

CAPACITY OF  
COMPRESSION  
MEMBERS IN RTA  
TIMBER TRUSS  
BRIDGES

BY AMIE NICHOLAS

# EXECUTIVE SUMMARY

## PURPOSE OF THIS INVESTIGATION:

The Roads and Traffic Authority of New South Wales (RTA) is constantly under pressure to replace or significantly upgrade many of the remaining timber bridges on NSW roads, because, among other reasons, they do not meet current loading standards and because of the large maintenance burden the bridges impose. Many of these bridges employ truss designs, are of heritage significance, and are listed on the State Heritage Register.

Using the best available information in the current Australian standard for design of timber structures, often members in these trusses must be assessed as theoretically under-capacity. The current standard for design of timber structures is not really intended for bridges, and there has not been a current timber bridge design standard since the NAASRA code in 1976. Timber bridges generally have been known to carry higher loadings than that predicted by design. No appreciable damage to members has been observed, even when bridges have been subjected to present heavy loadings. This suggests that the bridges are capable of carrying much heavier loads than current theory and codes would predict. There is a need for a method to assess the true load capacity of timber bridges to ensure safety to the public.

This is especially relevant for compression members, which are the focus of this investigation.

## EXISTING KNOWLEDGE ON THE SUBJECT:

The behaviour and design of steel compression members has been the focus of research for many years. In 1944, the Column Research Council was established in the United States. In January 2010, now called the Structural Stability Research Council (SSRC), they released the sixth edition of the "Guide to Stability Design Criteria for Metal Structures". Despite significant interest in the application of the Euler formula in the design of metal columns, it is evident in recent literature that little investigative effort has been given to the design of timber columns. Much of the research that has been done into timber columns has been done with the building industry in mind, rather than the bridge industry, and so much of it is not directly applicable.

Two large scale tests of RTA timber truss bridges have been conducted, one test to destruction by MBK in the 90s and another test of an instrumented bridge by the RTA in 2007.

## EXPERIMENTAL INVESTIGATION:

Four distinct aspects of the behaviour of RTA spaced columns were tested:

- **Buckling Mode:** Ten third size scale models of a typical DeBurgh truss vertical were tested to failure in order to observe the mode of failure and the ultimate capacity.
- **Bridge Timber Properties:** Timbers from an existing truss bridge were tested to determine the density and modulus of elasticity of timbers in RTA timber trusses.
- **Creep Effects:** A test was conducted to determine the extent of stress relieving of the bending stresses induced in timber compression members during fabrication.
- **Spacer Capacity:** The shear capacity of the bolt and spacer combination common in RTA timber truss compression members was investigated to inform the model for members not tested directly – both loose and tight bolts were investigated.

The buckling mode tests confirmed that the two flitches in a timber spaced column exhibit behaviour much closer to non-composite than complete composite action. However, they indicated that some advantage was gained, and so a rational buckling analysis of the assembly is a reasonable approach to assessing the true capacity of these assemblies.

The investigation of bridge timber properties tended to confirm the AS1720.1 values, whereby 16,000MPa is the average modulus of elasticity, but is subject to significant variation.

The creep test confirmed that stress relaxation does occur in timber subject to constant deflection. Approximately 15% of the initial load was lost in the 45 days duration of the test. A straight line could be fit fairly well to the data when load was plotted against log-time.

The results of the spacer capacity test proved that the primary component to carry shear in the timber spacers loaded perpendicular to grain is the bolts. Timber spacers showed very little resistance before splitting at the location of the bolts. A plot of the theoretical relationship between load and deflection for bolts fixed at both ends to induce double curvature shows that assuming fixity at the centre of the flitches provides a good prediction of strength and stiffness. Care must be taken to ensure that looseness of connections is also catered for.

### CONCLUSIONS AND RECOMMENDATIONS:

It is recommended that this simplification of the formula in AS 1720.1 Appendix E be used:

$$\left( \frac{M^*_{y}}{M_{d,y}} \right) + \left( \frac{N^*_{c}}{N_{d,cy}} \right) \leq 1.0$$

Since a quick calculation in accordance with the code requirements generally causes timber compression members in RTA bridges to fail, the following needs to take place:

- $M^*_{y}$  needs to be reduced (eg. by taking into account stress relaxation of timber)
- $M_{d,y}$  needs to be increased (eg. by modifying  $k_1$  factors)
- $N_{d,cy}$  needs to be increased by using a more detailed analytical design approach

Detailed recommendations are provided regarding the levels of stress relaxation which may be assumed and the new  $k_1$  factors to be used for various situations. Guidance is also provided on appropriate methods for modelling and conducting a critical buckling analysis.

It is not recommended that the design approach for spaced columns as outlined in AS1720.1 Appendix E be followed. This is because of the empirical nature of the formulas provided, and the difficulties in obtaining the theoretical basis of these formulas, as well as the fact that the arrangement of RTA spaced columns are significantly different from those described in the code. It is therefore concluded that a new approach would be simpler both to formulate and to implement. This is especially the case in the RTA design office where designers are relatively comfortable with Microstran so a rigorous buckling analysis is not difficult to achieve.

### FURTHER RESEARCH NEEDS:

Significant benefit could be gained by further research in the following specific areas:

- **Interaction equation for bending moment and axial force:** An investigation is required using actual bridge timbers, and full size sections as used in RTA bridges to determine the real behaviour in combined compression and bending.
- **Stress relaxation in timber subject to constant deflection:** Long term (minimum 24 months) timber stress relaxation tests are required using actual bridge timbers and full section sizes, but at a variety of stress levels and environmental conditions.
- **Relaxation rupture in timber with constant deflection:** This can be done in conjunction with the previous test, but looking specifically at failure due to time effects of timber subject to constant deflection. This may result in new  $k_1$  factors for bending.
- **Optimisation of bolt sizes in timber spacer connections:** A study needs to be done into the effect of increasing shear stiffness by increasing bolt diameters without excessively decreasing the compressive strength of the timber, which is also critical.
- **Influence of direction of grain of timber spacers:** Some trusses have spacers where direction of grain is different, and effects of this requires further investigation.

# TABLE OF CONTENTS

## CHAPTER ONE: LITERATURE REVIEW

RTA TIMBER TRUSS BRIDGES	5
TIMBER SPACED COLUMNS	6
MEMBER STABILITY	9
END RESTRAINT	9
GLOBAL STABILITY	13
CONCLUSION	13
BIBLIOGRAPHY	14

## CHAPTER TWO: THEORETICAL ANALYSIS

ANALYSIS IN ACCORDANCE WITH AS 1720.1 (NON-COMPOSITE)	15
Capacity Factor ( $\phi$ )	17
Duration of Load Factor ( $k_1$ )	17
Partial Seasoning Factor ( $k_4$ )	17
Modification Factor for Temperature ( $k_6$ )	17
Strength Sharing Factor ( $k_9$ )	17
Characteristic Strengths of Timber ( $f'_b$ & $f'_c$ )	17
Stability Factor ( $k_{12}$ )	18
Summary of Results for a Non-Composite Column	29
ANALYSIS IN ACCORDANCE WITH AS 1720.1 (SPACED COLUMN)	30

## CHAPTER THREE: EXPERIMENTATION

PURPOSE OF EXPERIMENTAL INVESTIGATION	33
METHOD AND RESULTS OF EXPERIMENTAL INVESTIGATION	33
Buckling Mode	33
Bridge Timber Properties	40
Creep Effects	42
Spacer Capacity	45

## CHAPTER FOUR: DISCUSSION AND CONCLUSIONS

FURTHER DISCUSSION IN THE LIGHT OF EXPERIMENTAL RESULTS	53
CONCLUSIONS AND RECOMMENDATIONS	60
FURTHER RESEARCH NEEDS	61

## APPENDIX A: SPACED COLUMN TEST RESULTS

DIMENSIONS FOR TIMBERS FOR SPACED COLUMNS	62
MODULUS OF ELASTICITY ABOUT X AND Y AXES	62
COMPRESSIVE STRENGTH OF TIMBERS FOR SPACED COLUMNS	66
EXPERIMENTAL RESULTS FOR SPACED COLUMN ASSEMBLY 11B12A	71
EXPERIMENTAL RESULTS FOR SPACED COLUMN ASSEMBLY 08A02A	74
EXPERIMENTAL RESULTS FOR SPACED COLUMN ASSEMBLY 11A10A	77
EXPERIMENTAL RESULTS FOR SPACED COLUMN ASSEMBLY 10B02B	80
EXPERIMENTAL RESULTS FOR SPACED COLUMN ASSEMBLY 05A04A	83
EXPERIMENTAL RESULTS FOR SPACED COLUMN ASSEMBLY 07B07A	86
EXPERIMENTAL RESULTS FOR SPACED COLUMN ASSEMBLY 01A01B	89
EXPERIMENTAL RESULTS FOR SPACED COLUMN ASSEMBLY 04B05B	92
EXPERIMENTAL RESULTS FOR SPACED COLUMN ASSEMBLY 06A12B	95
EXPERIMENTAL RESULTS FOR SPACED COLUMN ASSEMBLY 06B09B	98

# CHAPTER ONE

## LITERATURE REVIEW

### RTA TIMBER TRUSS BRIDGES:

The Roads and Traffic Authority of New South Wales (RTA) is constantly under pressure to replace or significantly upgrade many of the remaining timber bridges on NSW roads, because, among other reasons, they do not meet current loading standards and because of the large maintenance burden the bridges impose. Many of these bridges employ truss designs, are of heritage significance, and are listed on the State Heritage Register.<sup>1</sup>

There are five types of timber truss bridges remaining in NSW:

- Old Public Works Department trusses were built from 1860 to 1886. These bridges were designed by British engineers working in NSW, and adopted British styles of construction.
- McDonald trusses were built from 1886 to 1893, still using British styles of construction. They were designed for a distributed live load of 4.0 kPa or a 16 tonne traction engine.
- Allan trusses were built from 1893 to 1929. This design was similar to the American Howe truss design, with cast iron connection pieces. Designed for 6.7 kPa or a 16 tonne engine.
- DeBurgh trusses were built from 1899 to 1905. This was a pin-jointed design, similar to the American Pratt truss. In some cases steel replaced timber for the bottom chord.
- Dare trusses were built from 1905 to 1936. This design was very similar to the Allan truss with similar design loading, but the main difference being a steel bottom chord.



Figure 1.1: Photographs of Old PWD (left), Allan (centre) and DeBurgh (right) Trusses

A comparison of the design loads for the timber truss bridges (16 tonne traction engine) with the design loadings according to the current Australian Standard<sup>2</sup> for Bridge Design AS 5100 (SM1600 – approximately equivalent to four 40 tonne tri-axle loads (160 tonnes)) shows that with the provision of better roads and bridges, vehicles have become much heavier.

On a positive note, modern knowledge of the capacity of timber is more comprehensive, and permits the much more careful description of timber by species, resulting in increased capacities in the species used in timber bridges. For Ironbark and Tallowwood this increase is nearly 600% over McDonald's permissible stresses, and 155% over those used by Allan.<sup>3</sup>

However, even using the best available information in the current Australian standard for design of timber structures<sup>4</sup> and designing only for current legal loading (42½ tonne truck), often members in these old timber trusses must be assessed as theoretically under-capacity.

<sup>1</sup> RTA 2002

<sup>2</sup> AS 5100.2 Bridge Design Part 2: Design Loads (2004)

<sup>3</sup> DMR 1987

<sup>4</sup> AS 1720.1 Timber Structures Part 1: Design Methods (1997)

The current standard for design of timber structures is not really intended for bridges, and there has not been a current timber bridge design standard since the NAASRA<sup>5</sup> code in 1976. Timber bridges generally have been known to carry higher loadings than that predicted by design. No appreciable damage to members has been observed, even when bridges have been subjected to present heavy loadings. This suggests that the bridges are capable of carrying much heavier loads than current theory and codes would predict. There is a need for a method to assess the true load capacity of timber bridges to ensure safety to the public.

### TIMBER SPACED COLUMNS:

Compression members in many of the RTA's timber truss bridges take the form of spaced columns. These consist of compression members in two parts separated by timber spacers.

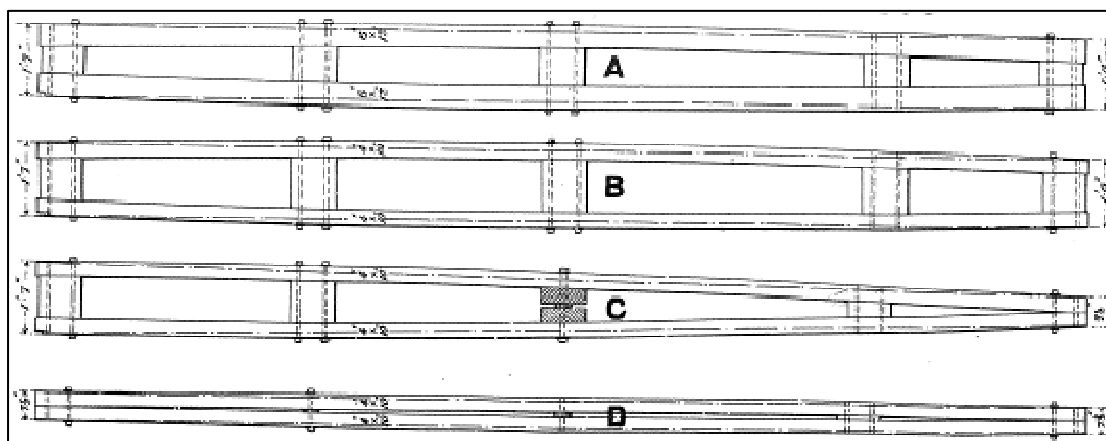


Figure 1.2: Typical Layouts of Spaced Columns – excerpt from Morpeth Bridge Plans

Although the packing blocks in spaced timber columns appear similar to batten plates in steel columns, the design of timber spaced columns is very different. Unless they are glued in place, the packing blocks in timber columns are not sufficiently rigid to enable the column to act as a unit. Even if they are tightly bolted up when the structure is first erected, the inevitable shrinkage will cause subsequent looseness, with a great reduction in strength.<sup>6</sup>

Buckling strength of a timber member is a function of a great number of complex parameters; these include those used for material failure and creep criteria, material variability, nonlinear material characteristics, the random dispersion of defects and initial crookedness.<sup>7</sup> To strive for a high degree of accuracy is inappropriate; many of the critical parameters that affect buckling strength are either unknown or vary significantly from one member to another.<sup>8</sup>

Wood with defects behaves as a non-linear ductile material in compression. Knots and material variability make it impossible to load a member with perfectly concentric axial loads.<sup>9</sup> Although there are provisions for spaced columns in the current code, they do not cover the kinds of spaced columns used in timber truss bridges. Difficulties for designers include:

- Load sharing between the two components of a spaced column with varying stiffness
- How to deal with the effects of initial curvature and resultant internal bending stresses
- Capacity of bolt in timber spacers loaded perpendicular to grain along the grain
- Unknown end fixity provided by cast iron shoes or timber to timber connections
- Difference in end fixity between Dare & Allan due to steel bottom chord
- How to deal with lack of fit and tolerance issues and their influence on end fixity

<sup>5</sup> NAASRA 1976

<sup>6</sup> CSIRO 1948

<sup>7</sup> Leicester 1986

<sup>8</sup> Leicester 1988

<sup>9</sup> Buchanan 1985

In the early 1990s the RTA had some load testing carried out on two timber truss bridges.<sup>10</sup>

A full size twin diagonal member from Euminbah Bridge was tested in compression at the University of NSW. The 3.185m long specimen failed at 1518kN with calculated stress of 35MPa. The twin diagonal tested had a straight member and a curved member and at failure load the straight member fractured about its major axis without any obvious buckling action.

A full size twin diagonal and single diagonal to top chord connection from Euminbah Bridge was tested with eccentric compressive axial forces in the diagonals to obtain moment-rotation relationship at top chord connection, axial stiffness in compression and elastic modulus of the diagonal members. Reported results, though difficult to interpret, are copied below:

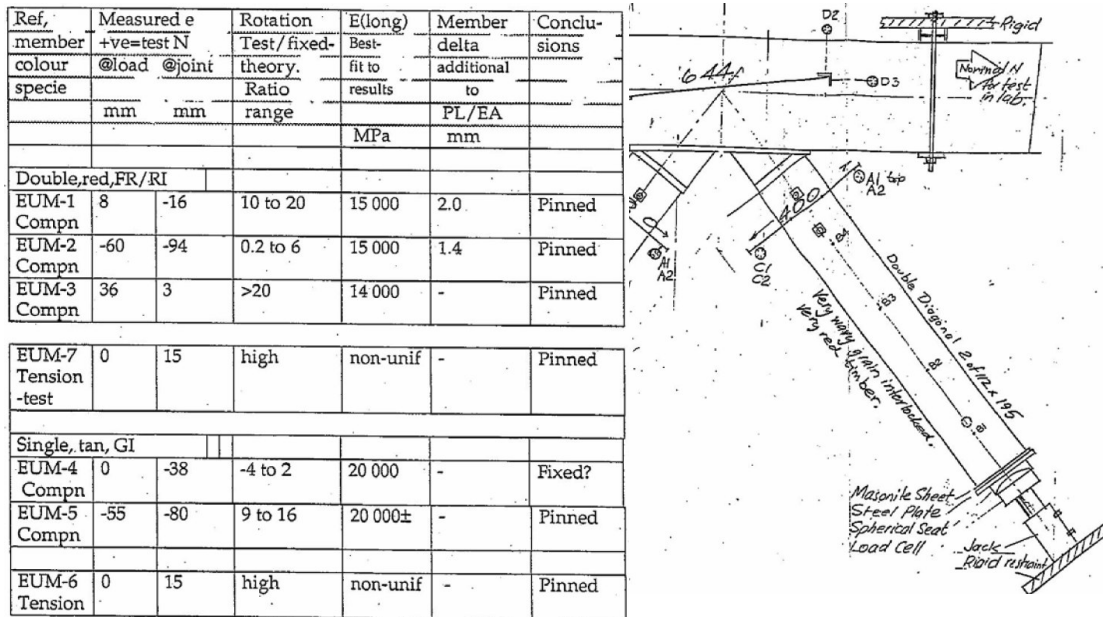


Figure 1.3: Full size Diagonal-to-Chord Connection Stiffness

Codes of practice around the world rely heavily on the concept of effective length when dealing with capacity of columns. However, there have been a number of different definitions of “effective length” including idealised cases in textbooks, maximum stress criteria, effective lengths decided by axial load only, or effective lengths at the elastic critical load factor.<sup>11</sup>

The MBK report concluded that pin-jointed action would probably be appropriate for estimating the effective lengths against buckling for diagonal members. This was because the measured rotation across the finite joint was many times expected rotation for a fixed joint under the applied loads. The measured large rotation was thought to be due primarily to the much lower E value perpendicular to the grain within the chord member.

In 2007 the RTA again did some load testing and strain gauging of an Allan truss bridge.<sup>12</sup>

Among other things, the load sharing between the two flitches of the spaced columns comprising the principals, diagonals and top chords of the truss was investigated. Results varied substantially with some members displaying almost equal strains in the two flitches (45% / 55%), while other members had differences in strain of up to 30% / 70%. Significantly, it was not always the inner flitch or the outer flitch that showed the highest strains, which may suggest that load sharing is highly dependent upon the variation of properties between the two timbers that make up the spaced column rather than on global effects in the truss.

<sup>10</sup> MBK 1994  
<sup>11</sup> Wood, 1974  
<sup>12</sup> Shah 2008



Diagonal Member (Note the sensor flitch)

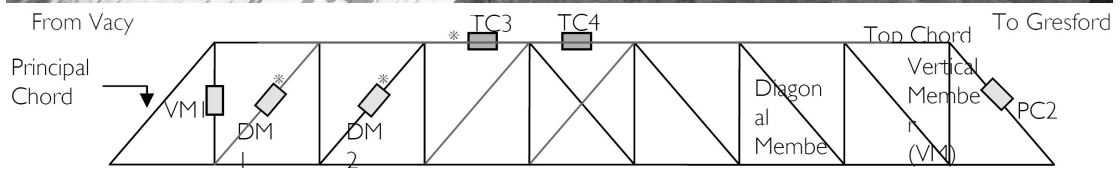


Figure 1.4: Load Testing and Strain Gauging of Vacy Bridge, Hunter Region<sup>13</sup>

<sup>13</sup> Shah 2008



**MEMBER STABILITY:**

The Euler formula for the elastic critical buckling load of a slender column is the earliest engineering design formula that is still in use today. The “Euler Load” is defined as the critical load at which a slender elastic column can be held in a bent configuration under axial load alone. In Euler’s time, columns were made of masonry or timber, the latter being considered by Euler as “subject to bending” and therefore appropriate for application of his formula.<sup>14</sup>

Despite the fact that the Euler formula is widely used, it is an idealisation, and many important fundamental problems and questions remain unanswered. Johnston helpfully outlines a number of them: Real columns are never perfectly straight nor can the degree of crookedness in a real structure be known. Real columns nearly always carry appreciable strength reducing bending moments, which can only be estimated. Real columns have lateral and rotational end restraints that may vary with the life of the structure, and these can only be estimated.<sup>15</sup>

The behaviour and design of real metal columns has been the subject of research for many years. In 1944, the Column Research Council was established in the United States.<sup>16</sup> In January 2010, now called the Structural Stability Research Council (SSRC), they released the sixth edition of the “Guide to Stability Design Criteria for Metal Structures”. Despite significant interest in the application of the Euler formula in the design of metal columns, it is evident in the literature that little investigative effort has been made into the design of timber columns.

**END RESTRAINT:**

Conventional procedures for the analysis of framed steel structures depend on the basic assumption that the member end-connections behave as either pinned or completely rigid. This is done despite the knowledge that few connections behave in either fashion.<sup>17</sup>

Since the presence of end restraint may be expected to affect column strength, it is desirable to make a proper allowance for this in design. The Euler approach enables the elastic critical load to be related directly to the stiffness of the restraint at either end through the concept of effective length where effective length is defined as the length of the equivalent pin-ended column that would have the same elastic critical load as the actual end-restrained column.<sup>18</sup>

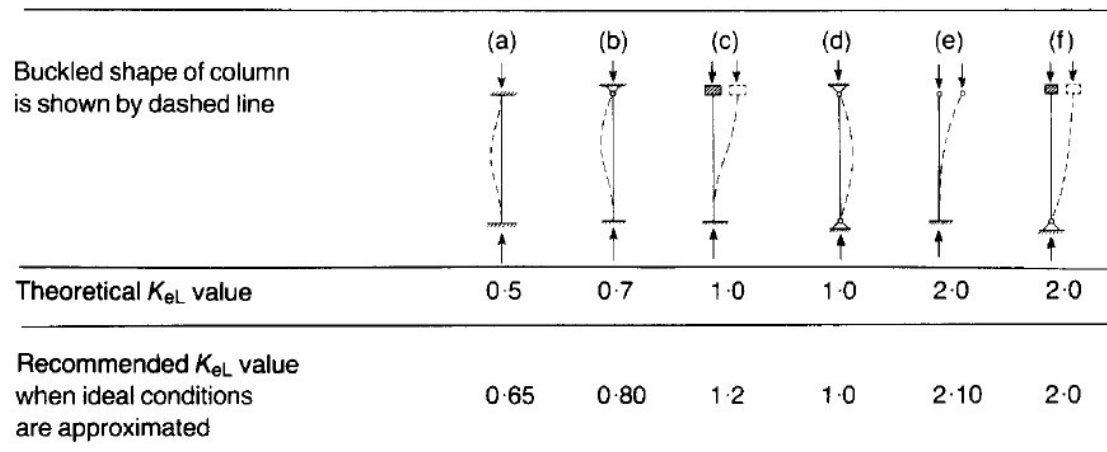


Figure 1.5: Effective Length ( $K_{eL}$ ) for centrally loaded columns as recommended by SSRC.<sup>19</sup> (The recommended design values of  $K$  are modifications of the ideal values, taking into account the fact that neither perfect fixity nor perfect flexibility is attained in practice – pg 48, fifth edition SSRC Guide)

<sup>14</sup> Johnston 1983  
<sup>15</sup> Johnston 1983  
<sup>16</sup> Chen 1980  
<sup>17</sup> Romstad 1970  
<sup>18</sup> Nethercot 1988  
<sup>19</sup> Nethercot 1988

	Braced member			Sway member		
Buckled shape						
Effective length factor ( $k_e$ )	0.7	0.85	1.0	1.2	2.2	2.2
Symbols for end restraint conditions	= Rotation fixed, translation fixed = Rotation free, translation fixed			= Rotation fixed, translation fixed = Rotation free, translation fixed		

AS4100 Figure 4.6.3.2 Effective Length Factors for Idealised Conditions of End Restraint<sup>20</sup>

It can be seen from the excerpt from AS4100 above that a similar concept has been accepted for use in Australian standards for design of steel structures. The effective lengths specified are a little different to those proposed by the SSRC, and the commentary to AS4100, Clause C4.6.3.2 notes that the values given assume that full fixity will not occur in practice.

Condition of end restraint	Effective length factor ( $g_{13}$ )
Flat ends	0.7
Restrained at both ends in position and direction	0.7
Each end held by two bolts (substantially restrained)	0.75
One end fixed in position and direction, the other restrained in position only	0.85
Studs in light framing	0.9
Restrained at both ends in position only	1.0
Restrained at one end in position and direction and at the other end partially restrained in direction but not in position	1.5
Restrained at one end in position and direction but not restrained in either position or direction at other end	2.0

AS1720.1 Table 3.2 Effective Length Factor for Columns without Intermediate Restraint<sup>21</sup>

It can be seen from comparing AS4100 to the excerpt from AS1720 above that the same effective length factors have been specified, with some additional information given that is relevant only to timber (studs in light framing, each end held by two bolts, etc). It is therefore implied that the underlying assumption remains that full fixity will not occur in practice.

Information concerning actual connection behaviour and analytical methods developed to incorporate this behaviour are cumbersome. However, the introduction of the computer has made it possible to incorporate better representations of true connection behaviour.<sup>22</sup>

<sup>20</sup> AS 4100 Steel Structures (1998)

<sup>21</sup> AS 1720.1 Timber Structures Part 1: Design Methods (1997)

<sup>22</sup> Romstad 1970

The best description of the flexural behaviour of a connection is the relationship between the moment transmitted by the connection and the rotation of the connected members relative to each other.<sup>23</sup> Methods of modelling moment-rotation curves have developed in step with experimental studies for metal connections starting in the 1930s, as summarised by Nethercot in the table below. Early models assumed a linear  $M-\phi$  relationship. In the 1960s, the  $M-\phi$  data was approximated to a polynomial function. In the 1970s and 1980 bilinear, trilinear and piecewise linear models were developed. Finally, an accurate representation of connection behaviour was achieved using fairly complicated cubic B-spline curve fitting techniques.<sup>24</sup>

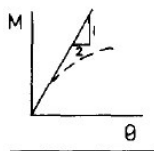
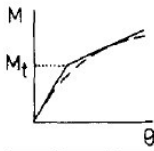
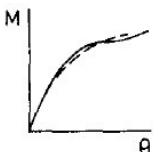

Type of Model	References	Year	Advantages	Disadvantages
1. Linear				
	Baker	1933	1. Simple to use	Inaccurate at high rotation values
	Rathbun	1936	2. Stiffness matrix only requires initial modification	
2. Bilinear				
	Lionberger & Weaver	1969	1. Simple to use	Inaccurate at some rotation values
	Romstad & Subramanian	1970	2. Curve follows $M-\theta$ curve more closely than Linear model	
3. Polynomial				
	Sommer	1970	Produce a close approximation to the shape of the $M-\theta$ data	1. Can produce inaccurate (even negative) connection tangent stiffness values
	Frye & Morris	1975		2. Nonlinear requires iterative evaluation
4. Cubic B-Spline				
	Jones <i>et al.</i>	1980	1. Produces a very close approximation to the $M-\theta$ data shape 2. Produces accurate values of connection stiffness	1. Nonlinear, therefore requires iterative evaluation 2. Requires special numerical procedures for evaluation

Figure 1.6: Methods of Modelling Moment Curvature Data for Metal Connections<sup>25</sup>

Razzaq has argued that an elastic-plastic restraints with the same maximum spring plastic moment may result in nearly the same maximum column load as other models, so consideration should be given to approximating nonlinear moment-rotation restraint characteristics by simple elastic-plastic properties, as opposed to more complicated ones.<sup>26</sup>

<sup>23</sup> Jones 1980

<sup>24</sup> Jones 1980

<sup>25</sup> Nethercot 1988

<sup>26</sup> Razzaq 1983

However the moment-rotation characteristics of the connections are modelled (and modelling of timber connections may be different anyway), a number of researchers have discovered the significant benefits to column capacity of even a small amount of connection rigidity.

Romstad<sup>27</sup> defined percent rigidity of a connection as the ratio of the moment required to produce a unit joint rotation with a partially rigid connection divided by the moment required to produce a unit joint rotation with a fully rigid connection. Rigidities of only 15% to 25% were discovered to provide a significant increase in buckling capacity over a pinned connection.

Jones<sup>28</sup> noted that the benefits of increased end restraint become more significant as the column becomes more slender. The strength increase at  $\lambda = 220$  was found to be 83% and 203% for web cleats and end plate connections respectively. Jones noted a significant reduction in deformations for both slender and stocky columns with some end restraint.

Similarly, Razzaq<sup>29</sup> has shown that only a moderate amount of end restraint is needed to enable a column to carry over 85% of the load for the nearly fixed column. This is contrary to the popular belief of the designers that a nominal restraint may be assumed as pinned.

Shen<sup>30</sup> plotted the strength of a column as a function of R (rotational stiffness of end restraint) for six selected values of  $\lambda$  (a non-dimensional slenderness ratio). The increases are expressed as percentages of the capacities of the respective columns with zero end restraint.

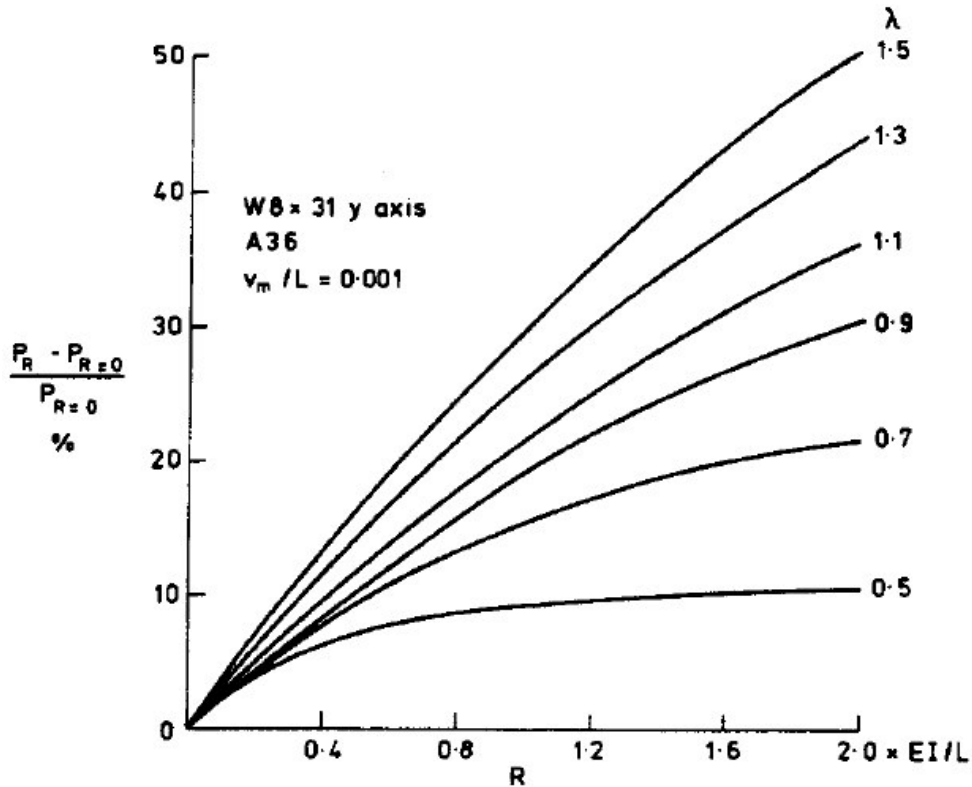


Figure 1.7: Increase in Column Strength due to End Restraint<sup>31</sup>

Goncalves has investigated the influence of joint flexibility on K-factor for both the inelastic and the elastic case and concluded that, for a narrow range of flexible connections, a small increase in joint stiffness results in a substantial decrease in the effective length factor.<sup>32</sup>

<sup>27</sup> Romstad 1970

<sup>28</sup> Jones 1982

<sup>29</sup> Razzaq 1983

<sup>30</sup> Shen 1983

<sup>31</sup> Shen 1983

<sup>32</sup> Goncalves 1992

## GLOBAL STABILITY:

Although there is an acknowledged interdependence between the maximum strength of frames and the maximum strength of the component members, the complexity involved in taking into account this interdependence means that the two aspects (stability of individual members and stability of the structure as a whole) are generally considered independently.<sup>33</sup>

The ultimate capacity of a frame depends on its connection flexibility in two ways: first, a stiffer connection tends to transfer more moment from the girder to the column, thus causing premature yielding in the column, and tending to decrease the capacity of the frame. On the other hand, a stiffer connection will provide greater rotational restraint on the column ends, which will tend to increase their buckling strength and to increase the frame capacity.<sup>34</sup>

The failure to include the effects of axial load in adjacent members restraining a critical buckling member can lead to serious error in determining its elastic critical buckling load.<sup>35</sup>

In trusses, the loads are generally applied at joints. If members are connected rigidly or semi-rigidly at the joints, the angle changes due to loading introduce secondary bending stresses. However, according to the SSRC investigations, these have little effect on the buckling strength of the truss members because the secondary moments dissipate due to local yielding of extreme fibres of the members near the joints as the truss is loaded to ultimate. The SSRC therefore recommends that web members in trusses designed for moving live-load systems be designed with  $K=0.85$  in the plane of the truss. This is because the position of live load that produces maximum force in the web member being designed will result in less than the maximum forces in members framing into it, so rotational restraints are developed.<sup>36</sup>

It is yet to be seen whether or not these recommendations are applicable to timber trusses.

## CONCLUSION:

The primary questions that remain unanswered are:

- What is the end fixity for the spaced columns in a cast iron shoe on timber or steel?
- If end fixity does exist, what is the moment curvature relationship of that connection?
- What effect does lack of fit and construction tolerance have on end fixity?
- How are loads distributed between the two flitches in a spaced column?
- What is the effect of the initial curvature induced during fabrication of members?
- What is the creep effect and how does it affect column strength over time?
- What affect does the variability of E have on the reliability of compressive strength?
- What is the effect of limited bolts at ends of spaced columns? Does it matter?
- To what extent are bolts in central spacers assisted by friction induced by curvature?
- To what extent are end bolts made less effective in shear by tension due to curvature?
- What effect does the limited capacity of the spacer bolts to transmit shear have?
- How does the global behaviour of a timber truss bridge affect its capacity?
- Is the current standard for design of timber compression members overly conservative?
  - Is it necessary to modify the stability factor  $k_{12}$ ?
  - Is it necessary to modify the effective length factor  $g_{13}$ ?

In looking into these questions using theoretical and experimental methods, the aim of this project is to provide guidelines that can be used by bridge design staff to allow reasonable prediction of compression strength of timber members in RTA timber truss bridges.

---

<sup>33</sup> Chen 1980

<sup>34</sup> Ackroyd 1983

<sup>35</sup> Bridge 1987

<sup>36</sup> Galambos, 1998 (pg 49-50)

**BIBLIOGRAPHY:**

- Ackroyd, M.H, Gerstle, K.H. (1983) “*Strength of Flexibly Connected Steel Frames*”, Engineering Structures, Volume 5, January 1983, pp 31-37
- Bridge, R.Q., Fraser, D.J. (1987), “*Improved G-Factor Method for Evaluating Effective Lengths of Columns*”, Journal of Structural Engineering, Volume 113, June 1987, pp 1341-1356
- Buchanan, A.H., Johns, K.C., Madsen, B (1985) “*Column Design Methods for Timber Engineering*” International Council for Building Research Studies and Documentation – Working Commission W18 – Timber Structures, Meeting 18, Israel
- Chen, W.-F., (1980), “*End Restraint and Column Stability*”, Journal of the Structural Division ASCE, Volume 106, November 1980, pp 2279-2295
- DMR (1987) “*Timber Truss Bridge Maintenance Handbook*”, Produced by Department of Main Roads New South Wales, February 1987
- CSIRO (1948) “*Handbook of Structural Timber Design – Third Edition*”, J.J. Gourley, Government Printer, Melbourne.
- Galambos, T.V. (1998) “*Guide to Stability Design Criteria for Metal Structures – Fifth Edition*”, John Wiley & Sons
- Goncalves S., R. (1992), “*New Stability Equation for Columns in Braced Frames*”, Journal of Structural Engineering, Volume 118, July 1992, pp 1853-1870
- Johnston, B.G. (1983), “*Column Buckling Theory: Historic Highlights*”, Journal of Structural Engineering, Volume 109, September 1983, pp 2086-2096
- Jones, S.W., Kirby, P.A., Nethercot, D.A. (1980) “*Effect of Semi-Rigid Connections on Steel Column Strength*”, Journal of Constructional Steel Research, Volume 1, September 1980, pp 38-46
- Jones, S.W., Kirby, P.A., Nethercot, D.A. (1982) “*Columns with Semirigid Joints*”, Journal of the Structural Division ASCE, Volume 108, February 1982, pp 361-372
- Leicester, R.H., (1986) “*Creep Buckling Strength of Timber Beams and Columns*”, International Council for Building Research Studies and Documentation – Working Commission W18 – Timber Structures, Meeting 19, Italy
- Leicester, R.H., (1988) “*Format for Buckling Strength*”, International Council for Building Research Studies and Documentation – Working Commission W18 – Timber Structures, Meeting 21, Canada
- MBK (1994) “*Report on Test Loading of Allan Truss Bridges (Euminbah Bridge) and Dare Truss Bridges (Dangar Bridge) in February and June 1993*”, June 1994
- NAASRA (1976) “*Bridge Design Specification*”, National Association of Australian State Road Authorities, 5<sup>th</sup> Edition 1976
- Nethercot, D.A., Chen, W.-F. (1988) “*Effects of Connections on Columns*”, Journal of Constructional Steel Research, Volume 10, 1988, pp 201-239
- Razzaq, Z. (1983) “*End Restraint Effect on Steel Column Strength*”, Journal of Structural Engineering, Volume 109, February 1983, pp 314-334
- Romstad, K.M., Subramanian, C.V. (1970) “*Analysis of Frames with Partial Connection Rigidity*”, Journal of the Structural Division ASCE, Volume 96, November 1970, pp 2283-2300
- RTA (2002) “*Timber Bridge Management*” January 2002
- Shah, P, Ton, P. (2008) “*Realistic Load Capacity Timber Truss Bridges by Performance Load Testing*” Presented at RTA Annual Bridge Seminar, December 2008
- Shen Z.-Y., Lu, L.-W. (1983) “*Analysis of Initially Crooked, End Restrained Steel Columns*”, Journal of Constructional Steel Research, Volume 3, 1983, pp 10-18
- Standards Australia (1997) AS1720.1 – Timber Structures Part 1: Design Methods
- Standards Australia (1998) AS4100 Steel Structures
- Standards Australia (2004) AS5100.2 - Bridge Design Part 2: Design Loads
- Wood, R.H. (1974) “*Effective Lengths of Columns in Multi-Storey Buildings*”, The Structural Engineer, Volume 52, July 1974, pp 235-244

## CHAPTER TWO

# THEORETICAL ANALYSIS

### ANALYSIS IN ACCORDANCE WITH AS 1720.1 FOR A NON-COMPOSITE COLUMN:

Compression members in many of the RTA's timber truss bridges take the form of spaced columns. These consist of compression members in two parts separated by timber spacers. The spacers are generally of different widths, so that a bow is created in the compression members. The bow is typically 25mm for each member, but does vary for some truss types. The existence of this bow means that bending stresses must be considered in addition to compressive stresses. Two types of bending stresses must be considered. Firstly, the bending stresses induced due to fabrication of the member with initial curvature and secondly, the secondary bending stresses due to eccentricity when a compressive force is applied.

Although AS 1720.1 - 2010<sup>37</sup> does not cover the case of minor axis bending with axial compression, the Timber Design Handbook<sup>38</sup> does provide a formula which is a simplification of the biaxial bending formula given in AS 1720.1 Appendix E. The formula is given here:

$$\left( \frac{M_y^*}{M_{d,y}} \right) + \left( \frac{N_c^*}{N_{d,cy}} \right) \leq 1.0$$

A bending strength assessment is undertaken in accordance with Clause 3.2.1 of AS 1720.1

$M_d \geq M^*$  where  $M_d = \phi k_1 k_4 k_6 k_9 k_{12} f'_b Z$

$M_d$	=	design capacity in bending
$M^*$	=	design action effect in bending
$\phi$	=	capacity factor (0.75 for F22 timber)
$k_1$	=	duration of load factor (0.57 for dead load, 0.97 for ultimate live load)
$k_4$	=	partial seasoning factor (1.0 for RTA truss timbers)
$k_6$	=	modification factor for temperature (1.0 for RTA truss bridges)
$k_9$	=	strength sharing factor (1.0 for RTA truss members)
$k_{12}$	=	stability factor (1.0 for bending about the minor axis)
$f'_b$	=	characteristic value in bending (55MPa for F22)
$Z$	=	section modulus which equals $db^2/6$ for bending about minor axis

Similarly, a compressive strength assessment is undertaken in accordance with Clause 3.3.1

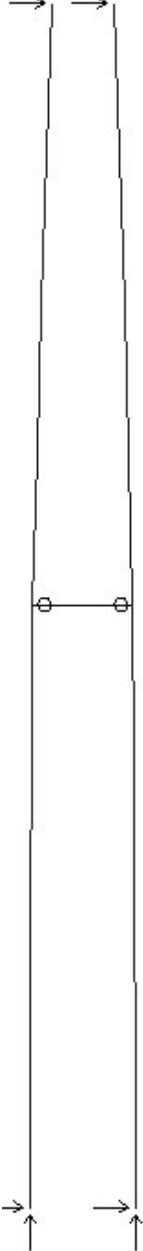
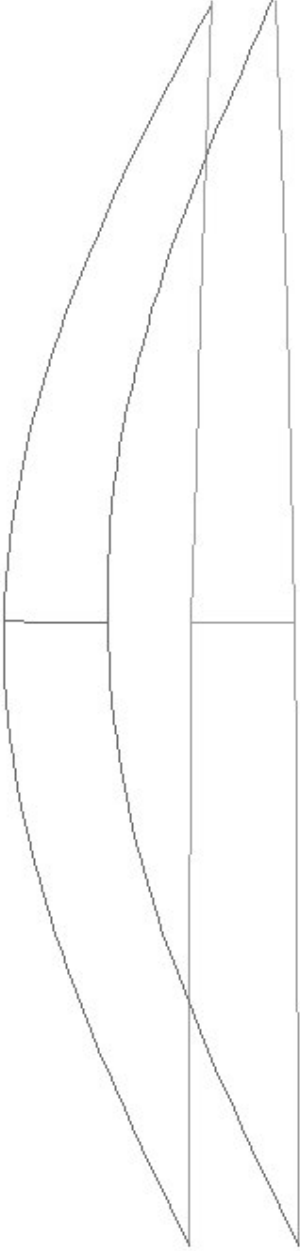
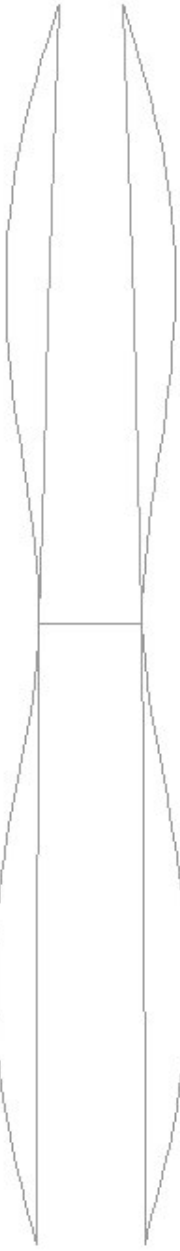
$N_{d,c} \geq N_c^*$  where  $N_{d,c} = \phi k_1 k_4 k_6 k_{12} f'_c A_c$

$N_{d,c}$	=	design capacity in compression
$N_c^*$	=	design action effect in compression
$\phi$	=	capacity factor (0.75 for F22 timber)
$k_1$	=	duration of load factor (0.57 for dead load, 0.97 for ultimate live load)
$k_4$	=	partial seasoning factor (1.0 for RTA truss timbers)
$k_6$	=	modification factor for temperature (1.0 for RTA truss bridges)
$k_{12}$	=	stability factor
$f'_c$	=	characteristic value in compression parallel to grain (42MPa for F22)
$A_c$	=	cross-sectional area of column

<sup>37</sup> AS 1720.1 – 2010 Timber Structures Part 1: Design Methods (2010)

<sup>38</sup> SAA HB108-1998 Timber Design Handbook

When a typical compression member is assessed assuming non-composite action, it is modelled as two independent flitches joined by spacers that are pinned at both ends. The top of each of the flitches is restrained from lateral movement, but free to move in the vertical direction, while the base is fixed in both horizontal and vertical directions. Below is shown a typical arrangement of a compression member for a De Burgh truss along with the two primary buckling modes to be assessed assuming non-composite action of the two flitches.

Microstran Model	Buckling Mode 1	Buckling Mode 2
	<p data-bbox="603 472 943 741">The possible buckling mode shown below assumes that the initial curvature is insufficient to exclude the possibility of the curvature of one flitch reversing under compression loads, and the two flitches together deflecting to one side.</p> 	<p data-bbox="986 472 1326 741">The possible buckling mode shown below assumes that the initial curvature prevents buckling mode 1 from occurring, and so buckling is confined to the areas between the timber spacers, and there is no reversal of initial curvature in either flitch.</p> 



### CAPACITY FACTOR ( $\phi$ )

The capacity factor ( $\phi$ ) is obtained from Table 2.1. For truss timbers in RTA timber truss bridges, the appropriate category is Category 3, which applies to primary structural members in structures intended to fulfil an essential service or post disaster function. This is entirely appropriate for these heritage structures. All members in a truss are primary structural members whose failure could result in collapse of the bridge. Not only do many of these structures fulfil an essential transportation service to the travelling public, but the RTA is also required by law to maintain them well into the future due to their significant heritage value.

In accordance with RTA QC Specification 2380<sup>39</sup>, all truss timbers supplied for RTA timber truss bridges have a minimum stress grade of F22. Therefore, the capacity factor is 0.75.

### DURATION OF LOAD FACTOR ( $k_1$ )

In accordance with Clause 2.4.1.1 of AS 1720.1, for any given combination of loads of differing duration, the factor  $k_1$  to be used is that appropriate to the action that is of the shortest duration. Generally, the forces due to dead load in most timber elements in a bridge are quite small compared to those caused by live loads. However, some components in large span trusses may be subject to very high dead load forces. Permanent effects alone should, therefore, also be considered separately using the  $k_1$  factor of 0.57 for permanent actions. This would generally include dead loads as well as permanent forces due to fabrication.

The appropriate  $k_1$  factor for ultimate vehicular loading (T44 vehicle with load factor of 2.0 in accordance with the Austroads Bridge Design Code<sup>40</sup>) on timber truss bridges is obtained from Table 2.3 for five hours duration. Therefore,  $k_1$  for member strength shall be 0.97. If a lesser loading is being considered, such as legal loading (42.5 tonne semi trailer with a load factor of 2.0), then the number of anticipated significant load events would increase, and so the cumulative duration of load should be taken as five days, giving a  $k_1$  factor of 0.94.

The relevant  $k_1$  factor for serviceability vehicular loading is 0.8 assuming five months duration.

### PARTIAL SEASONING FACTOR ( $k_4$ )

Due to the fact that RTA bridge truss timbers generally have a least dimension of 100mm or more, the appropriate  $k_4$  factor in accordance with Clause 2.4.2 is generally 1.0.

### MODIFICATION FACTOR FOR TEMPERATURE ( $k_6$ )

As the RTA generally maintains bridges only in NSW, the appropriate  $k_6$  factor is 1.0.

### STRENGTH SHARING FACTOR ( $k_9$ )

As noted by the RTA Timber Bridge Manual<sup>41</sup>, truss members with multiple components should generally be taken as discrete parallel systems for the purposes of determining  $k_9$ . Nearly all compression members are detailed with the components spaced apart, and although they are joined at intervals along the length, this does not properly represent a combined parallel system. Therefore, in accordance with Clause 2.4.5.2, the strength sharing factor  $k_9$  should be taken as 1.0 unless there are three or more members in the system.

### CHARACTERISTIC STRENGTHS OF TIMBER ( $f'_b$ & $f'_c$ )

In accordance with RTA 2380, all truss timbers supplied for RTA timber truss bridges have a minimum stress grade of F22. Characteristic values are therefore obtained from Table H2.1:

$$\begin{aligned} f'_b &= 55 \text{ MPa (where depth of member is less than or equal to 300mm)} \\ f'_c &= 42 \text{ MPa} \end{aligned}$$

<sup>39</sup> RTA QC Specification 2380: Timber for Bridges

<sup>40</sup> Austroads Bridge Design Code 1996

<sup>41</sup> Timber Bridge Manual, RTA Bridge Engineering, June 2008

STABILITY FACTOR ( $k_{12}$ )

The stability factor ( $k_{12}$ ) is defined differently for bending and compression members.

For the purposes of studying compression members in RTA timber truss bridges, the stability factor for bending relates to bending about the minor axis, for which  $k_{12}$  is taken as 1.0.

In accordance with Clause 3.3.3, the stability factor ( $k_{12}$ ) for compression is given by:

for $\rho_c S \leq 10$	$k_{12} = 1.0$
for $10 \leq \rho_c S \leq 20$	$k_{12} = 1.5 - 0.05 \rho_c S$
for $\rho_c S \geq 10$	$k_{12} = 200 / (\rho_c S)^2$

The stability factor for columns therefore depends upon two primary variables.

The first ( $\rho_c$ ) is a material constant that, according to the Timber Design Handbook, allows for:

- initial curvature of the member
- creep buckling of the compression member; and
- ratio of stiffness to compressive strength

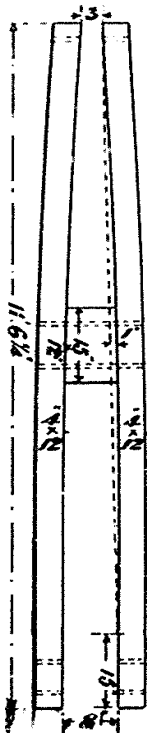
For F22 timbers which are used in RTA timber truss bridges,  $\rho_c$  can be calculated as follows:

$$\begin{aligned} \rho_c &= 9.29 (E/f'_c)^{-0.367} r^{-0.146} \\ E &= 16,000 \text{ MPa (Table H2.1)} \\ f'_c &= 42 \text{ MPa (Table H2.1)} \end{aligned}$$

Therefore,

$$\begin{aligned} \rho_c &= 1.05 r^{-0.146} \\ r &= (\text{temporary design action effect}) / (\text{total design action effect}) \end{aligned}$$

As stated in the Timber Design Handbook, it is to be recognised that the formulas in AS 1720.1 use an empirical relationship to derive  $\rho_c$ . The applicability of this material constant in the spaced columns on RTA timber truss bridges is questionable for the following reasons:



- 1) The material constant allows for initial curvature of the member. This assumes a single stand-alone member not constrained to a particular curvature. The members of interest in this study have opposing curvatures restrained by bolts and timber spacers so that the system is in equilibrium.
- 2) The curvatures assumed in AS 1720.1 are likely to be considerably less than the curvatures that are induced in RTA timber truss bridge members. The initial curvature induced in truss members is very significant, well defined and easily measureable, and should therefore be considered separately rather than being included in an empirically derived material constant.
- 3) The material constant allows for creep buckling of the compression member. The effects of creep are unlikely to be the same for a single stand-alone member when compared with the members of interest in this study. Once again, there may be significant benefits to be gained from the opposing curvatures of the two flitches of the spaced columns, which not only define the curvature of the flitches, but also limit additional deflections due to creep.
- 4) Creep may cause lateral deflection to increase between the spacers, thereby increasing secondary bending stresses in the member. However, creep is also likely to decrease the internal bending stresses in the member which resulted from the fabrication process forcing curvature into the member. It is possible that the positive effect of creep in reducing the stresses would outweigh the negative effect of secondary stresses due to lateral deflection.

The second variable upon which the stability factor depends is the slenderness coefficient (S).

The value of the slenderness coefficient is obtained in Appendix E in the following equation:

$$S = \sqrt{\left(\frac{\pi^2}{12}\right)\left(\frac{EA}{N_{cr}}\right)}$$

Where

E	=	16,000 MPa (Table H2.1)
A	=	cross sectional area of column
$N_{cr}$	=	$\pi^2 EI/L_{eff}^2$ (critical elastic axial buckling load of column)
I	=	$db^3/12$ (for buckling about the minor axis)
d	=	depth of member
b	=	breadth of member
$L_{eff}$	=	effective length of member

The most critical aspect in determining an appropriate slenderness coefficient (S) for a column is to determine the effective length ( $L_{eff}$ ) of the member. The effective length is found by modifying the actual length by an effective length factor ( $g_{13}$ ) which is obtained from Table 3.2 of AS 1720.1, from which the relevant portion is copied below.

Condition of end restraint	$g_{13}$
Flat ends (perfectly flat ends bearing on flat unyielding bases)	0.7
Restrained at both ends in position and direction	0.7
Each end held by two bolts (substantially restrained)	0.75
One end fixed in position and direction, the other restrained in position only	0.85
Studs in light framing	0.9
Restrained at both ends in position only	1.0

Often in truss analysis, one would assume that both ends of a timber compression member are restrained in position only, giving a  $g_{13}$  factor of 1.0. Indeed, as outlined in the literature review, some testing has been undertaken which did conclude that pin-jointed action would probably be appropriate for estimating the effective lengths against buckling. This was because the measured rotation across the finite joint was many times the expected rotation for a fixed joint under the applied loads. The measured large rotation was thought to be due primarily to the much lower E value perpendicular to the grain within the chord member

However, as also noted in the literature review, a small increase in joint stiffness may result in a substantial decrease in the effective length. Therefore, it is worth investigating whether or not a less conservative assumption of end restraint is warranted for RTA timber bridges.

It does seem reasonable at least to assume a  $g_{13}$  factor of 0.9 which is given for “studs in light framing”. Although timber truss compression members are obviously not studs in light framing, they are compression members nominally cut square and effectively bearing on timber perpendicular to grain at both ends (except for the case of bridges with steel bottom chords, where additional restraint may be expected due to the stiffness of the metal). This is similar to the explanation of “studs in light framing” in the Timber Design Handbook.

For the case of timber truss bridges with steel bottom chords and steel cross girders, it may be appropriate to assume a shorter effective length due to the significant restraint afforded by the steel connections at the base of the column. If the top connection is also assumed to provide some restraint, then the appropriate  $g_{13}$  factor would be  $(0.9+0.7)/2 = 0.8$ . An example of this is Tabulam Bridge which is a De Burgh truss bridge with a steel bottom chord. Although originally the cross girders were timber, they have now been replaced by steel cross girders as shown in the photograph.



The next option to consider is a  $g_{13}$  factor of 0.75 which applies when each end of the member is held by two bolts, which is alleged to provide “substantial restraint”. Although RTA timber trusses often have two bolts at each end, these bolts provide resistance to rotation at the ends about the major axis rather than the minor axis, and so this not relevant to this study.

The final consideration is a  $g_{13}$  factor of 0.7 which assumes full restraint at both ends. This full restraint can be provided either by perfectly flat ends bearing on flat unyielding bases, or by other means such as mentioned for the case of Tabulam Bridge above. For RTA timber truss bridges, it is not reasonable to assume perfectly flat ends because even if ends are perfectly flat at the time of construction, these structures are subject to environmental factors which cause deterioration over time so that flat ends will not remain flat for the life of the structure. In addition to this, compression members in RTA timber truss bridges do not bear on flat unyielding bases at both ends. This is because even though a member might bear on a flat unyielding cast iron shoe, this shoe is bearing on timber perpendicular to grain at the top chord and often at the bottom chord also. Therefore, resistance to rotation must be supplied at both ends of a member by other means before a  $g_{13}$  factor of 0.7 could be used.

It should be noted at this point that there is significant inbuilt conservatism in the timber structures code, as there is for other codes. The theoretical value of  $g_{13}$  for a compression member that is fully restrained at both ends is 0.5 as opposed to 0.7 in the code. Similarly, the theoretical value for a compression member that is fully restrained at one end and pinned at the other end is 0.7 as opposed to 0.85 in the code. Theoretically, a compression member fully restrained at both ends has a critical elastic buckling load equal to four times that of the same member pinned at both ends ( $1/0.5^2=4$ ). According to the code, a compression member fully restrained at both ends has a critical elastic buckling load equal to only two times that of the same member pinned at both ends ( $1/0.7^2=2$ ). Therefore, the code value of the critical elastic buckling load is only 50% of the theoretical value. Similarly, for a member fixed at one end and pinned at the other, the code value is only 70% of the theoretical value.

Another detail to note is that the value for the coefficient of slenderness is independent of E:

$$S = \sqrt{\left(\frac{\pi^2}{12}\right)\left(\frac{EA}{N_{cr}}\right)} = \sqrt{\left(\frac{1}{12}\right)\left(\frac{AL_{eff}^2}{I}\right)}$$

Therefore, the only place where the modulus of elasticity comes into the design of slender timber columns is in the material constant ( $\rho_c$ ) which includes an allowance for the ratio of stiffness to compressive strength ( $E/f_c$ ). Although AS 1720.1 gives a value of 16,000 MPa for E, this value is an average value which includes an allowance of about 5% for shear deformation. This average value is used in the calculation of the material constant ( $\rho_c$ ).

In Appendix B, a rough estimate of the lower fifth-percentile values of the modulus of elasticity are given and for F22 timber, the calculated value is 8,000 MPa (50% of the average modulus of elasticity). When the lower fifth-percentile values of the modulus of elasticity are used, the theoretical critical elastic buckling load is only 50% of the value obtained using the average.

It could be argued that the use of an E value higher than the lower bound 5<sup>th</sup> percentile value could be warranted due to the fact that we have two separate flitches carrying the load and so the likelihood of both flitches having a lower than average E value is decreased. However, this is not necessarily the case as the two flitches of a column are often sourced from the same tree to ensure similar strengths, and so the likelihood of two flitches both with very low E values is greater in RTA timber truss bridges than say in a random distribution.

Timber becomes less flexible as it loses moisture. Seasoned timber has a moisture content less than 15%. Unseasoned timber has a moisture content greater than 25%. Extra moisture will make a seasoned timber member more flexible, and the loss of moisture will make an unseasoned member stiffer. The choice of E value has a significant effect on bending as well as compression in the RTA timber truss bridges. A lower modulus of elasticity would significantly decrease the internal bending stresses induced at construction due to the initial curvature, while a higher value would increase these internal bending stresses.

For RTA timber truss bridges, the calculated value of the slenderness coefficient (S) is generally greater than 20, and so the appropriate formula to obtain  $k_{12}$  is as follows:

$$k_{12} = 200 / (\rho_c S)^2$$

For the sake of compatibility, we shall look only at the case of a short term load. This means that the ratio  $r = 1$  and so the material constant ( $\rho_c$ ) = 1.05. To find the nominal capacity of a column under immediate short term loading, the formula in accordance with AS 1720.1 is:

$$\begin{aligned} N &= k_{12} f'_c A_c \\ &= 200 f'_c A_c / (S \rho_c)^2 \\ &= 2400 f'_c I / (1.05 L)^2 \end{aligned}$$

This can then be compared with the theoretical capacity for a slender member which is:

$$N = \pi^2 E I / L^2$$

The theoretical value is therefore different by a factor of  $((1.05\pi)^2 E / 2400 f'_c)$ . For F22 timbers, which are used in RTA timber truss bridges, this equates to 0.86. Therefore, if the AS 1720.1 values for effective length are used in both cases, then the theoretical lower bound 5<sup>th</sup> percentile capacity is approximately 15% less than that given by the code.

All of this may best be illustrated by a worked example. Tabulam Bridge is an early example of a DeBurgh timber truss road bridge. It was constructed over the Clarence River in 1903. It has five timber truss spans of 104 feet (approximately 32m) each. The bridge provides a single lane carriageway with a width between kerbs of approximately 4.6m. The bridge is located at Tabulam which is in the north of the State on the Bruxner Highway between Casino and Tenterfield. This is a significant route for heavy vehicles, and is assessed here for legal loading, which consists of a single 42.5 tonne semi-trailer as illustrated below.

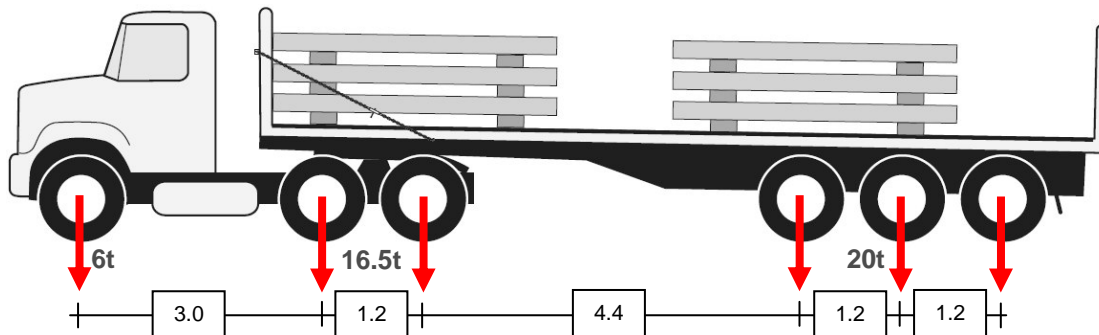


Figure 2.1: NSW Legal Load 42.5 tonne Semi-Trailer

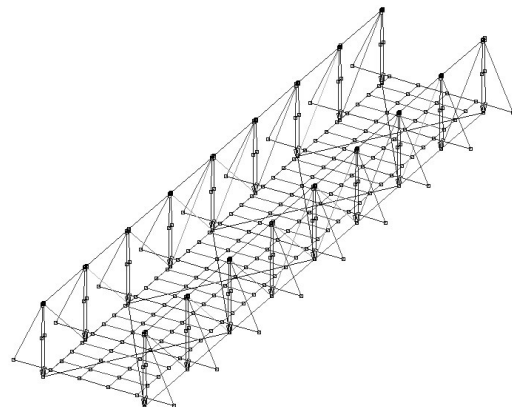


Figure 2.2: Photograph and Microstran Model of Tabulam Bridge – DeBurgh Truss

The critical compression members in a DeBurgh Truss such as Tabulam Bridge are the end verticals, located over the piers. This vertical compression member comprises two timber flitches cut from F22 timber to dimensions 100mm x 300mm. Each flitch is then bent to induce an offset curvature of 25mm at approximately mid height. The length is 3510mm.

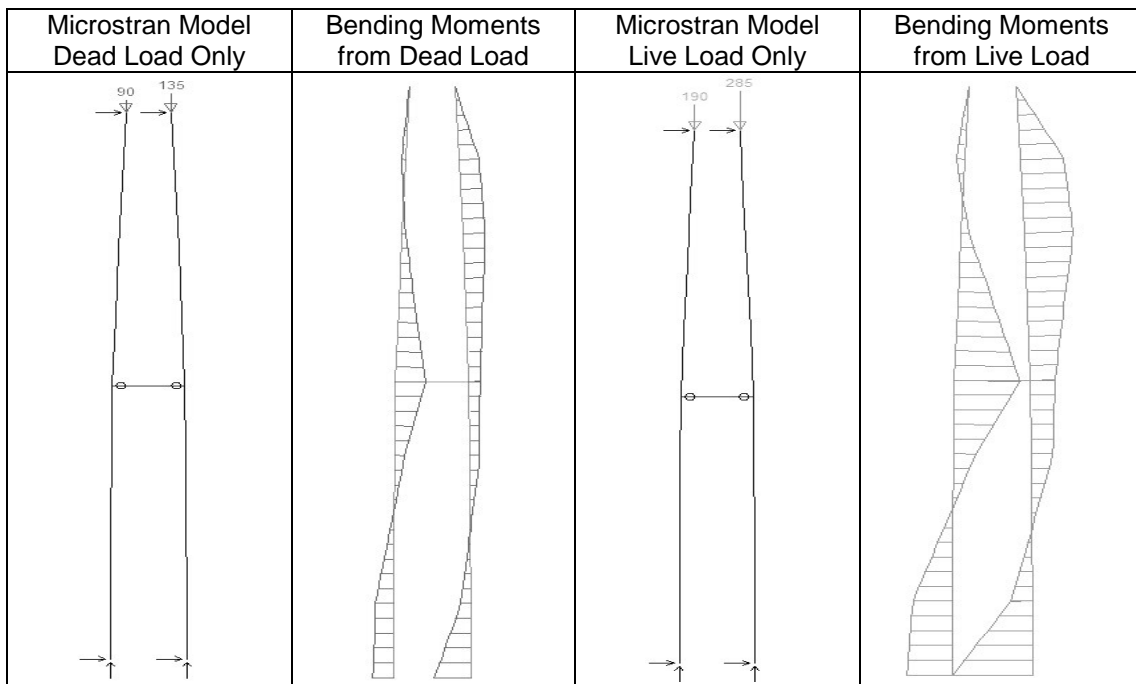
The design compressive forces calculated for this vertical member are as follows:

$$\begin{aligned} N_c^* \text{ (ULS live load)} &= 475\text{kN (LF = 2.0; DLA = 0.2)} \\ N_c^* \text{ (ULS dead load)} &= 225\text{kN (LF = 2.25)} \end{aligned}$$

Compressive forces obtained from the global model shown in Figure 2.2 are transferred to a local model shown in Figure 2.3. In this model, the load distribution between the two flitches is assumed to be 40% / 60%. This is due to the uncertainties in actual behaviour of the two flitches. They are unlikely to be each taking exactly the same loading due to the following:

- Lack of fit - if one is slightly longer than the other the longer will take more load
- Variability in Modulus of Elasticity (E) – the stiffer member will take the greater load
- Out of straightness – if one member has a different curvature to the other, this will affect its stiffness and so more load will be taken by the straighter member
- Global truss behaviour – bending in the top and bottom chord will affect load transfer

For simplicity at this stage, the verticals at Tabulam can be reasonably assumed in their current state to be fixed at the base and pinned at the top, and this is reflected in the model.



The design compressive and bending forces obtained for a single flitch are as follows:

$$\begin{aligned} N_c^* \text{ (ULS dead load)} &= 135 \text{ kN} && \text{(duration: 50+years)} \\ N_c^* \text{ (ULS live load)} &= 285 \text{ kN} && \text{(duration: 5 days)} \\ N_c^* \text{ (ULS dead load + live load)} &= 420 \text{ kN} && \text{(duration: 5 days)} \\ M^* \text{ (fabrication load)} &= 10 \text{ kNm} && \text{(duration: 50+years)} \\ M^* \text{ (secondary effects, dead load)} &= 0.5 \text{ kNm} && \text{(duration: 50+years)} \\ M^* \text{ (total permanent effects)} &= 10.5 \text{ kNm} && \text{(duration: 50+years)} \\ M^* \text{ (secondary effects, live load)} &= 1.0 \text{ kNm} && \text{(duration: 5 days)} \\ M^* \text{ (total permanent load + live load)} &= 11.5 \text{ kNm} && \text{(duration: 5 days)} \end{aligned}$$

Since the modulus of elasticity is a critical consideration in the buckling strength of a slender column, the lower bound 5<sup>th</sup> percentile value of E is used here, and the theoretical nominal capacity of a single flitch in compression (fixed one end, pinned at other) is found by:

$$N = \pi^2 E_{0.05} I / L_{eff}^2 (= \pi^2 \times 8000 \times 300 \times 100^3 / (12 \times (0.7 \times 3510)^2)) = 325 \text{ kN}$$

Now, taking into account the capacity and load duration, the theoretical design capacity is:

$$\begin{aligned} N_{d,c} &= \phi k_1 k_4 k_6 N \\ &= 0.75 \times 0.94 \times 1.0 \times 1.0 \times 325 = 230 \text{ kN (includes no creep allowance)} \end{aligned}$$

The nominal capacity of the same flitch in compression is now calculated using AS 1720.1.

First we can analyse a temporary design action effect alone ( $r = 1$ ):

$$\begin{aligned} \rho_c &= 1.05 \\ N_{cr} &= \pi^2 EI / L_{eff}^2 (= \pi^2 \times 16000 \times 300 \times 100^3 / (12 \times (0.85 \times 3510)^2)) = 443.5 \text{ kN} \\ S &= \sqrt{[(\pi^2 E A) / (12 N_{cr})]} \\ &= \sqrt{[(\pi^2 \times 16000 \times 100 \times 300) / (12 \times 443.5)]} = 29.835 \\ k_{12} &= 200 / (\rho_c S)^2 \\ &= 200 / (1.05 \times 29.835)^2 = 0.20 \\ N &= k_{12} f'_c A_c \\ &= 0.20 \times 42 \times 300 \times 100 = 255 \text{ kN} \end{aligned}$$

Note that this value is less than 80% of the theoretical nominal lower bound solution (325 kN).

We now consider the actual ultimate limit states dead load plus live load combination:

$$\begin{aligned} r &= 285/420 = 0.68 \\ \rho_c &= 1.05 r^{-0.146} \\ &= 1.05 (0.68)^{-0.146} = 1.11 \\ S &= 29.835 \\ k_{12} &= 200 / (\rho_c S)^2 \\ &= 200 / (1.11 \times 29.835)^2 = 0.18 \\ N &= k_{12} f'_c A_c \\ &= 0.18 \times 42 \times 300 \times 100 = 230 \text{ kN} \end{aligned}$$

Now, taking into account the capacity and load duration, the capacity using AS 1720.1 is:

$$\begin{aligned} N_{d,c} &= \phi k_1 k_4 k_6 k_{12} f'_c A_c \\ &= 0.75 \times 0.94 \times 1.0 \times 1.0 \times 230 = 160 \text{ kN} \end{aligned}$$

Therefore capacity obtained from the code is less than 70% of the theoretical solution.

Similarly, we can consider the actual ultimate limit states of dead load only:

$$\begin{aligned} \rho_c &= 1.28 \\ S &= 29.835 \\ k_{12} &= 200 / (\rho_c S)^2 \\ &= 200 / (1.28 \times 29.835)^2 = 0.137 \\ N &= k_{12} f'_c A_c \\ &= 0.137 \times 42 \times 300 \times 100 = 175 \text{ kN} \end{aligned}$$

Now, taking into account the capacity and load duration, the capacity using AS 1720.1 is:

$$\begin{aligned} N_{d,c} &= \phi k_1 k_4 k_6 k_{12} f'_c A_c \\ &= 0.75 \times 0.57 \times 1.0 \times 1.0 \times 175 = 75 \text{ kN} \end{aligned}$$

Therefore capacity obtained from the code is approximately 30% of the theoretical solution.

A critical issue that does not appear to be clarified in AS 1720.1 is whether or not it is actually appropriate to use the duration of load modification factor  $k_1$  for slender columns at all.

As noted in the Timber Design Handbook, the duration of load factor models the progressive microscopic damage to wood fibres that occurs as they stretch and move relative to one another under continued loading. This damage aggregates over long periods of loading and eventually reduces the strength of the timber. Wood cells are very small, spirally wound tubes held together with lignin. Under loading, the fibres stretch, some more than others. If one cell breaks, it releases its load to those nearby. Over a long period of loading, quite a few fibres may break. This can substantially increase the stress level in the remaining fibres. Eventually, under prolonged loading, the load carrying capacity of the section is reduced.

Duration of load for the strength limit state models microscopic damage that is not recoverable, so it accumulates throughout the life of the structural element. The duration of load factor allows for the accumulation of all peak load events over the life of the structure.

Now, for slender columns, it is not the material strength that governs, but the material stiffness (modulus of elasticity). Although a very minor and almost imperceptible shortening would occur under compressive loads, there is no significant deflection until elastic buckling occurs. It is therefore possible that the results obtained using AS 1720.1 are excessively conservative especially when the permanent design actions are under consideration.

Although our column appears to have already failed both short term and long term ultimate limit states in compression, we must now turn our attention to the bending capacity.

Once again, we find that the modulus of elasticity is a critical consideration in determining the design bending moment in a single flitch due to the 25mm curvature put into each member.

The mid-span deflection of a simply supported beam under a central point load is:

$$\delta = \frac{WL^3}{48EI}$$

This can be re-arranged to find the point load required to induce the desired deflection:

$$W = \frac{48EI\delta}{L^3}$$

We also know that the maximum bending moment due to a centrally located point load is:

$$M = \frac{WL}{4}$$

Combining the above equations, we obtain the design action effect in bending is as follows:

$$M^* = \frac{12EI\delta}{L^2}$$

Assuming average E, the bending moment due to the 25mm curvature at midpoint is:

$$M^* = 12 \times 16,000 \times (300 \times 100^3/12) \times 25 / 3510^2 = 9.74 \text{ kNm}$$

However if the lower bound 5<sup>th</sup> percentile value of E is used, then the bending moment is:

$$M^* = 12 \times 8,000 \times (300 \times 100^3/12) \times 25 / 3510^2 = 4.87 \text{ kNm}$$

Presumably, if the upper bound 5<sup>th</sup> percentile value of E was used, it would be:

$$M^* = 12 \times 24,000 \times (300 \times 100^3/12) \times 25 / 3510^2 = 14.61 \text{ kNm}$$

These can now be compared with the design capacity obtained from AS 1720.1:

$$\begin{aligned} M_d &= \phi k_1 k_4 k_6 k_9 k_{12} f'_b Z \\ &= 0.75 \times 0.57 \times 1.0 \times 1.0 \times 1.0 \times 55 \times 300 \times 100^2 / 6 = 11.75 \text{ kNm} \end{aligned}$$



From this simple analysis, it would seem that our columns may be overloaded due to lack of bending capacity alone, even before we combine bending with compression. However, there are two issues worth further consideration before these members are confirmed inadequate.

Firstly, there is the possibility of initial out of straightness. Timbers used in RTA trusses are generally visually graded to AS 2082.<sup>42</sup> According to Table C1 of this standard, the maximum permissible bow in a 100mm thick piece of sawn timber of 3.6m length is 20mm. If the timber already has a bow, then less force is required in order to increase the bow to 25mm. If the initial bow is 20mm, the required force is 20% of that required for an initially straight member. Therefore, depending upon initial straightness, the actual bending moment for the flitches in question will be somewhere between 20% and 100% of the calculated value.

Possibly a more important consideration is creep in the timber. As noted in the Timber Design Handbook, creep in a member subject to bending occurs due to the inelastic shortening of cells on the compression side of the member. The sum of these microscopic movements can contribute to substantial movement in the member. AS 1720 includes allowances for the increase in deflection with load duration with a duration factor  $j_2$ .

The Timber Design Handbook distinguishes between two primary types of creep:

- Recoverable creep is time-dependent deflection that upon release of the load will be fully recovered. It is associated with the squashing of the timber fibres. As the fibres squash, the crystalline structure of the fibres is rearranged. Movement of moisture through the fibres lubricates them allowing the easier rearrangement in response to the stresses. The squashing of cell walls may also release some moisture over time and allow a reduction in the volume of the cell wall causing further strain.
- Irrecoverable creep is time-dependent deflection that is not recovered when the load is released. There is microscopic damage to the fibre structure so that the load paths change and there is no stress on the structure to encourage it to return to its former configuration. This type of creep is also accelerated by moisture movements.

The assumptions behind AS 1720.1 which give the values of  $j_2$  given are most appropriate for a uniform moisture environment. Where there is wetting and drying of the timber such as in RTA timber bridges, then the creep deformations can be more than twice those given.

Closely related to creep is relaxation. Whereas creep involves an increase in strain under constant stress, relaxation is the decrease in stress experienced over a period of time by a material subjected to a constant strain. Although AS 1720 includes provisions for creep for serviceability calculations, it does not provide any guidance for the positive effect that creep may have on the internal bending stresses in columns that are constrained to a constant curvature. AS 1720 gives a multiplier by which the deflection can be increased over time while the bending moment remains unchanged. However, it does not give any guidance as to how much the bending moment might decrease over time if the deflection is kept constant.

For example, in our vertical member on Tabulam Bridge, a point load is applied by means of inserting a timber spacer at mid span to induce a 25 mm deflection in each flitch. This curvature is generally applied when the timber is partially seasoned, so we could reasonably assume a 20% moisture content. We would expect, if this load remained constant and the member was free to deflect further, that the deflection would increase to approximately 2.5 times the initial deflection over the first year ( $j_2 = 2.5$  from Table 2.4, therefore deflection at one year equals 62.5 mm). Further considering that the timber is exposed to constant cycles of wetting and drying, we might expect an even greater deflection due to creep.

However, instead of having a constant load, we have a fixed deflection. It is reasonable to assume that inelastic shortening of cells on the compression side of the member will still occur, along with movement of moisture through the fibres lubricating them and allowing the redistribution of stresses. However, we are without guidelines to calculate the load reduction.

---

<sup>42</sup> AS 2082-2007 Timber – Hardwood – Visually stress-graded for structural purposes

A possible approach, however, may be as follows:

We know the mid-span deflection of a simply supported beam under a central point load is:

$$\delta = \frac{WL^3}{48EI}$$

If we assume as a conservative estimate that the deflection might increase by 50% in one year (the code seems to indicate a possible increase in deflection of 500% in a year), then we would have to reduce the modulus of elasticity by about 30% to maintain equilibrium. We know that the load, the length, the depth and the width remain constant, so the modulus of elasticity is the only parameter in the above equation which is subject to change with time.

We know that the initial central point load required to induce a desired mid-span deflection is:

$$W = \frac{48EI\delta}{L^3}$$

For Tabulam Bridge, assuming an average Modulus of Elasticity, the load can be found:

$$W_{\text{initial}} = 48 \times 16,000 \times (300 \times 100^3/12) \times 25 / 3510^3 = 11.1\text{kN}$$

Now, if we assume again that the modulus of elasticity reduces with time, we can recalculate:

$$W_{\text{1year}} = 48 \times 2/3 \times 16,000 \times (300 \times 100^3/12) \times 25 / 3510^3 = 7.4\text{kN}$$

We also know that the maximum bending moment due to a centrally located point load is:

$$M = \frac{WL}{4}$$

And so we can see that a 50% increase in deflection is equivalent to a 1/3 decrease in E, which causes a 1/3 decrease in W and also a 1/3 decrease in M\* over the period of one year. We would expect half of this to occur in the first 20 days (ie. 1/6 decrease in W and M\*).

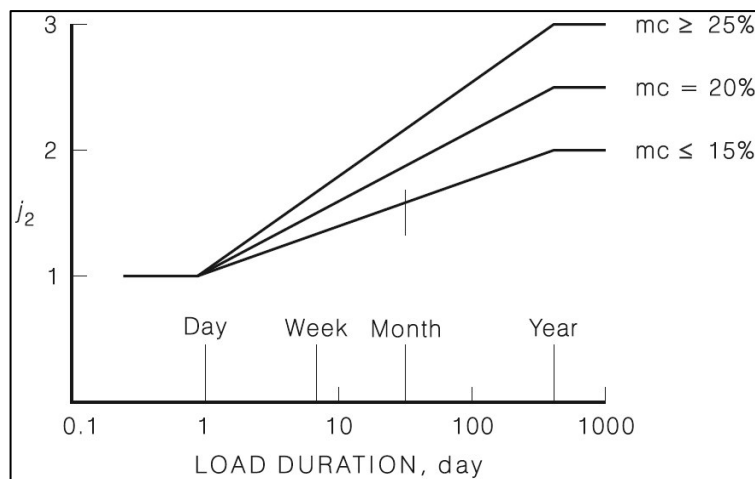


Figure 2.3: AS1720.1 Bending and Compression Deformations

Considering the fact that the timbers used in bridges are often bent to shape in the early stages of seasoning ( $mc > 25\%$ ), and then are subjected to outdoor conditions with large variations in temperature and moisture, a  $j_2$  factor of 0.5 may be overly conservative.

An upper bound case may be to assume a deflection of 300%, which would then give a decrease in modulus of elasticity of 2/3, and so the design bending stresses after a year would only be 1/3 of the initial stresses (ie. 2/3 decrease in W and M\* after one year).

It is clear that considerable benefits could be gained from further investigation of the effects of stress relaxation due to creep effects in RTA timber bridges. If the design bending moments could be reduced, the design capacity remaining for compression is thereby increased.

Another closely related subject is the duration of load factor which models the progressive microscopic damage to wood fibres that occurs as they stretch and move relative to one another under continued loading, eventually reducing the strength of the timber.

At low stress levels, wood can be considered as a linear, viscoelastic material.<sup>43</sup> In such cases, the creep deformation under sustained loading can be divided into two stages: a primary stage where the creep rate decreases; and a secondary stage where the creep rate is nearly constant. At higher stress levels, in addition to the primary and secondary stages, a tertiary stage, where the creep rate increases, will occur and lead to eventual creep-rupture.

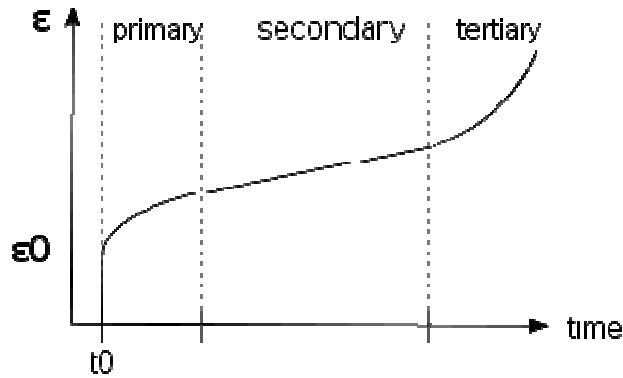


Figure 2.4: Typical Creep Curve

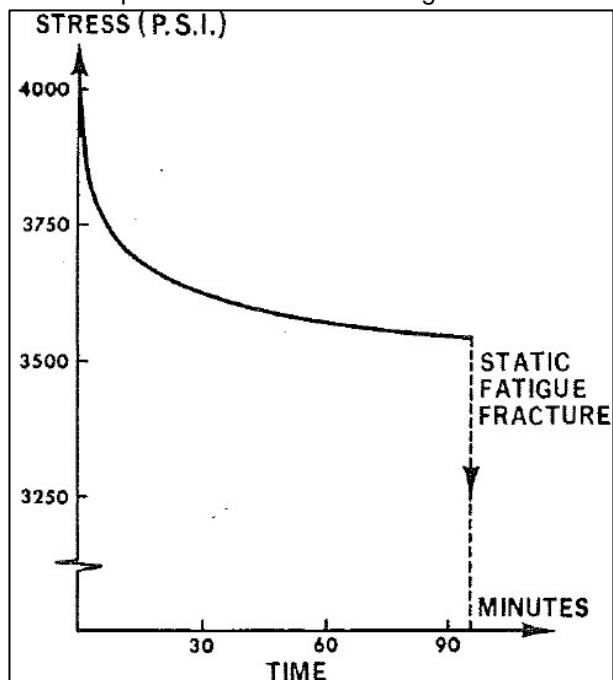
The load duration factor ( $k_1$ ) is a factor that aims to ensure that the member being designed does not proceed into the tertiary stage of creep, thereby avoiding eventual creep-rupture.

Creep failure of timber under gravity loads is a well-known phenomenon that has received considerable attention in the literature. However, failure under constant strain has received very limited attention, and the only relevant experimentation investigating this phenomenon is a single study conducted by the Forest Products Laboratory in Vancouver reported in 1967.<sup>44</sup>

In this study, Bach conducted stress-relaxation experiments on 40 woody tissue specimens at relatively high constantly kept tensile strain. The specimens were 0.1 x 2.5 x 80mm in dimensions, their moisture content was 8% and temperature was 22°C. The grain orientation of specimens was parallel to the longitudinal axis of each piece, and the specimens were strained to 90% of the estimated ultimate strain, and then that strain was kept constant.

There are two things to note from Bach's study. Firstly, his study confirms that stress does actually decrease with time when strain is kept constant. Secondly, Bach observed failure in more than half of the stress-relaxing specimens in less than 1000 minutes.

However, Bach himself noted that this study was exploratory, and that further work is required in order to determine the influence of various strain levels, climatic conditions and wood characteristics. Unfortunately, there is no record of any such work being done.



<sup>43</sup> Encyclopedia of Materials: Science and Technology ISBN: 0-08-0431526 pp. 9616-9620

<sup>44</sup> Lars Bach, 1967, "Static Fatigue of Wood Under Constant Strain", Forest Products Laboratory, Vancouver, British Columbia, Information Report VP-X-24

Possibly the reason for no further work being conducted in this area is that constant strain is less common in real engineering applications for timber structures than various gravity loads (constant loads, ramp loads, cyclic loads, intermittent loads) which have received all the attention in the laboratories. However, in RTA bridges, it is this constant strain that proves to be a critical factor in the theoretical load carrying capacity of the timber spaced columns.

The  $k_1$  factor of 0.57 for permanent effects is there to protect against tertiary creep which leads to creep rupture. Perhaps a different factor would be more suitable to guard against relaxation-rupture. Bach's experiment shows that relaxation-rupture is a possibility, but the testing that he did is vastly dissimilar to the situation encountered in RTA timber truss bridges:

	Forest Products Laboratory	RTA Timber Truss Bridges
<b>Size of Sample</b>	0.1 x 2.5 x 80 mm	Approx 100 x 300 x 3500 mm
<b>Type of Loading</b>	Constant Strain - Tension	Constant Strain - Bending
<b>Load Intensity</b>	Approx 90% of ultimate	Approx 35% of ultimate
<b>Temperature</b>	Constant 22°C	Variable – outdoor climate
<b>Moisture Content</b>	Constant 8%	Variable – outdoor climate
<b>Timber Species</b>	Douglas Fir & Norway Spruce	Eucalypt & Corymbia species
<b>Wood Characteristics</b>	Clear samples of woody tissue	Large section timbers

Perhaps it is appropriate for design bending moment after one year to be written:

$$M^* = \Phi_{relaxation} \frac{12EI\delta}{L^2}$$

where appropriate values for  $\Phi_{relaxation}$  may be in the range of 0.35 to 0.65.

Similarly, it might be appropriate for the design bending capacity to be written:

$$M_d = \phi k_{relaxation} k_4 k_6 k_9 k_{12} f'_b Z$$

where appropriate values for  $k_{relaxation}$  may be in the range of 0.57 to 0.80.

We can now revisit our primary formula:

$$\left( \frac{M^*_y}{M_{d,y}} \right) + \left( \frac{N^*_c}{N_{d,cy}} \right) \leq 1.0$$

We can see that if we were to reduce  $M^*_y$  by 35-65% and / or increase  $M_{d,y}$  by up to 23% then the value of  $(M^*_y / M_{d,y})$  would decrease significantly, thereby allowing higher design loads in compression. For example, if we apply these new formulas to Tabulam Bridge we get:

For Permanent Effects (Dead Loads):

	CODE VALUE	LOWER BOUND	UPPER BOUND
$M^*_y$	$12 \times 16000 \times 25 \times 10^6 \times 25 / 3510^2$ =9.74 kNm	$0.65 \times 12 \times 16000 \times 25 \times 10^6 \times 25 / 3510^2$ =6.33 kNm	$0.35 \times 12 \times 16000 \times 25 \times 10^6 \times 25 / 3510^2$ =3.41 kNm
$M_d$	$0.75 \times 0.57 \times 55 \times 0.5 \times 10^6$ =11.75 kNm	$0.75 \times 0.57 \times 55 \times 0.5 \times 10^6$ =11.75 kNm	$0.75 \times 0.80 \times 55 \times 0.5 \times 10^6$ =16.50 kNm
$M^*/M_d$	$(9.74/11.75) = 0.83$	$(6.33/11.75) = 0.53$	$(3.41/16.50) = 0.21$
Result	17% remains for axial	47% remains for axial	79% remains for axial

For Permanent Loads plus Live Loads (vehicles):

	CODE VALUE	LOWER BOUND	UPPER BOUND
$M^*_y$	$12 \times 16000 \times 25 \times 10^6 \times 25 / 3510^2$ =9.74 kNm	$0.65 \times 12 \times 16000 \times 25 \times 10^6 \times 25 / 3510^2$ =6.33 kNm	$0.35 \times 12 \times 16000 \times 25 \times 10^6 \times 25 / 3510^2$ =3.41 kNm
$M_d$	$0.75 \times 0.94 \times 55 \times 0.5 \times 10^6$ =19.39 kNm	$0.75 \times 0.94 \times 55 \times 0.5 \times 10^6$ =19.39 kNm	$0.75 \times 0.94 \times 55 \times 0.5 \times 10^6$ =19.39 kNm
$M^*/M_d$	$(9.74/19.39) = 0.50$	$(6.33/19.39) = 0.33$	$(3.41/19.39) = 0.18$
Result	50% remains for axial	67% remains for axial	82% remains for axial

SUMMARY OF RESULTS FOR A NON-COMPOSITE COLUMN:

Results from the analysis of the end verticals at Tabulam assuming non-composite behaviour strictly in accordance with AS 1720.1 can be summarised as follows:

$$\left( \frac{M^*_{y}}{M_{d,y}} \right) + \left( \frac{N^*_{c}}{N_{d,cy}} \right) \leq 1.0$$

For ultimate limit states dead load plus live load:

$$\begin{aligned} M^* &= 11.5 \text{ kNm} \\ M_d &= \phi k_1 k_4 k_6 k_9 k_{12} f'_b Z \\ &= 0.75 \times 0.94 \times 1.0 \times 1.0 \times 1.0 \times 55 \times 300 \times 100^2/6 = 19.4 \text{ kNm} \\ N^*_c &= 420 \text{ kN} \\ N_{d,c} &= \phi k_1 k_4 k_6 k_{12} f'_c A_c \\ &= 0.75 \times 0.94 \times 1.0 \times 1.0 \times 0.18 \times 42 \times 300 \times 100 = 160 \text{ kN} \end{aligned}$$

Therefore,  $(M^*/M_d) + (N^*/N_d) = (11.5/19.4) + (420/160) = 3.2 > 1.0$  therefore, FAIL!

For ultimate limit states permanent effects only:

$$\begin{aligned} M^* &= 10.5 \text{ kNm} \\ M_d &= \phi k_1 k_4 k_6 k_9 k_{12} f'_b Z \\ &= 0.75 \times 0.57 \times 1.0 \times 1.0 \times 1.0 \times 55 \times 300 \times 100^2/6 = 11.8 \text{ kNm} \\ N^*_c &= 135 \text{ kN} \\ N_{d,c} &= \phi k_1 k_4 k_6 k_{12} f'_c A_c \\ &= 0.75 \times 0.57 \times 1.0 \times 1.0 \times 0.14 \times 42 \times 300 \times 100 = 75 \text{ kN} \end{aligned}$$

Therefore,  $(M^*/M_d) + (N^*/N_d) = (10.5/11.8) + (135/75) = 2.7 > 1.0$  therefore, FAIL!

As noted previously, the following factors are worth further consideration:

- Use of theoretical buckling capacity with lower bound 5<sup>th</sup> percentile value of E but effective lengths as given in AS 1720.1 will yield compressive capacities as follows:
  - approximately 15% less than AS 1720.1 for  $r = 1$  (short term load alone)
  - approximately equal for  $r = 0.625$  (such as for Tabulam Bridge verticals)
  - approximately 28% greater than AS 1720.1 for  $r = 0$  (permanent effects)
- The theoretical buckling capacity is directly proportional to E, so if E was known more accurately for RTA truss timbers, then perhaps a value greater than half of the average E given in the code could be used, and capacity would increase accordingly.
- Use of theoretical buckling capacity with theoretical effective length rather than code recommendations will yield a compressive capacity approximately 40% greater.
- Disregarding the  $k_1$  factor for slender columns in compression would increase the compressive capacity by up to 75% for permanent effects.
- Inclusion of creep effects in bending would lower the design bending moment by an unknown amount, possibly up to 50%, but testing is required to confirm.
- Use of upper bound 5<sup>th</sup> percentile value of the modulus of elasticity to calculate the design bending moment may increase design bending moment by 50%.

It is clear from all this that without some level of composite action between the two flitches of a compression member, these members would be unable to reliably carry today's legal loads.

**ANALYSIS IN ACCORDANCE WITH AS 1720.1 FOR A SPACED COLUMN:**

Although the compression members in the RTA's timber truss bridges clearly do not meet the requirements in AS 1720.1 for spaced columns, the formulas in Appendix E are a good place to start when we try to consider the extent to which the RTA columns may behave compositely, and how capacity may be reasonably increased by this composite action.

**E4.2.4 Spacing of intermediate packing pieces:** *The centre-to-centre distance between packing pieces shall not exceed the least of the following:*

- (a) *One-third of the distance between centres of the end packing pieces.*
- (b) *Thirty times the thickness of the thinnest shaft.*
- (c) *The value such that the slenderness coefficient of the portion of an individual shaft between any pair of packing pieces is not greater than 0.7 times the maximum slenderness coefficient of the whole column.*

**E4.2.5 Distance between shafts:** *The clear space between individual shafts shall not exceed 3 times the thickness of the thinnest shaft measured in the same plane.*

**E4.3.1 Design shear force:** *The connections between the packing pieces of spaced columns shall be designed to transmit the stresses resulting from the design action effect produced by strength limit states design loads in lateral shear:*

$$\begin{aligned}
 V^* &= V_1^* + V_2^* \\
 V_1^* &= \text{shear action effect produced by strength limit states design loads} \\
 V_2^* &= \text{shear action effect due to curvature of the column} \\
 &= 0.075 N^* \text{ for end packing pieces} \\
 &= 0.001 N^* (L_{ay}/d) \text{ for intermediate packing pieces} \\
 N^* &= \text{design action effect in axial compression} \\
 L_{ay} &= \text{distance between points of lateral restraint on the spaced columns.} \\
 d &= a + 2 t_s \text{ (} a = \text{distance between shafts; } t_s = \text{shaft thickness)}
 \end{aligned}$$

**E4.3.2 Force effects on packing pieces:** *The interface of each packing piece and its connection shall be designed to transmit a shear force  $V_{pack}^*$  equal to:*

$$\begin{aligned}
 V_{pack}^* &= V^* L_s/a \\
 V^* &= \text{resulting lateral force as defined above} \\
 L_s &= \text{the centre-to-centre distance of packing pieces} \\
 a &= \text{distance between shafts}
 \end{aligned}$$

**E4.4.1.1 Slenderness coefficients of individual shafts:** *The effective length ( $L_s$ ) of individual shafts of spaced columns shall be taken as the distance measured along the column axis between centroids of the fastener groups in adjacent packing pieces.*

**E4.4.1.2 Slenderness coefficient of composite cross-sections:** *For spaced columns with packing pieces, composed of two shafts of timber, the slenderness coefficient for bending about the y-axis ( $S_5$ ) is given by the following equation:*

$$\begin{aligned}
 S_5 &= 0.3 g_{13} g_{28} L (A / I)^{1/2} \\
 g_{13} &= \text{effective length factor as per simple column design} \\
 g_{28} &= \text{modification factor for the effective length of spaced columns} \\
 L &= \text{length of composite column} \\
 A &= \text{net cross-sectional area of the shafts} \\
 I &= \text{second moment of area of the composite section about the y-axis}
 \end{aligned}$$

**E4.4.2 Design procedure:** *The design capacity shall be taken as the least of:*

- (a) *the design capacity for a solid column whose area is that of the sum of the cross sectional areas of the shafts, bending about the x-axis;*
- (b) *the design capacity for a column bending about the y-axis, whose geometrical properties of cross-section are those of the composite column, but whose slenderness coefficient is as given above; and*
- (c) *the sum of the design capacity for the individual shafts where the design capacity for each shaft is equal to that for a solid column, the effective length of which is equal to the values of  $L_s$  defined above.*

Again, we shall examine the implications of requirements of AS 1720.1 for Tabulam Bridge.



Firstly, there are requirements regarding the spacing of intermediate packing pieces. In Tabulam Bridge, the centre to centre distance between packing pieces exceeds one third the distance between centres of the end packing pieces, as there is only one intermediate packer. The value of the slenderness coefficients are as follows:

$$\begin{aligned} S_{(\text{single})} &= L/d = 1660 / 100 = 16.6 \\ 0.7S_5 &= 0.7 \times 0.3 g_{13} g_{28} L (A/I)^{1/2} \\ &= 0.21 \times 0.85 \times 2.7 \times 3510 (60,000 / 1311.5 \times 10^6)^{1/2} = 11.4 \end{aligned}$$

Therefore, the slenderness coefficient of the individual shaft is greater than 0.7 times the slenderness coefficient of the whole column. Therefore, the spaced column at Tabulam twice fails the criteria for spacing of intermediate packing pieces.

Next, the design shear force for the packing piece connections must be calculated:

$$\begin{aligned} V^* &= V_1^* + V_2^* \\ V_1^* &= \text{shear action effect} = 0 \\ V_2^* &= 0.075 N^* \text{ for end packing pieces} \\ &= 0.075 \times 700 = 52.5 \text{ kN} \\ &= 0.001 N^* (L_{ay}/d) \text{ for intermediate packing pieces} \\ &= 0.001 \times 700 \times (3510 / 390) = 6.3 \text{ kN} \end{aligned}$$

Therefore, the design shear force for each packing piece and its connection can be found:

$$\begin{aligned} V_{\text{pack}}^* &= V^* L_s/a \\ &= 52.5 \times 1660/190 = 460 \text{ kN (at end packers)} \\ &= 6.3 \times 1660/190 = 55 \text{ kN (at intermediate packers)} \end{aligned}$$

Clearly, a shear capacity of 460 kN at end packers is not achieved with current connections.

Despite failing the criteria for spaced columns, the design capacity that could be achieved if the columns were assessed as spaced columns according to AS 1720.1 is the least of:

#### CASE 1

$$\begin{aligned} S &= g_{13}L/d = 0.85 \times 3510 / 300 = 9.945 \\ \rho_c &= 1.05 r^{-0.146} = 1.05 (0.68)^{-0.146} = 1.11 \\ K_{12} &= 1.5 - 0.05 \rho_c S = 1.5 - 0.05 (1.11 \times 9.945) = 0.948 \\ N_{(\text{case1})} &= \phi k_1 k_4 k_6 k_{12} f'_c A_c \\ &= 0.75 \times 0.94 \times 1.0 \times 1.0 \times 0.948 \times 42 \times 60,000 = 1685 \text{ kN} \end{aligned}$$

#### CASE 2

$$\begin{aligned} S_5 &= 0.3 g_{13} g_{28} L (A/I)^{1/2} \\ &= 0.3 \times 0.85 \times 2.7 \times 3510 (60,000 / 1311.5 \times 10^6)^{1/2} = 16.3 \\ \rho_c &= 1.05 r^{-0.146} = 1.05 (0.68)^{-0.146} = 1.11 \\ K_{12} &= 1.5 - 0.05 \rho_c S = 1.5 - 0.05 (1.11 \times 16.3) = 0.59 \\ N_{(\text{case2})} &= \phi k_1 k_4 k_6 k_{12} f'_c A_c \\ &= 0.75 \times 0.94 \times 1.0 \times 1.0 \times 0.59 \times 42 \times 60,000 = 1048 \text{ kN} \end{aligned}$$

#### CASE 3

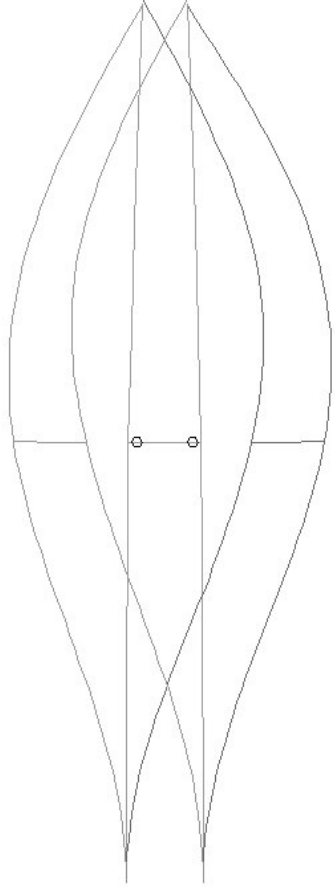
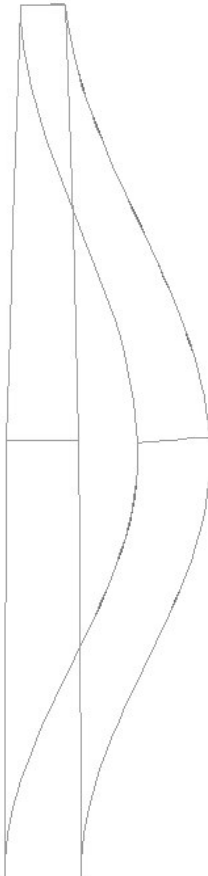
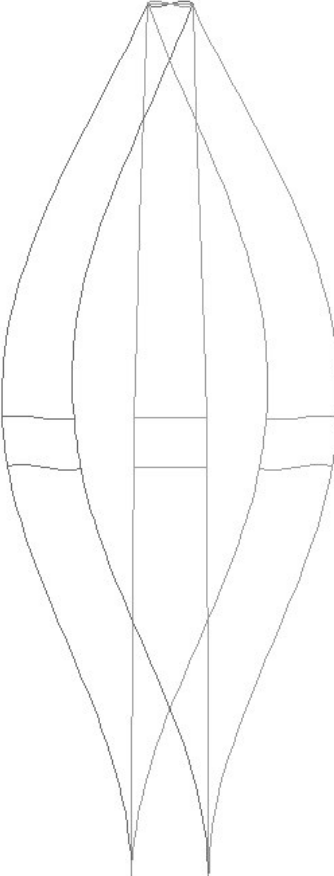
$$\begin{aligned} S &= L/d = 1660 / 100 = 16.6 \\ \rho_c &= 1.05 r^{-0.146} = 1.05 (0.68)^{-0.146} = 1.11 \\ K_{12} &= 1.5 - 0.05 \rho_c S = 1.5 - 0.05 (1.11 \times 16.6) = 0.58 \\ N_{(\text{case3})} &= \phi k_1 k_4 k_6 k_{12} f'_c A_c \\ &= 2 \times 0.75 \times 0.94 \times 1.0 \times 1.0 \times 0.58 \times 42 \times 30,000 = 1030 \text{ kN} \end{aligned}$$

Therefore, the compression capacity (using section properties at mid-height) assuming spaced column behaviour is 1030 kN, which is equivalent to 515 kN per flitch, which is 3.2 times the capacity obtained for an individual flitch behaving non-compositely.

However, to this point we have obviously overlooked some important aspects:

- Flitches are not parallel, so section properties change along the length of the column
- Loads are not necessarily equally distributed to the two flitches
- There are not enough spacers to ensure that flitches deflect together
- Bending stresses due to fabrication and secondary effects need to be considered
- End connections are woefully inadequate, both due to the fact that there are not enough bolts, and then also due to the fact that the bolts are already loaded heavily in tension, and so there will not be a tight interface between the flitch and the spacer at the top and bottom of the column. In addition to the tension in the bolts, the end spacer are difficult to keep tight due to the ends of the flitches bearing on a steel shoe where the friction would need to be overcome in order to tighten the bolts.

We can now do some sensitivity analysis in Microstran using different assumptions. The relevant analysis to perform is an elastic critical load analysis using the lower bound 5<sup>th</sup> percentile modulus of elasticity for the timber ( $E = 8,000 \text{ MPa}$ ). Microstran then provides the critical buckling mode shape as well as the critical buckling load for the system. Two cases were investigated, one where flitches were loaded equally (50 kN to each flitch), and another where flitches were loaded unequally (40 kN to one and 60 kN to the other). Interestingly, the distribution of loads did not significantly affect the total critical buckling load of the system.

Non-composite behaviour (confirms theoretical result) <b>LOWER BOUND SOLUTION</b> Critical Buckling Load: 650 (325 kN per flitch)	Fully fixed timber spacers top and centre (assumes no slip) <b>UPPER BOUND SOLUTION</b> Critical Buckling Load: 1330 (665 kN per flitch)	Ignore spacers and assume fully fixed steel bolts (2/22mm @ top; 4 @ centre): Critical Buckling Load: 960 (480 kN per flitch)
		
The design capacity for this assumption would be: $N_{d,c} = \phi N = 485 \text{ kN}$	The design capacity for this assumption would be: $N_{d,c} = \phi N = 995 \text{ kN}$	The design capacity for this assumption would be: $N_{d,c} = \phi N = 720 \text{ kN}$



# CHAPTER THREE

## EXPERIMENTATION

### PURPOSE OF EXPERIMENTAL INVESTIGATION:

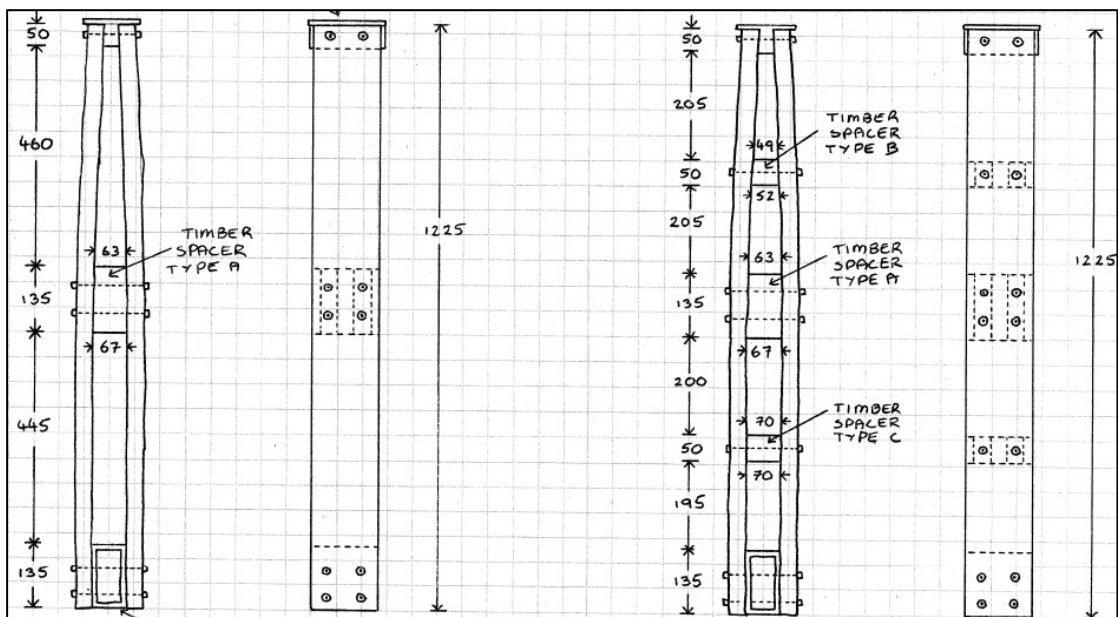
A number of aspects of the behaviour of RTA spaced columns will be tested:

- **Buckling Mode:** A third size scale model of a typical DeBurgh truss vertical will be tested to failure in order to observe the mode of failure and the ultimate capacity. Properties of the timbers used in the scale model will also be tested.
- **Bridge Timber Properties:** Timbers from an existing truss bridge will be tested to determine the density and modulus of elasticity of timbers in RTA timber trusses.
- **Creep Effects:** Tests will be conducted to determine the extent of stress relieving of the bending stresses induced in timber compression members during fabrication.
- **Spacer Capacity:** The shear capacity of the bolt and spacer combination common in RTA timber truss compression members will be investigated to inform the model for members not tested directly – both loose and tight bolts will be investigated.

### METHOD AND RESULTS OF EXPERIMENTAL INVESTIGATION:

#### BUCKLING MODE:

The column assemblies for the experimental investigation were fabricated from two 140 x 35 mm pieces of F22 kiln dried timber 1,225mm long to represent a third scale model of a typical compression strut found in a DeBurgh truss. A fabricated steel shoe was provided at the top of the column assembly, and a fabricated steel box was provided at the base to represent a steel cross girder. The two flitches were bent to shape, thereby providing an 8.5mm offset from straight at the centre. Two lengths of 8mm threaded rod were provided at the top shoe, and four at the base. A pinned connection was provided at the top, while the base was supported on the flat floor of the testing rig. Five assemblies had only a central timber packer bolted with four lengths of 8mm threaded rod with 40 x 40 x 3 mm washers, while another five assemblies had two additional packers with two lengths of threaded rod used to attach each.



A separate investigation was undertaken to determine the shear capacity and behaviour of the spacer and bolt configurations. This is because there were at least three possible options to represent a third scale model of the existing 22mm bolts. The options were as follows:

- If bending stiffness of the bolt is critical, 17mm bolts are appropriate ( $I = \pi d^4/64$ ).
- If shear strength of the bolt is critical, 13mm bolts are appropriate ( $A = \pi r^2$ ).
- If bearing area on the timber edge is critical, 8mm bolts are appropriate.

Prior to fabrication, the individual flitches were tested in bending about both the major and minor axes. The modulus of elasticity in bending was determined from a simply supported four point beam test configuration as outlined in AS/NZS 4063.1-2010.

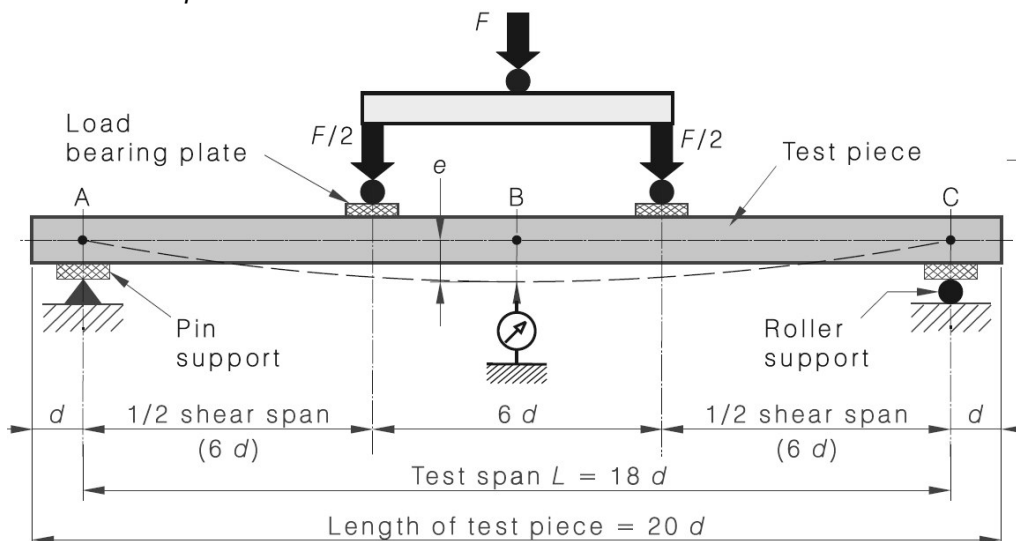
The requirements of AS/NZS 4063.1-2010 are summarised as follows:

**2.4.1 General:** *The over-all length of a test piece shall be 20 d and the length of the test span, L, shall be 18 d between the reactions on which the test piece is supported. The total load, F, shall be applied equally at the third points of the test span. A test piece shall be adequately restrained to prevent lateral buckling during loading.*

**2.4.2 Apparent modulus of elasticity in bending:** *The apparent modulus of elasticity in bending, E, shall be determined from the measurement of the vertical displacement, e, of point B on the centreline at mid-span relative to the points A and C on the centreline at the end supports of the test piece. A load, F, shall be applied to a test piece at a uniform rate of loading. The apparent modulus of elasticity in bending, E, of a test piece shall be calculated from the following equation:*

$$E = \frac{23}{108} \left( \frac{L}{d} \right)^3 \left( \frac{\Delta F}{\Delta e} \right) \frac{1}{b}$$

*The linear portion of the load-deformation line shall be used to determine  $\Delta F/\Delta e$ .*



In addition to testing the modulus of elasticity, the actual compressive strength of the timbers was tested so that the ultimate capacities could be compared with code design capacities. The 140x35mm lengths of F22 timber have previously been used to make a Stress Laminated Timber (SLT) deck, and so they had a number of  $\phi 35$ mm holes in them. Although these holes are unlikely to have a significant impact on the bending strength or stiffness of the timbers, they are likely to have a significant impact on the compressive strength of the timber. Therefore, care was taken to test some lengths with holes and some without in compression.

Flitches were paired up matching the modulus of elasticity about the minor axis of each flitch as closely as possible. For the purposes of fabrication and inducing appropriate curvature in the members, it is critical that the two flitches are closely matched, otherwise the stiffer flitch would have inadequate curvature while the flitch with a lower modulus of elasticity would have excessive curvature induced, thereby forcing eccentricities in the load paths.

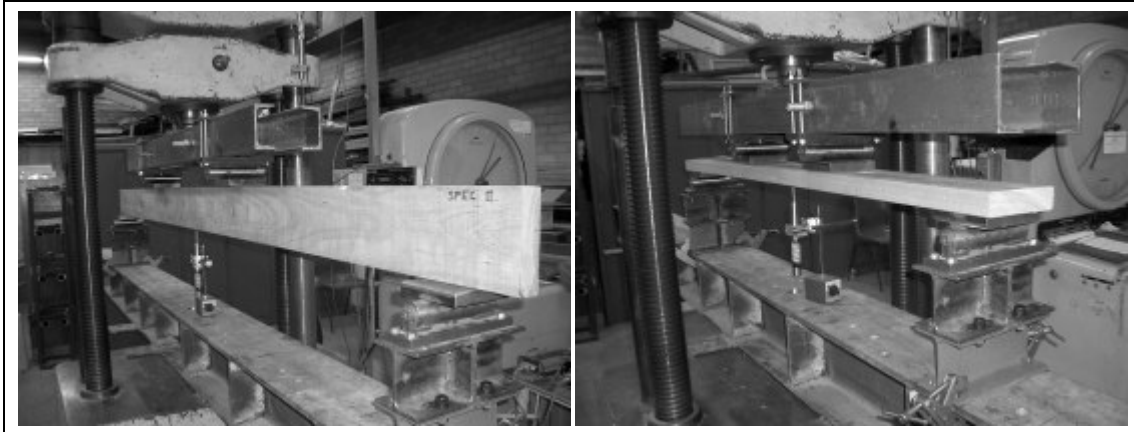


Figure 3.1: Photographs of modulus of elasticity test (x axis on left, and y axis on right)

Twelve lengths of timber each 2.8m long were marked (Spec 1 to Spec 12), measured and then tested for Modulus of Elasticity about the x axis. Each specimen was then cut in half and the two halves marked (Spec 1A and 1B to 12A and 12B). The 1.4m lengths were then tested for Modulus of Elasticity about the y axis. Results can be seen in Table 3.4.

Samples were then paired to match modulus of elasticity as closely as possible. Some considerable effort was then spent attempting to minimise the effect of the existing  $\phi 35\text{mm}$  holes in the timber by ensuring that the new drilled holes for bolts were kept a maximum distance from the large SLT strand holes. Timbers were cut to size (required length of 1225mm) in such a way as to avoid clashes between planned 10mm bolt holes and existing SLT strand holes. Pairs were also assigned to either Type A (single central spacer) or Type B (three spacers) depending primarily upon whether or not clashes would occur with holes.

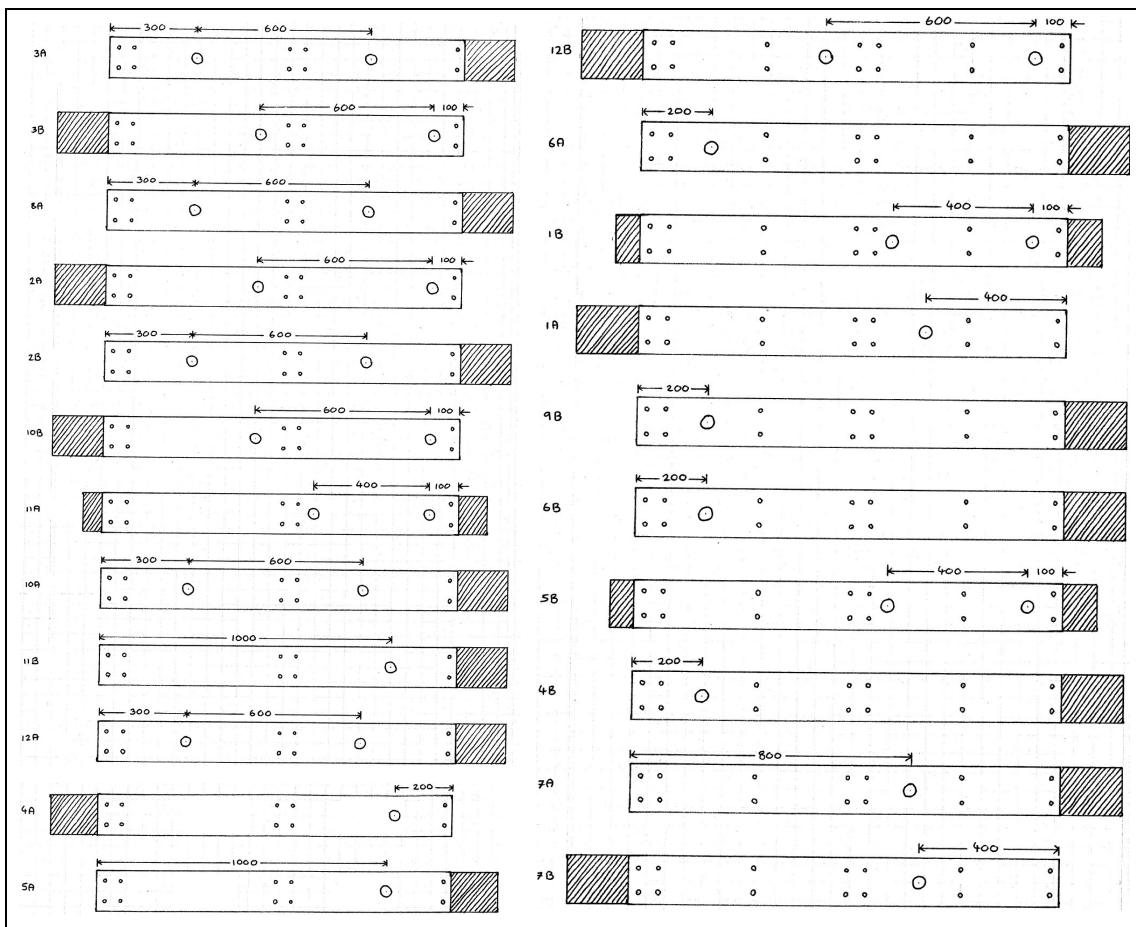


Figure 3.2: Plan for cutting timbers to size and drilling holes to avoid clashes with SLT holes

The off-cuts from the 1.4m lengths of timber were then tested in compression. There were three samples where tests could not be conducted due to the sample sizes being too short to give reasonable results due to the cutting configurations necessitated by the SLT holes. However, the results obtained give a good indication of the compressive strength of the timber as well as the effect of the holes in reducing the compressive strength of the timber. It was found that although the holes only reduced the cross sectional area by approximately 25%, they caused a reduction in strength of approximately 33%. The holes were therefore plugged with timber dowel cut from Tasmanian Oak in the fabricated assemblies to be tested.

	no hole	half a hole at edge	full central hole
<b>Minimum Compression Load (kN)</b>	<b>330</b>	<b>250</b>	<b>240</b>
<b>Maximum Compression Load (kN)</b>	<b>410</b>	<b>335</b>	<b>265</b>
<b>Average Compression Load (kN)</b>	<b>364</b>	<b>290</b>	<b>250</b>

Figure 3.3: Summary of Results showing effect of  $\phi 35\text{mm}$  holes on compression strength

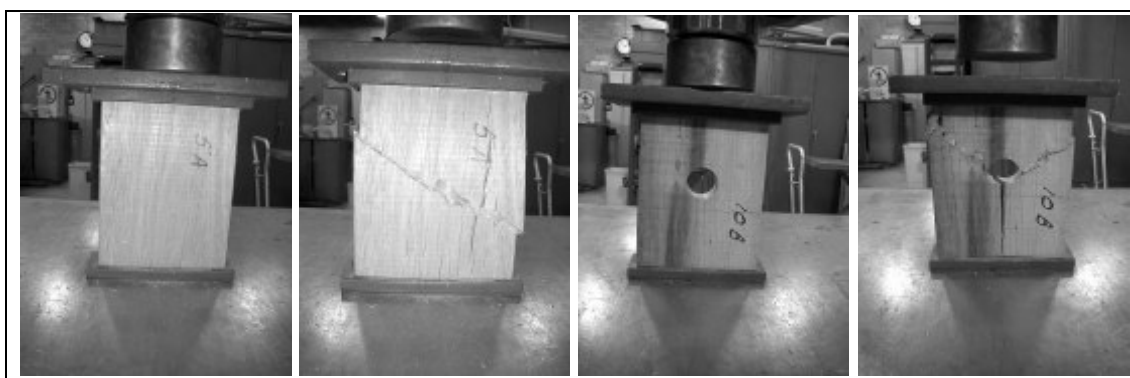


Figure 3.4: Photographs of compression strength test (clear sample on left, with hole on right)

Type		MoE (y) (MPa)	MoE (x) (MPa)	Axial (kN)	
Assembly Type A (single central spacer)	8A	15,789	16,456	330	no holes - clear sample
	2A	16,228	15,539	245	hole in middle of sample
Assembly Type A (single central spacer)	2B	16,309	15,539	340	no holes - clear sample
	10B	16,336	17,162	240	hole in middle of sample
Assembly Type A (single central spacer)	11A	16,770	16,845		
	10A	16,863	17,162	350	no holes - clear sample
Assembly Type A (single central spacer)	11B	17,619	16,845	345	no holes - clear sample
	12A	17,707	18,428	365	no holes - clear sample
Assembly Type A (single central spacer)	4A	21,543	18,064	250	hole at edge of sample
	5A	22,414	19,824	380	no holes - clear sample
Assembly Type B (three spacers)	12B	17,710	18,428	265	hole in middle of sample
	6A	17,732	17,868	285	hole at edge of sample
Assembly Type B (three spacers)	1B	19,197	18,674		
	1A	20,034	18,674	390	no holes - clear sample
Assembly Type B (three spacers)	9B	20,144	19,135	335	hole at edge of sample
	6B	20,366	17,868	305	hole at edge of sample
Assembly Type B (three spacers)	5B	20,857	19,824		
	4B	21,075	18,064	275	hole at edge of sample
Assembly Type B (three spacers)	7A	24,327	23,754	410	no holes - clear sample
	7B	25,745	23,754	370	no holes - clear sample
<b>Maximum Value</b>		<b>25,745</b>	<b>23,754</b>	<b>410</b>	
<b>Minimum Value</b>		<b>15,137</b>	<b>14,735</b>	<b>240</b>	
<b>Average Value</b>		<b>18,878</b>	<b>18,063</b>	<b>322</b>	

Figure 3.5: Tabulation of Results for Modulus of Elasticity and Compressive Strength

For the buckling tests, each assembly had eight strain gauges attached. Since the strain gauges were attached after fabrication of the assemblies, the gauges only recorded changes in strain during compressive testing, and did not record the initial strain already in the members due to the bending stresses induced at fabrication. Where possible, the strain gauges were attached at the centre of the width of the column, but where the strain gauges were located near a SLT strand hole, they were attached 25mm from the edge of the column. Similarly, for the strain gauges on the inside faces of the assembly, strain gauges were attached 25mm from the edge due to limited space to attach gauges on the inside faces.

Strain gauges used were BCM 40mm 120ohm gauges.  
To attach gauges the following process was followed:

- Sand timber at proposed strain gauge location
- Clean timber with ethanol and cotton wool
- Mark up exact location & direction with pencil
- Stick gauge to timber with tape
- Peel back tape & apply Loctite 406 adhesive
- Press down gauge and tape for 10 seconds
- Remove tape and pull back wires
- Cut off a small section of circuit board (veroboard)
- Sand both sides of circuit board
- Glue circuit board to timber with Loctite 406
- Sand circuit board again to remove excess glue
- Solder strain gauge wire to copper on circuit board
- Check with voltmeter to ensure no short circuit
- Cut off excess wire from strain gauges
- Number strain gauges 1 to 8 on each assembly
- Solder wires to connect data taker to strain gauges
- Tape wires to timber to relieve gravity loads of wires



Gauges 1 to 4 were located 135mm above the top line of bolts for the central timber spacer on all assemblies.

- Strain Gauge 1 is on the left hand outer face.
- Strain Gauge 2 is on the left hand inner face.
- Strain Gauge 3 is on the right hand inner face.
- Strain Gauge 4 is on the right hand outer face.

Gauges 5 to 8 were located 135mm above the top line of the bolts for the bottom steel box on all assemblies.

- Strain Gauge 5 is on the left hand outer face.
- Strain Gauge 6 is on the left hand inner face.
- Strain Gauge 7 is on the right hand inner face.
- Strain Gauge 8 is on the right hand outer face.

Except for gauges located at the centre of the width of the timber (ie. on outer faces a minimum 200mm from SLT strand holes), all gauges were located 25mm from the front edge of the assemblies. All gauges were aligned vertically.



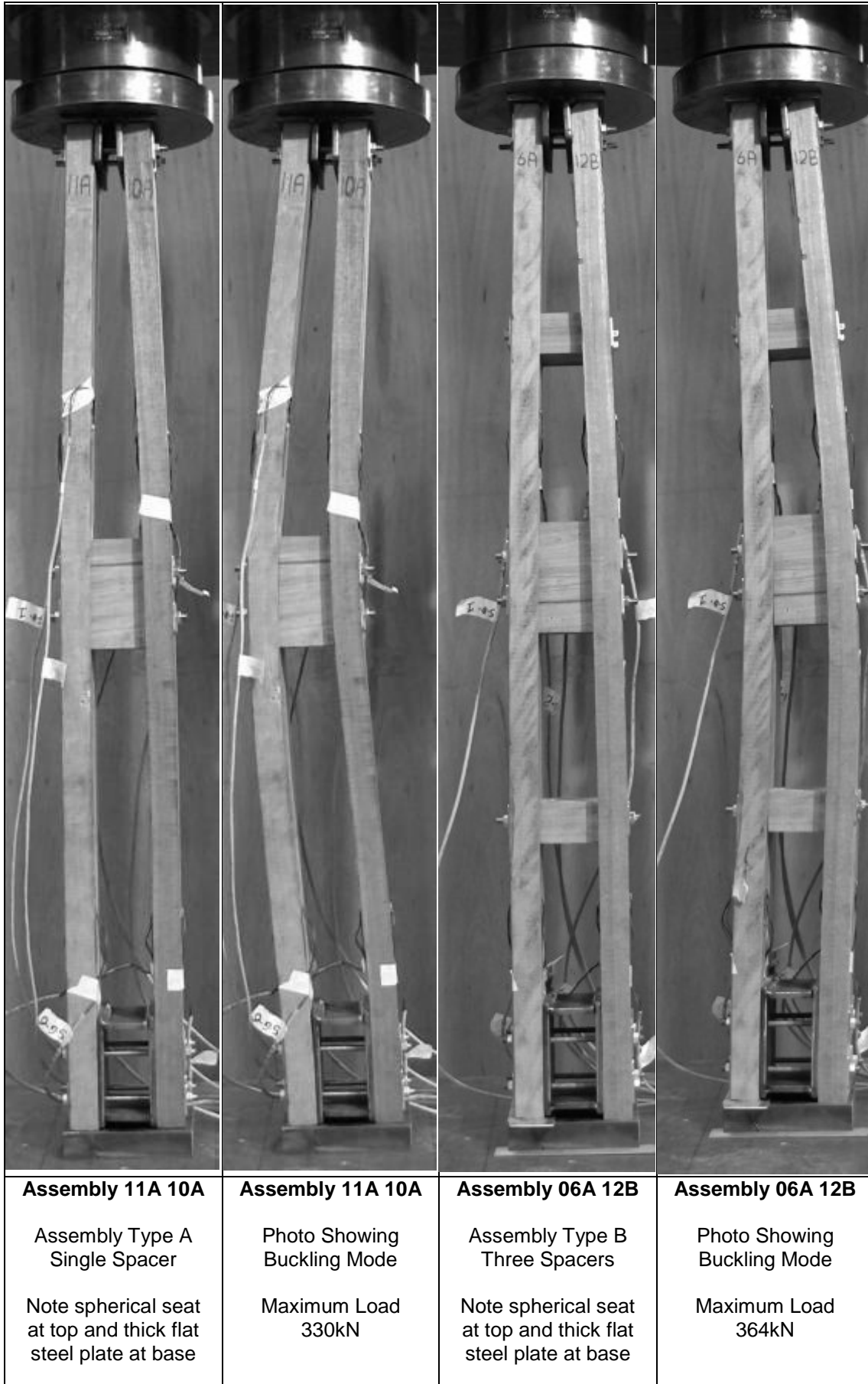


Figure 3.6: Photographs of Buckling Modes for Types A & B Spaced Columns

Assembly		MoE (y)	MoE (x)	Failed Towards	Theoretical Minimum Load	Actual Experiment Load	Actual
							Calculated
11B 12A	11B	17,619	16,845	12A	237.7	301.0	1.3
	12A	17,707	18,428				
08A 02A	8A	15,789	16,456	08A	217.8	275.5	1.3
	2A	16,228	15,539				
11A 10A	11A	16,770	16,845	11A	226.3	331.0	1.5
	10A	16,863	17,162				
10B 02B	10B	16,336	17,162	10B	219.3	302.5	1.4
	2B	16,309	15,539				
05A 04A	5A	22,414	19,824	05A	300.8	463.0	1.5
	4A	21,543	18,064				

Figure 3.7: Buckling Results for Type A Spaced Columns (single central spacer)

Assembly		MoE (y)	MoE (x)	Failed Towards	Theoretical Minimum Load	Actual Experiment Load	Actual
							Calculated
07B 07A	7B	25,745	23,754	07A	345.6	457.0	1.3
	7A	24,327	23,754				
01A 01B	1A	20,034	18,674	01B	268.9	454.5	1.7
	1B	19,197	18,674				
04B 05B	4B	21,075	18,064	04B	282.9	345.5	1.2
	5B	20,857	19,824				
06A 12B	6A	17,732	17,868	12B	238.0	364.0	1.5
	12B	17,710	18,428				
06B 09B	6B	20,366	17,868	09B	273.4	444.5	1.6
	9B	20,144	19,135				

Figure 3.8: Buckling Results for Type B Spaced Columns (three timber spacers)

Some interesting points to note from the results tabulated above are as follows:

- The critical factor affecting the maximum load appeared to be the location of the SLT holes – where SLT holes were too close to the centre (point of maximum bending moment) or the ends (near where the compression loads were applied) then failure was initiated prematurely at the location of the SLT holes.
- Of the 10 assemblies tested, seven failed prematurely at SLT hole locations:
  - 08A 02A (Type A – single spacer) – failed at SLT hole near centre
  - 11A 10A (Type A – single spacer) – failed at SLT hole near centre
  - 10B 02B (Type A – single spacer) – failed at SLT hole near centre
  - 07B 07A (Type B – three spacers) – failed at two SLT holes near centre
  - 01A 01B (Type B – three spacers) – failed at two SLT holes near top
  - 04B 05B (Type B – three spacers) – failed at SLT hole near centre and top
  - 06A 12B (Type B – three spacers) – failed at SLT holes near top and base
- The lowest value of actual/calculated minimum load was 1.2 for assembly 06A12B – this assembly did not have the SLT holes plugged with Tasmanian Oak as per the other assemblies, but the holes were left unplugged. Another difference between this assembly and the others was that 10mm threaded rod was used rather than 8mm threaded rod which was used for all connections on all the other assemblies.
- The maximum load obtained was from a “Type A” assembly with only a single spacer.
- Assembly 11B 12A had a surprisingly low load considering that it did not fail prematurely at an SLT hole (compare 11B 12A with 05A 04A). This lower maximum load is most probably explained by the fact that there was a problem with the fabrication of the steel top shoe and bottom box for this assembly, and so the holes were reamed out to oversize in the steelwork in order to be able to fit the bolts in.

Details and photographs of all ten tests are provided in Appendix A.

BRIDGE TIMBER PROPERTIES:

Tabulam Bridge is a DeBurgh timber truss bridge, constructed in 1903 located in the far north of NSW. It is the longest DeBurgh truss bridge remaining in service, with five timber truss spans and thirteen timber girder approach spans. Due to deterioration of the timbers, some of the vertical truss compression members have recently been replaced, and so the timbers that have been removed from the bridge were transported to the laboratory for testing.



Figure 3.9: Photograph of Modulus of Elasticity testing for timber from Tabulam Bridge

Each length of timber was measured and weighed before the modulus of elasticity was determined using the four point bending test as described previously. Results are as follows:

	weight (kg)	width (mm)	length (mm)	height (mm)	density (kN/m <sup>3</sup> )	MoE (MPa)
1	95	285	3,320	100	9.8	17,078
2	110	295	3,480	100	10.5	18,037
3	100	290	3,310	100	10.2	17,471
4	90	280	3,470	100	9.1	19,925
5	95	280	3,460	100	9.6	21,047
7	70	285	3,100	100	7.8	14,765
9	95	290	3,480	100	9.2	16,452
11	100	290	3,330	100	10.2	19,904

Figure 3.10: Modulus of Elasticity & Density for sound timber from Tabulam Bridge

	weight (kg)	width (mm)	length (mm)	height (mm)	density (kN/m <sup>3</sup> )	MoE (MPa)
6	70	280	3,290	100	7.5	12,869
8	90	290	3,485	100	8.7	8,189
10	80	280	3,365	100	8.3	6,056

Figure 3.11: Modulus of Elasticity & Density for rotted timber from Tabulam Bridge



The tables below plot load in kN (vertical axis) against mid-span deflection in mm (horizontal):

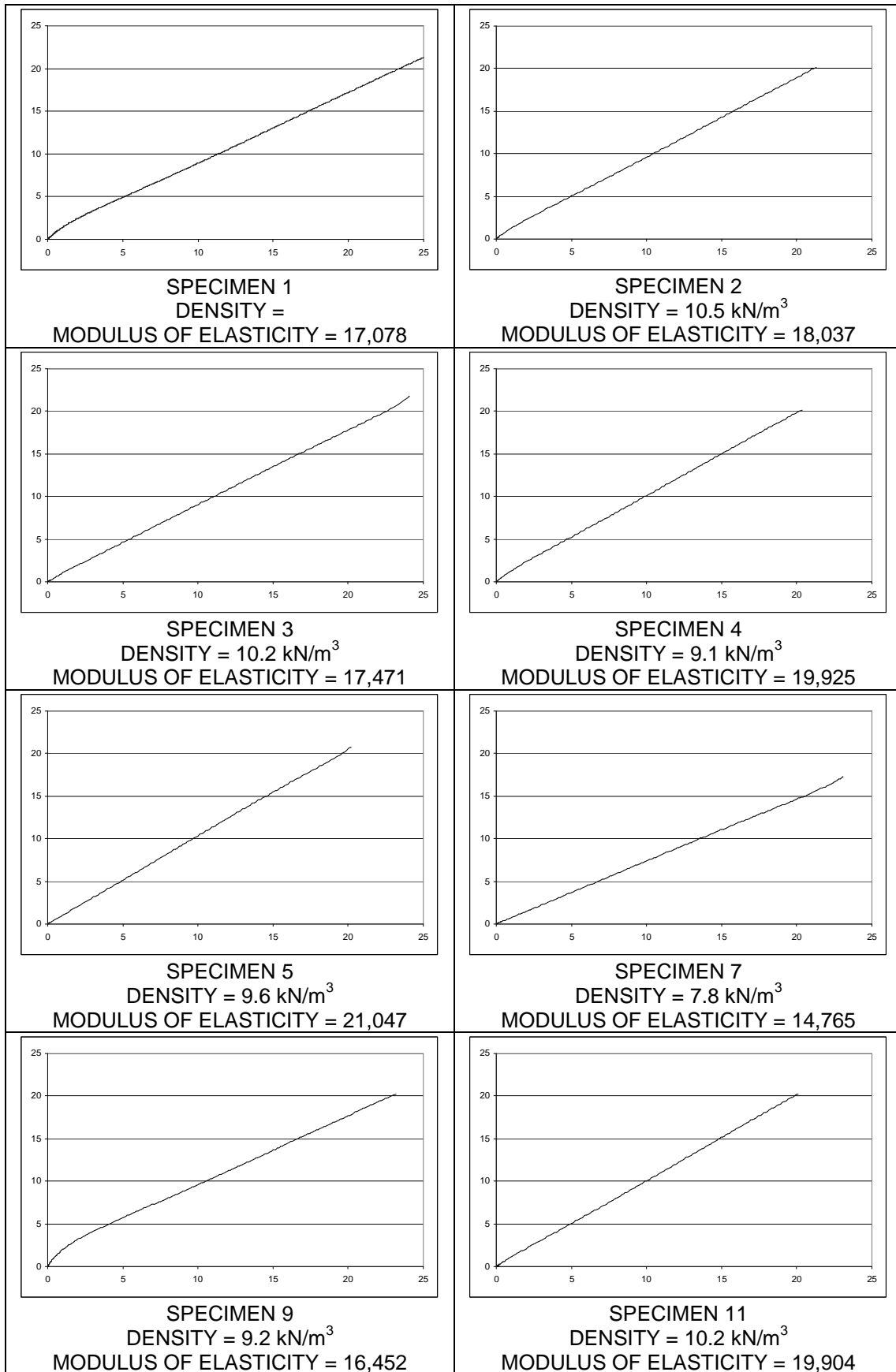


Figure 3.12: Graphs from which Modulus of Elasticity was calculated for bridge timbers

CREEP EFFECTS:

With another pair of timbers from Tabulam Bridge, a 45 day creep test was conducted.

Two full length (3510mm) pieces of timber that had been a pair in Tabulam Bridge were chosen and their curvature was measured. One length of timber had 9mm existing offset to straight at mid-length and the other had 35mm existing offset to straight at mid-length.

The pieces of timber were then placed on three timber packers (one at each end and one near the centre) and a 45kN S-type load cell was fitted between the lengths of timber. A spherical seat was provided on one side of the load cell to ensure a proper seating, and 20mm thick steel plates each 300mm x 300mm in dimension were placed on each side of the load cell to provide a reasonable bearing area for the timber as shown in Figure 3.14.

Bolts that had been removed from Tabulam Bridge were fitted at each end of the assembly. Due to the limited length of thread on the bolts, a number of thick steel washers were provided so that nuts could be tightened to induce the desired force in the load cell.

At 4pm on Thursday 16<sup>th</sup> December 2010, the bolts were tightened until the load cell was reading just over 10kN. The nuts had been tightened approximately 30mm to obtain this load.

The curvature of the timbers were measured at four stages, and the offsets to straight were:

Before Tightening	35 mm	9 mm
After Tightening	55 mm	21 mm
After 45 Days	55 mm	21 mm
After Disassembly	38 mm	9 mm

A display unit constantly showed the load in the load cell, and a data logger was programmed to take readings of load at intervals of 1 hour for a period of 45 days until 31<sup>st</sup> January 2011.

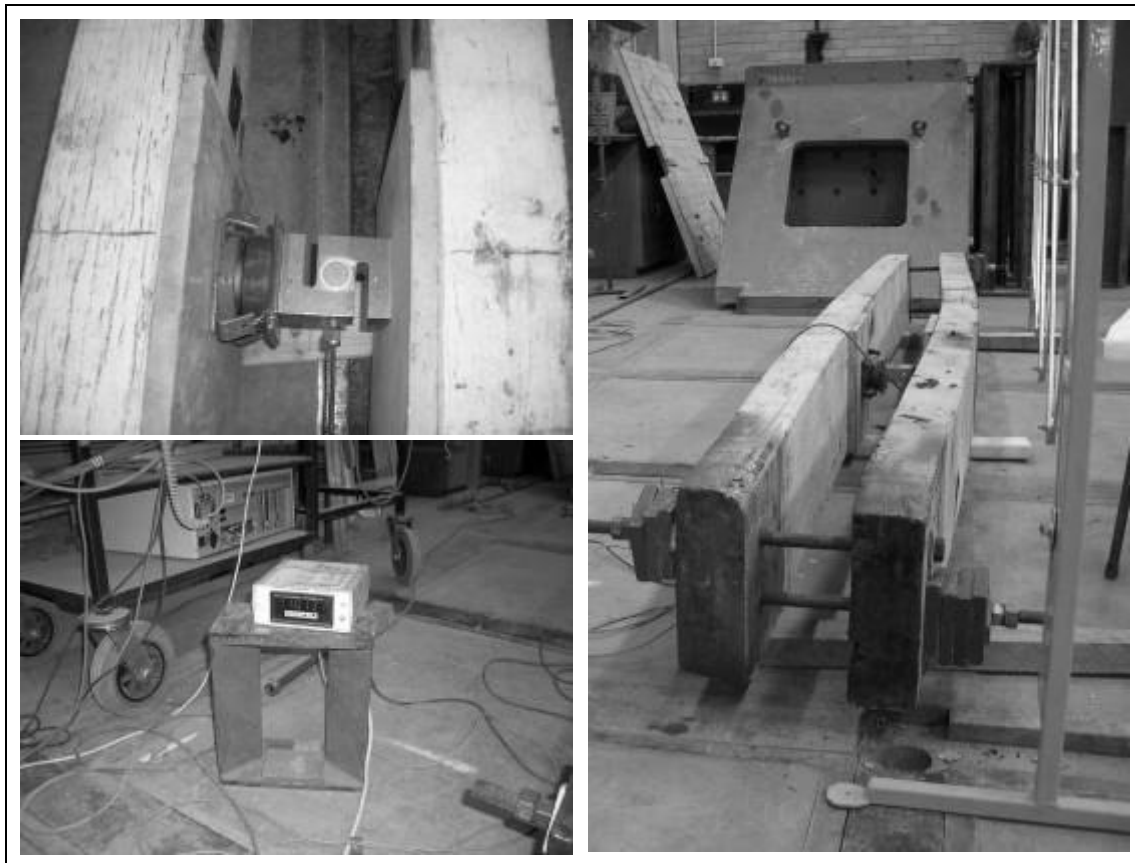


Figure 3.13: Photographs of setup for 45 Day Constant Deflection Creep Test



Figure 3.14: Photograph of 45 Day Constant Deflection Creep Test

After the 45 days, the curvatures of the timbers were checked again to confirm that deflection had indeed remained constant for the 45 day period, and this was found to be so. Also the load cell had a calibration check performed immediately after dismantling the experiment in order to confirm that the load cell itself was not experiencing creep effects during the test. The load cell gave results within 1% of the calibration load cell and was confirmed accurate.

Below are the readings of load taken from the data-logger over the 45 day period:

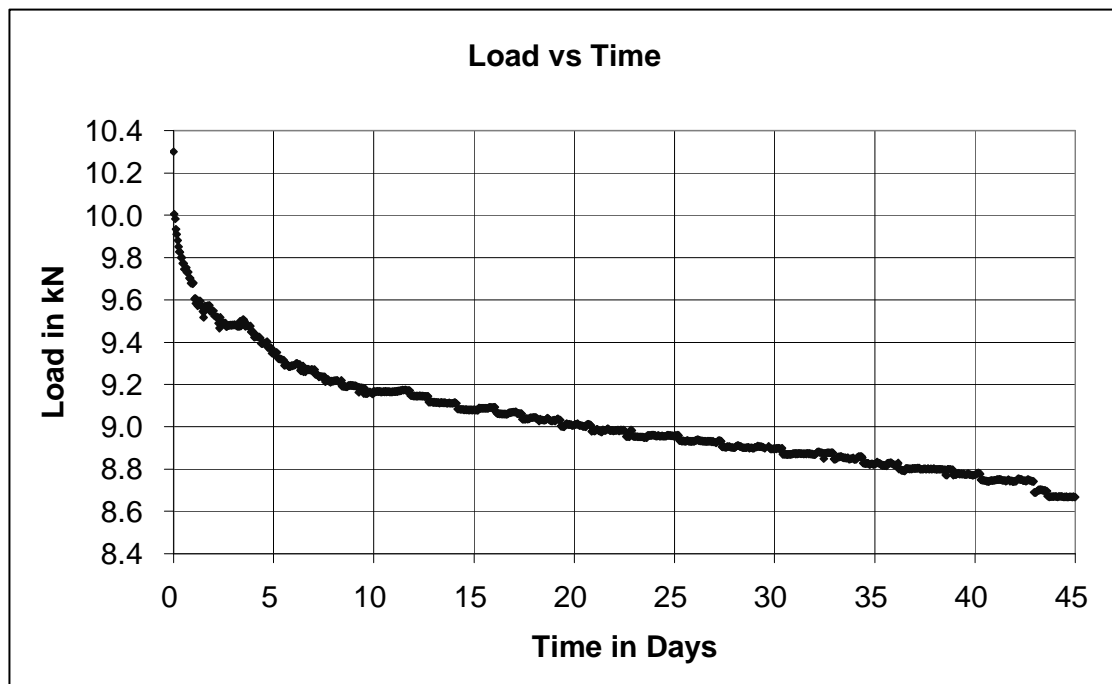


Figure 3.15: Graph of Load vs Time for 45 Day Constant Deflection Creep Test

As can be seen from Figure 3.15, approximately 15% of the initial load was lost in 45 days.

The same data from this experiment can be plotted on a logarithmic scale as per AS 1720.1:

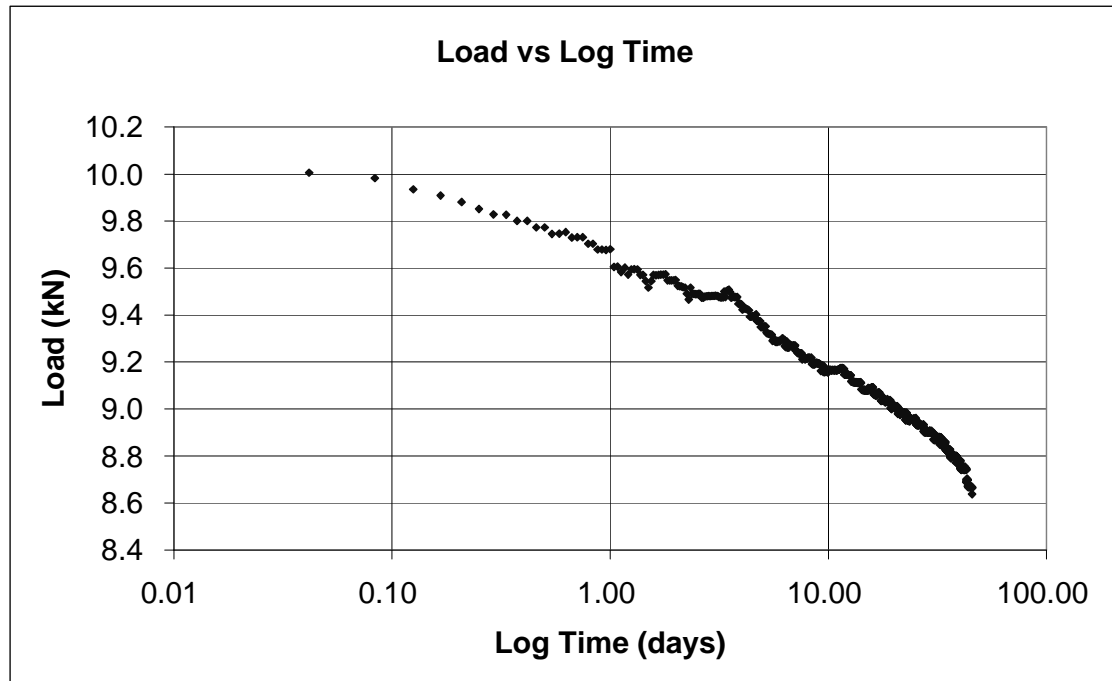


Figure 3.16: Graph of Load vs Log Time for 45 Day Constant Deflection Creep Test

It can be seen from this graph that a straight line could be fit fairly well to this data. There was a slight acceleration in the loss of load in the last week or so of the experiment, and this could possibly be due to the increase in temperature during that week. Although the experiment was undertaken inside in a relatively controlled environment, there was a discernable increase in temperature inside the laboratory during the last week of the test. The 15% drop in load is significant considering the age of the timber and the level of stress.

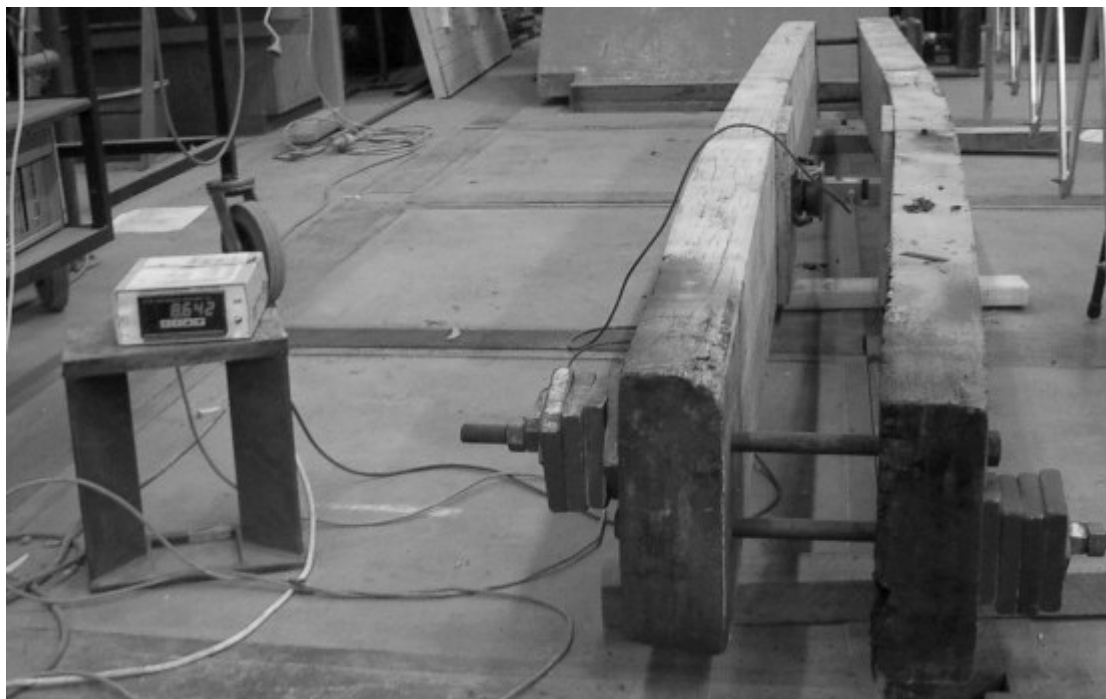


Figure 3.17: Photograph at end of 45 Day Constant Deflection Creep Test

SHEAR CAPACITY:

Using the same pieces of timber that had been tested for modulus of elasticity and density, another experiment was conducted to investigate the shear capacity of the timber spacers.

Assembly		weight (kg)	width (mm)	length (mm)	height (mm)	density (kN/m <sup>3</sup> )	MoE (MPa)
03-11	3	100	290	3,310	100	10.2	17,471
	11	100	290	3,330	100	10.2	19,904
05-07	5	95	280	3,460	100	9.6	21,047
	7	70	285	3,100	100	7.8	14,765
02-09	2	110	295	3,480	100	10.5	18,037
	9	95	290	3,480	100	9.2	16,452

Figure 3.18: Pairing of Timbers for Construction of Shear Test Assemblies

Six central timber spacers had been provided from Tabulam Bridge for testing, and so three assemblies were made. Eight new 22mm diameter holes were drilled into the timber flitches to match the four existing holes in each of the timber spacers. New holes were drilled clear of existing holes in the timber flitches so that the connections would not be adversely affected by deterioration in the region of the existing bolt holes. The existing holes in the timber spacers were in relatively good condition prior to testing, although the timber spacers did exhibit significant splitting, probably due to shrinkage, as is common in spacers in RTA bridges.



Figure 3.19: Photograph of assembly 03-11 to test shear capacity of timber spacers

All six spacers were of similar dimensions. They were each approximately 370mm long, 290mm wide, and slightly trapezoidal in shape, being 190mm high at one end and 180mm high at the other. The direction of grain in all the timber spacers was vertical.

For the first assembly (Assembly 03-11), the M20 bolts that had been removed from Tabulam Bridge were used. However, for the other two assemblies (Assembly 05-07 and 02-09) new M20 bolts were used due to the fact that there were insufficient bolts from the bridge to conduct the three tests. Washers that had been removed from the bridge were used at each end of the bolts – the steel plate washers measured 65mm x 65mm x 5mm with a 24mm hole.



Figure 3.20: Photograph before bolting of assemblies 05-07 (left) and 02-09 (right)



*Figure 3.21: Photograph showing setup for shear test*

In order to conduct the experiment, the bottom timber flitch was held down at two or three points (depending upon the length of the bottom flitch in the assembly) along its length and fixed to the floor of the Structures Laboratory. The end was also restrained from moving horizontally by steel packing plates against a fixed horizontal restraint. The top timber flitch was loaded horizontally by a hydraulic jack, and deflections were monitored at five positions while the assembly was being loaded. Two LVDTs (which monitor deflections) were placed at the loaded end each side of the hydraulic jack. Three LVDTs also monitored vertical movements, one at the loaded end of the assembly, and one above each timber spacer. Videos were taken of two of the tests, and photographs were taken before and after testing.

The first assembly was tested three times, with three different configurations of load cells, hydraulic jacks and pumps. This was because the behaviour of these spacers prior to the test was largely unknown, and so we started testing with lower capacity instrumentation and machinery to get accurate readings at lower forces, and then increased from there.

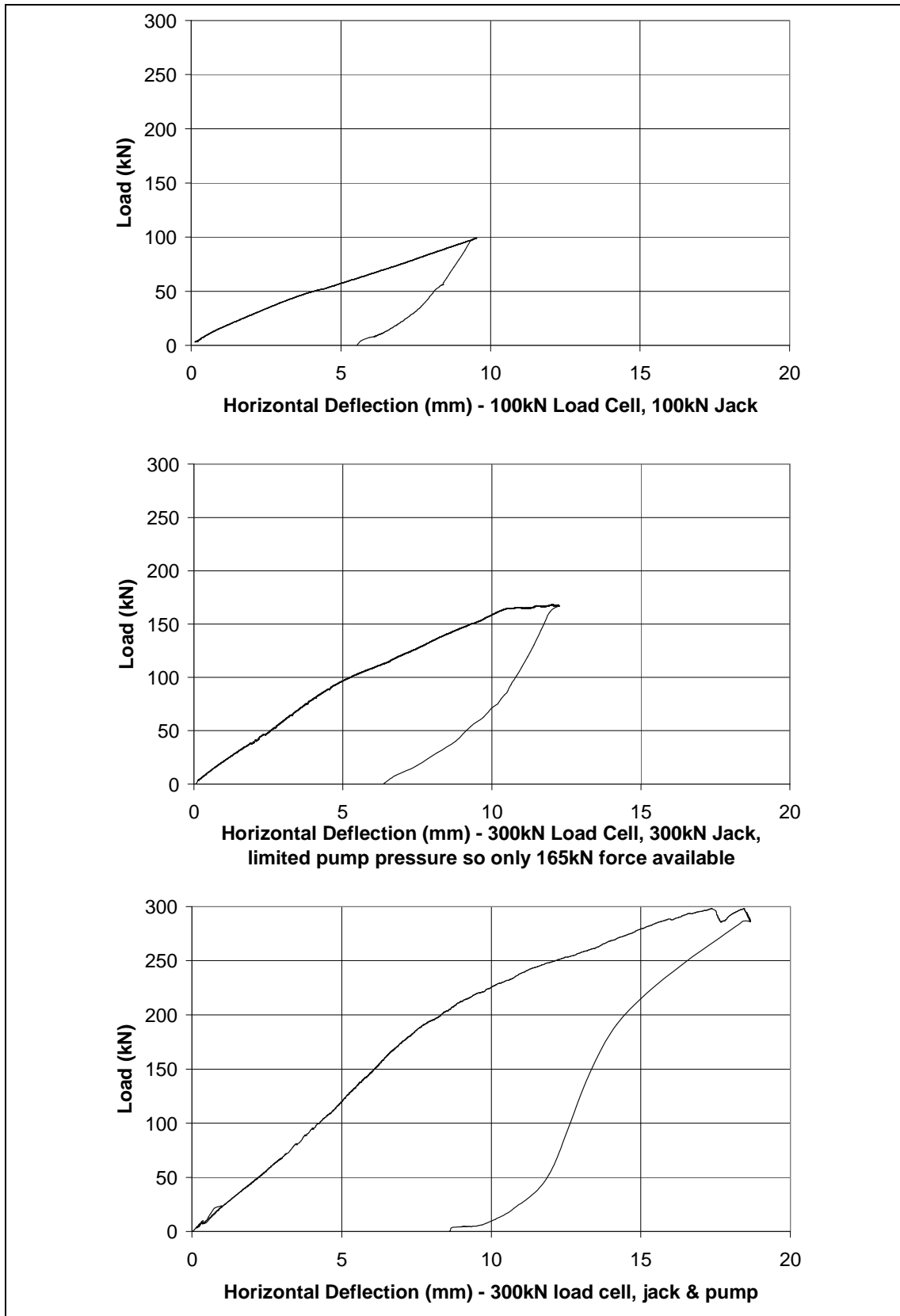


Figure 3.22: Graphs of Load vs Horizontal Deflection for Assembly 03-11



Figure 3.23: Photographs showing double curvature of one pair of bolts in Assembly 03-11



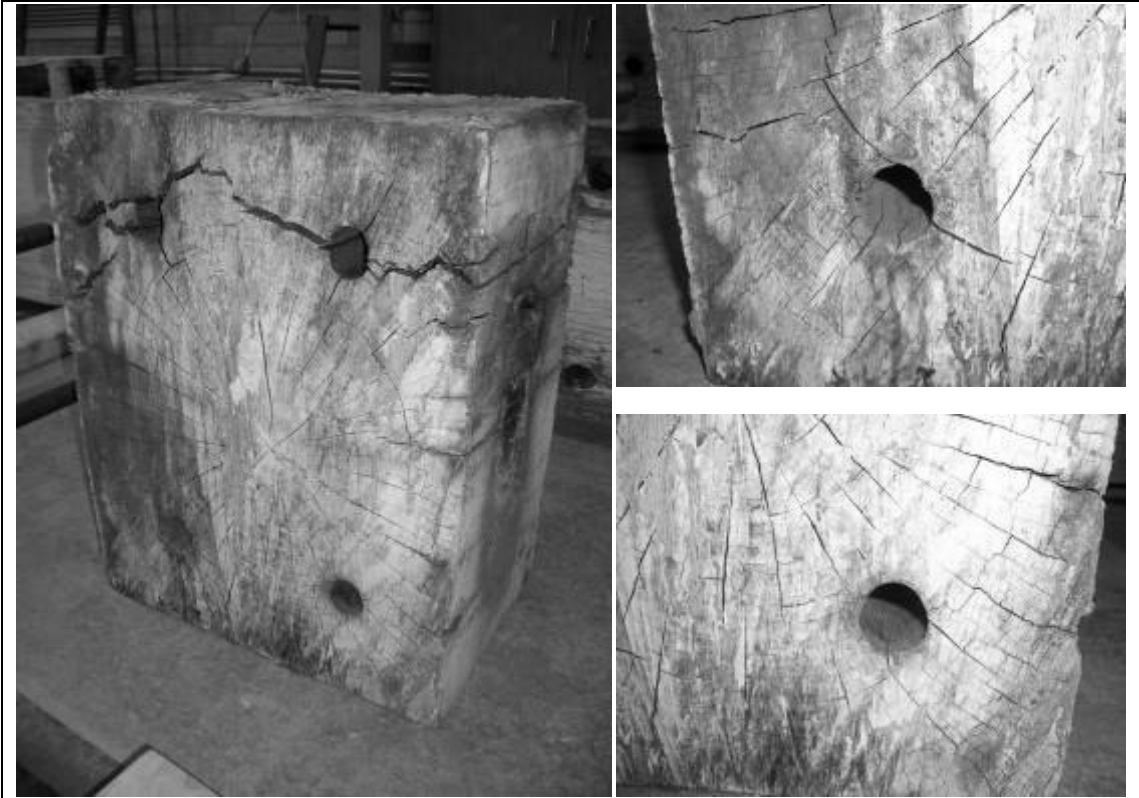


Figure 3.24: Photographs showing spacer bolt holes after testing in Assembly 03-11



Figure 3.25: Photographs showing bolts after testing in Assembly 03-11

The second and third assemblies were only tested once each, with a 1,000kN capacity jack. The setup for Assembly 05-07 was exactly the same as the first test, whereas the bolts for Assembly 02-09 were deliberately left loose in order to compare results and failure modes. None of the assemblies were tested to complete failure, but the load was released after a significant deflection had been reached (50mm for Assembly 05-07 and 70mm for 02-09).

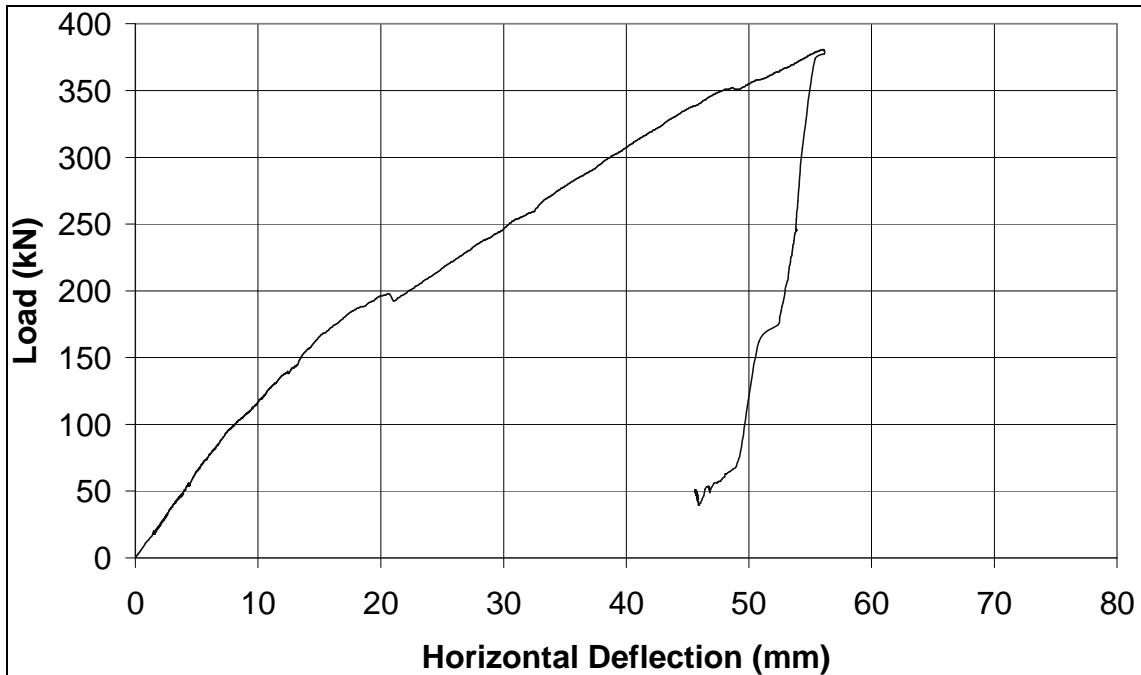


Figure 3.26: Graph of Load vs Horizontal Deflection for Assembly 05-07

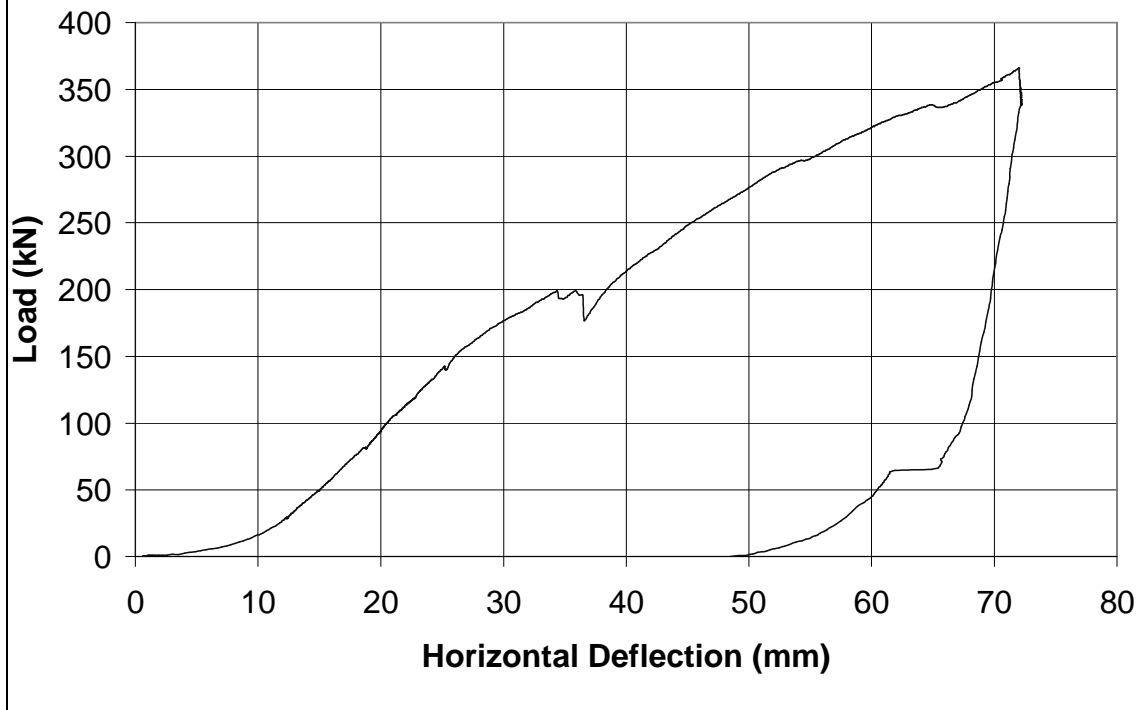


Figure 3.27: Graph of Load vs Horizontal Deflection for Assembly 02-09

It is clear that the tightness of the bolts does have a significant effect on the initial deflection that occurs before significant load is taken. However, the assembly tested with loose bolts still displayed a similar failure mode to the one tested with tight bolts, and the slope of the load deflection graph for the two assemblies is very similar after the initial slack is taken up.

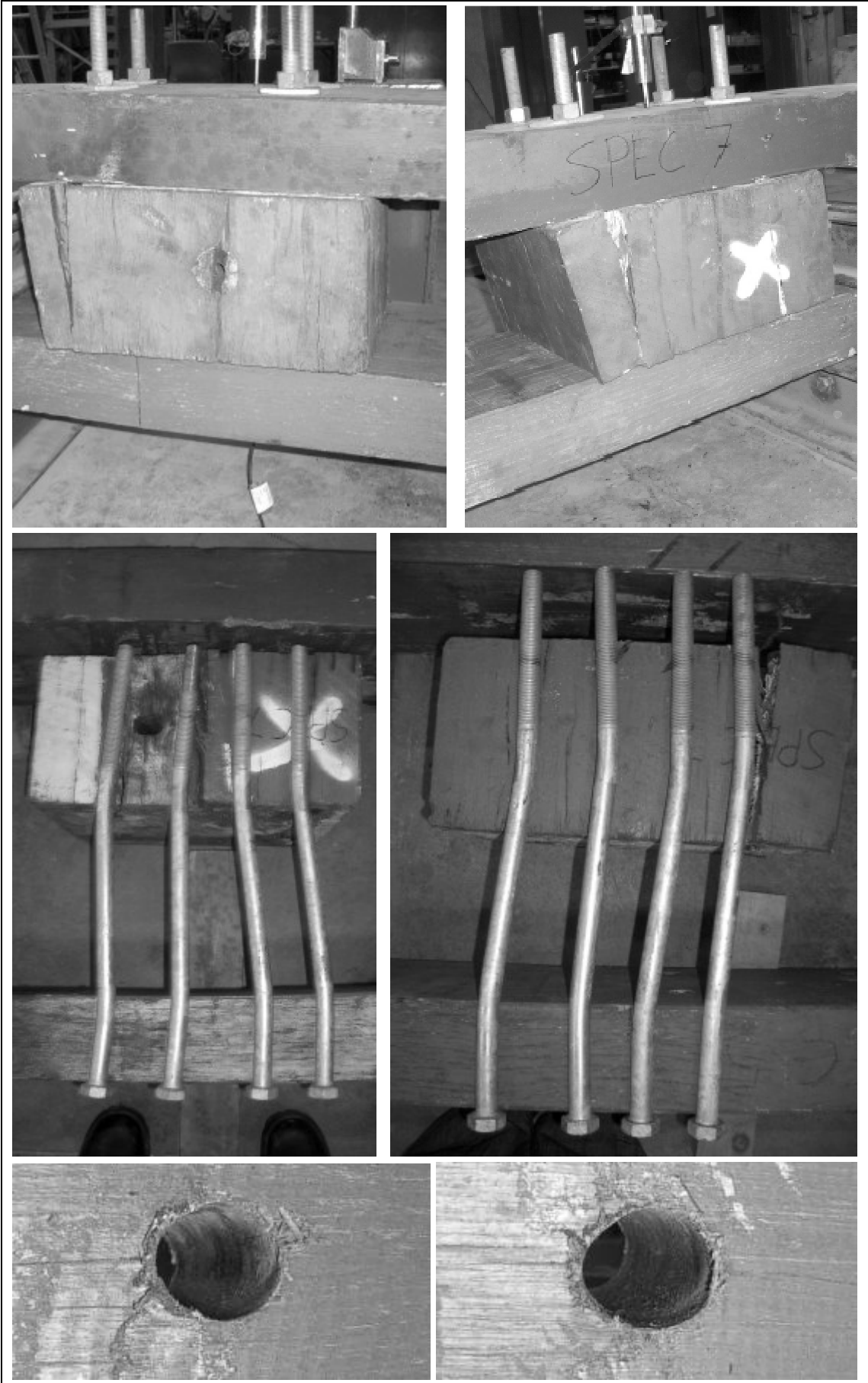


Figure 3.28: Photographs of spacers, bolts and bolt holes in flitches for Assembly 05-07

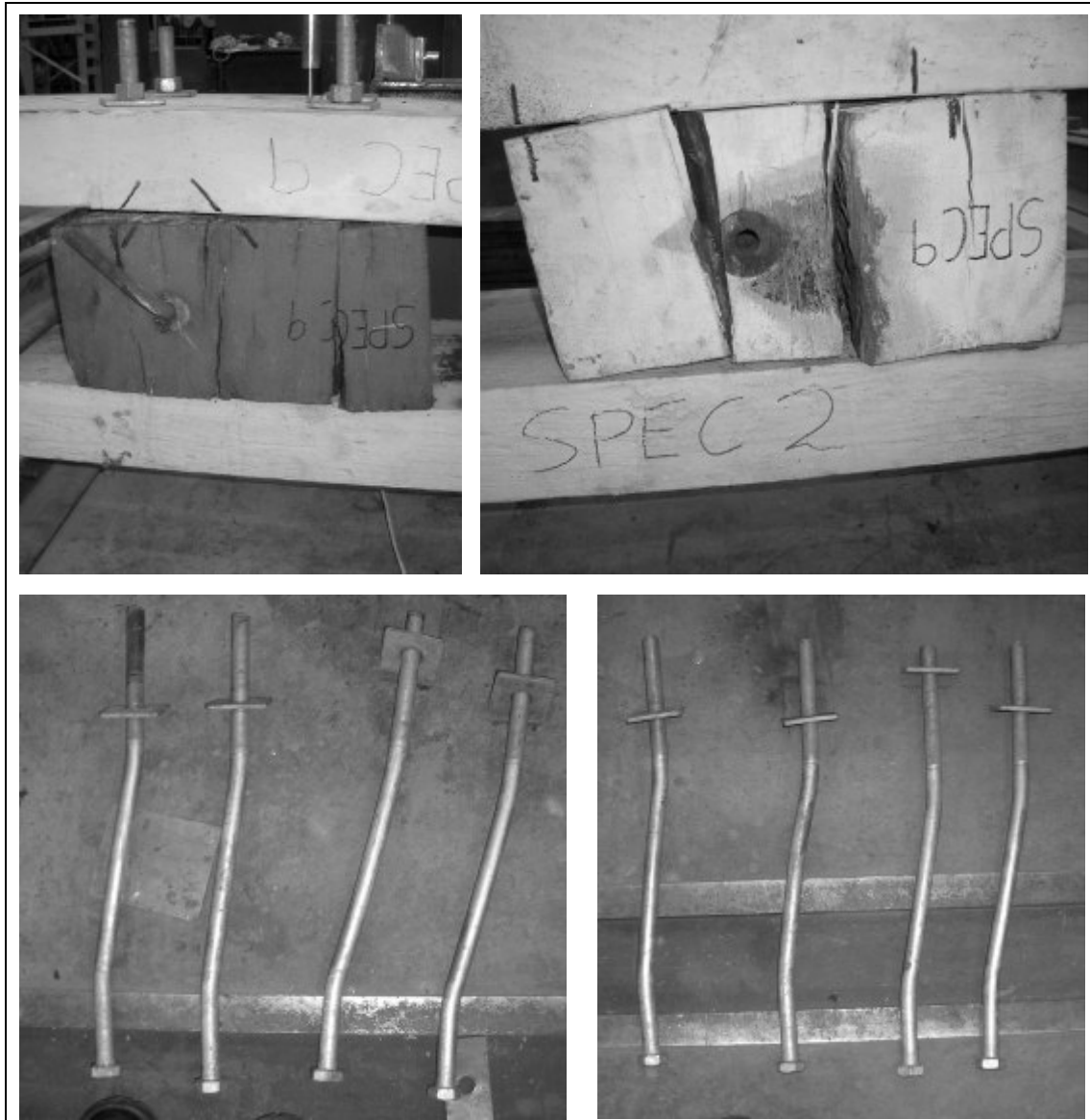
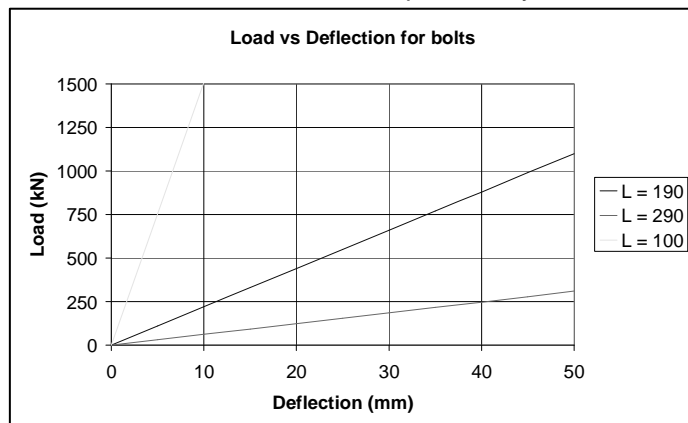


Figure 3.29: Photographs showing spacers and bolts for Assembly 02-09 after testing

It can be seen from the results of this test that the primary component to carry shear in the timber spacers is the bolts. There was only one location (Assembly 03-11) where the timber spacer appeared to contribute to the strength and stiffness of the system in shear. This was indicated by the fact that the bolt deformed in double curvature over a very short length in the area of the interface between one flitch and the timber spacer. This must have been due to a local characteristic in that timber spacer at that location which made it particularly resistant.

All the other spacers showed very little resistance before splitting at the location of the bolts. If we plot the theoretical relationship between load and deflection for eight bolts fixed at both ends to induce double curvature, we see that assuming fixity at the centre of the flitches does provide a good prediction of strength and stiffness, although care has to be taken to ensure that looseness of connections is also catered for.



## CHAPTER FOUR

### DISCUSSION AND CONCLUSIONS

#### FURTHER DISCUSSION IN THE LIGHT OF EXPERIMENTAL RESULTS:

As previously noted, the approach in AS 1720.1<sup>45</sup> to the case of minor axis bending with axial compression is obtained by simplification of the biaxial bending formula given in Appendix E:

$$\left( \frac{M_y^*}{M_{d,y}} \right) + \left( \frac{N_c^*}{N_{d,cy}} \right) \leq 1.0$$

Perhaps there is room for improvement even in this fundamental formula. As Steiger<sup>46</sup> has helpfully pointed out, most of the older design models and codes suggest a linear interaction of bending moment and axial force, which in case of high bending moments and moderate compression forces that are simultaneously acting on stocky columns presents a conservative approach, since the interaction in that case is considerably non-linear. The degree of non-linearity of the interaction curve, according to Steiger, depends on the slenderness of the column, on the ratio of flexural and axial stresses and on the strength of the timber.

Buchanan<sup>47</sup> notes that as far back as 1940, tests were carried out which showed some deviation from a straight line for small clear specimens. From these experiments, a parabolic interaction equation was suggested for slender columns which could be written as follows:

$$\left( \frac{M_y^*}{M_{d,y}} \right)^2 + \left( \frac{N_c^*}{N_{d,cy}} \right) \leq 1.0$$

On the other hand, Steiger notes that the European Code for timber structures<sup>48</sup> takes plastic deformations of the compression zone into account in members subject to high bending stresses and low axial stresses by squaring the compression part of the interaction model:

$$\left( \frac{M_y^*}{M_{d,y}} \right) + \left( \frac{N_c^*}{N_{d,cy}} \right)^2 \leq 1.0$$

Without further investigation in this area, we are constrained to keep the AS 1720.1 formula. Therefore, the aim of this thesis is to explain how timber bridges can meet this requirement. Since a quick calculation in accordance with the code requirements generally causes timber compression members in RTA bridges to fail, one or more of the following need to take place:

- $M_y^*$  could be reduced (eg. by taking into account stress relaxation of timber)
- $M_{d,y}$  could be increased (eg. by modifying  $k_1$  factors)
- $N_{d,cy}$  could be increased by using a more detailed analytical design approach

Of course, another approach would be to follow the design approach for spaced columns as outlined in AS1720.1. However, due to the empirical nature of the formulas provided, and the difficulties in obtaining the theoretical basis of these formulas, as well as the fact that the arrangement of RTA spaced columns are significantly different from those described in the code, it is thought that a new approach would be simpler both to formulate and to implement. This is especially the case in the RTA design office where all designers are relatively comfortable with Microstran, so a fairly rigorous buckling analysis is not difficult to achieve.

<sup>45</sup> AS 1720.1 – 2010 Timber Structures Part 1: Design Methods (2010)

<sup>46</sup> Steiger, R. & Fontana, M. (2005), "Bending moment and axial force interacting on solid timber beams" *Materials and Structures* 38 (June 2005) pp 507-513

<sup>47</sup> Buchanan, A.H. (1984) "Strength Model and Design Methods For Bending and Axial Load Interaction in Timber Members" PhD Thesis, The University of British Columbia

<sup>48</sup> European Committee for Standardization CEN, "EN 1995-1-1 Eurocode 5 Design of timber structures, Part 1-1: General – Common rules and rules for buildings", 2003

We will now revisit our investigation of a 42.5 tonne truck on Tabulam Bridge. As shown previously, the design compressive and bending forces for a single flitch are as follows:

$$\begin{aligned} N^*_c \text{ (ULS dead load)} &= 135 \text{ kN} && \text{(duration: 50+years)} \\ M^* \text{ (total permanent effects)} &= 10.5 \text{ kNm} && \text{(duration: 50+years)} \\ \\ N^*_c \text{ (ULS dead load + live load)} &= 420 \text{ kN} && \text{(duration: 5 days)} \\ M^* \text{ (total permanent load + live load)} &= 11.5 \text{ kNm} && \text{(duration: 5 days)} \end{aligned}$$

If we reduce long term  $M^*_y$  by 35% with the assumption of stress relaxation, we get:

$$\begin{aligned} N^*_c \text{ (ULS dead load)} &= 135 \text{ kN} && \text{(duration: 50+years)} \\ M^* \text{ (total permanent effects)} &= 6.8 \text{ kNm} && \text{(duration: 50+years)} \\ \\ N^*_c \text{ (ULS dead load + live load)} &= 420 \text{ kN} && \text{(duration: 5 days)} \\ M^* \text{ (total permanent load + live load)} &= 7.8 \text{ kNm} && \text{(duration: 5 days)} \end{aligned}$$

Looking at bending first, as it is simplest, as calculated previously, for permanent effects only:

$$\begin{aligned} M_d &= \phi k_1 k_4 k_6 k_9 k_{12} f'_b Z \\ &= 0.75 \times 0.57 \times 1.0 \times 1.0 \times 1.0 \times 55 \times 300 \times 100^2/6 = 11.8 \text{ kNm} \end{aligned}$$

However, if we modify  $k_1$  so that for bending moments due to constant deflection  $k_1 = 0.65$

$$\begin{aligned} M_d &= \phi k_1 k_4 k_6 k_9 k_{12} f'_b Z \\ &= 0.75 \times 0.65 \times 1.0 \times 1.0 \times 1.0 \times 55 \times 300 \times 100^2/6 = 13.4 \text{ kNm} \end{aligned}$$

No change is recommended to the procedure for temporary effects, as calculated previously:

$$\begin{aligned} M_d &= \phi k_1 k_4 k_6 k_9 k_{12} f'_b Z \\ &= 0.75 \times 0.94 \times 1.0 \times 1.0 \times 1.0 \times 55 \times 300 \times 100^2/6 = 19.4 \text{ kNm} \end{aligned}$$

Therefore, by these adjustments to bending moment calculations, we can see the following:

	Code Recommendations	Capacity remaining	New Recommendations	Capacity remaining
Permanent $M^*_y / M_{d,y}$	10.5/11.8 = 0.89	11%	6.8/13.4 = 0.51	49%
Temporary $M^*_y / M_{d,y}$	11.5/19.4 = 0.59	41%	7.8/19.4 = 0.40	60%

Recommendations result in a 19% increase in available compression capacity for temporary effects and a 38% increase in available compression capacity for permanent effects. Room is left for further improvement if further research is conducted in stress relaxation and  $k_1$  factors.

Now we can look at compression, and here we need to consider two things:

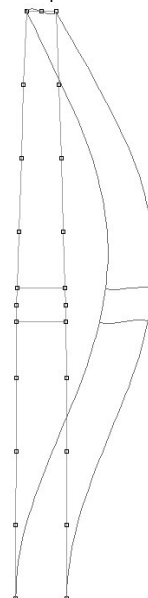
Material compression failure is a limiting criterion and so the following applies:

$$\begin{aligned} N_{d,c} &= \phi k_1 k_4 k_6 f'_c A_c \\ &= 0.75 \times 0.57 \times 1.0 \times 1.0 \times 1.0 \times 42 \times 300 \times 100 = 538.6 \end{aligned}$$

And similarly, for temporary effects:

$$\begin{aligned} N_{d,c} &= \phi k_1 k_4 k_6 f'_c A_c \\ &= 0.75 \times 0.94 \times 1.0 \times 1.0 \times 1.0 \times 42 \times 300 \times 100 = 888.3 \end{aligned}$$

Now, if we were to assume an average modulus of elasticity as given by the code, then we could prepare a model in Microstran of the column assembly, apply our design loads, and find the critical buckling load, which turns out to be 1590 kN (or 795 kN per flitch), giving a design capacity of 596.3 kN per flitch. It can then be seen the material failure is critical for permanent effects.



Therefore, by using this more accurate method of assessment, we see the following:

PERMANENT EFFECTS	Code Recommendations	New Recommendations
$M_y^* / M_{d,y} =$	$10.5/11.8 = 0.89$	$6.8/13.4 = 0.51$
$N^* / N_{d,c} =$	$135/75 = 1.80$	$135/538.6 = 0.25$
$(M_y^* / M_{d,y}) + (N^* / N_{d,c}) =$	$0.89+1.80 = 2.69$ (FAIL)	$0.51+0.25 = 0.76$ (OK)

TEMPORARY EFFECTS	Code Recommendations	New Recommendations
$M_y^* / M_{d,y} =$	$11.5/19.4 = 0.59$	$7.8/19.4 = 0.40$
$N^* / N_{d,c} =$	$420/160 = 2.63$	$420/596.3 = 0.70$
$(M_y^* / M_{d,y}) + (N^* / N_{d,c}) =$	$0.59+2.63 = 3.22$ (FAIL)	$0.40+0.70 = 1.10$ (FAIL)

We now examine the effect of a lower modulus of elasticity by revisiting our calculations:

The design compressive and bending forces for a single flitch (E=8,000MPa) are as follows:

$N_c^*$ (ULS dead load)	=	135 kN	(duration: 50+years)
$M^*$ (total permanent effects)	=	3.4 kNm	(duration: 50+years)
$N_c^*$ (ULS dead load + live load)	=	420 kN	(duration: 5 days)
$M^*$ (total permanent load + live load)	=	4.4 kNm	(duration: 5 days)

Bending strengths remain the same, but compressive strength will be affected. If we assume a lower fifth percentile value for the modulus of elasticity (E=8,000MPa), then we can adjust the model in Microstran of the column assembly, apply our design loads, and find the critical buckling load, which turns out to be 902 kN (or 451 kN per flitch), giving a design capacity of 338.3 kN per flitch. Therefore, material failure is no longer critical for permanent effects.

Similarly, we can examine the effect of a higher than average modulus of elasticity:

The design compressive and bending forces for a single flitch (E=24,000MPa) are as follows:

$N_c^*$ (ULS dead load)	=	135 kN	(duration: 50+years)
$M^*$ (total permanent effects)	=	10.2 kNm	(duration: 50+years)
$N_c^*$ (ULS dead load + live load)	=	420 kN	(duration: 5 days)
$M^*$ (total permanent load + live load)	=	11.2 kNm	(duration: 5 days)

Bending strengths remain the same, but compressive strength will be affected. If we assume an upper fifth percentile value for the modulus of elasticity (E=24,000MPa), then we can adjust the model in Microstran of the column assembly, apply our design loads, and find the critical buckling load, which turns out to be 2256 kN (or 1128 kN per flitch), giving a design capacity of 846.0 kN per flitch. Therefore, material failure governs again for permanent effects.

Therefore, we can compare the effects of varying the modulus of elasticity as follows:

PERMANENT EFFECTS	E = 8,000	E = 16,000	E = 24,000
$M_y^* / M_{d,y} =$	$3.4/13.4 = 0.25$	$6.8/13.4 = 0.51$	$10.2/13.4 = 0.76$
$N^* / N_{d,c} =$	$135/338.3 = 0.40$	$135/538.6 = 0.25$	$135/538.6 = 0.25$
$(M_y^* / M_{d,y}) + (N^* / N_{d,c}) =$	0.65 (OK)	0.76 (OK)	1.01 (FAIL)

TEMPORARY EFFECTS	E = 8,000	E = 16,000	E = 24,000
$M_y^* / M_{d,y} =$	$4.4/19.4 = 0.23$	$7.8/19.4 = 0.40$	$11.2/19.4 = 0.58$
$N^* / N_{d,c} =$	$420/338.3 = 1.24$	$420/596.3 = 0.70$	$420/846.0 = 0.50$
$(M_y^* / M_{d,y}) + (N^* / N_{d,c}) =$	1.47 (FAIL)	1.10 (FAIL)	1.08 (FAIL)

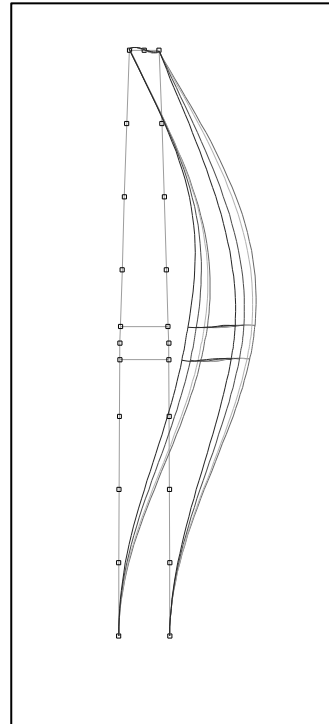
Note that we still fail to meet the requirements, but we fail by 10-50% rather than over 300%.

Using the same Microstran Model of a single column assembly from Tabulam Bridge, and assuming an average modulus of elasticity of 16,000MPa, an analytical investigation was conducted of the effects of applying the load unequally between the two flitches. Four different load distributions were considered and the results are as follows:

Application of Load	Critical Buckling Load
Load distributed 50% / 50%	1591 kN
Load distributed 40% / 60%	1591 kN
Load distributed 20% / 80%	1567 kN
Load distributed 0% / 100%	1516 kN

It can clearly be seen from this analysis that it is overly conservative to design each flitch to take more than 50% of the load, as the load distribution even in very extreme cases (where 100% of the load is going to only one flitch) has only a minimal effect (approx 5%) on the capacity of the assembly as a whole.

It is therefore confirmed that despite uncertainties due to lack of fit, variability of modulus of elasticity, out of straightness and the global truss behaviour, the two flitches of each assembly provide sufficient support to the other to prevent premature buckling even in the case of uneven distribution of load.



Another important discussion is how these recommendations compare with the full scale bridge testing that was conducted by MBK<sup>49</sup> in the early 1990s as mentioned in Chapter One. The bridge in question used to cross the Barwon River at Euminbah and had three 90 foot spans with a carriageway width of approximately 4.6m. This timber Allan truss bridge carried traffic on the Castlereagh Highway north of Walgett until it was taken out of service in 1991 due to deterioration in the piers and large distortions in the top chords of the truss spans.

The setup for testing is shown in Figure 4.1. The MBK report notes that at a total load of 4x380kN, failure occurred in the diagonal member third from the end of the downstream truss in combined bending and compression. Loads were then further applied to the upstream truss until a similar failure occurred in the corresponding member at a load of 2x490kN.

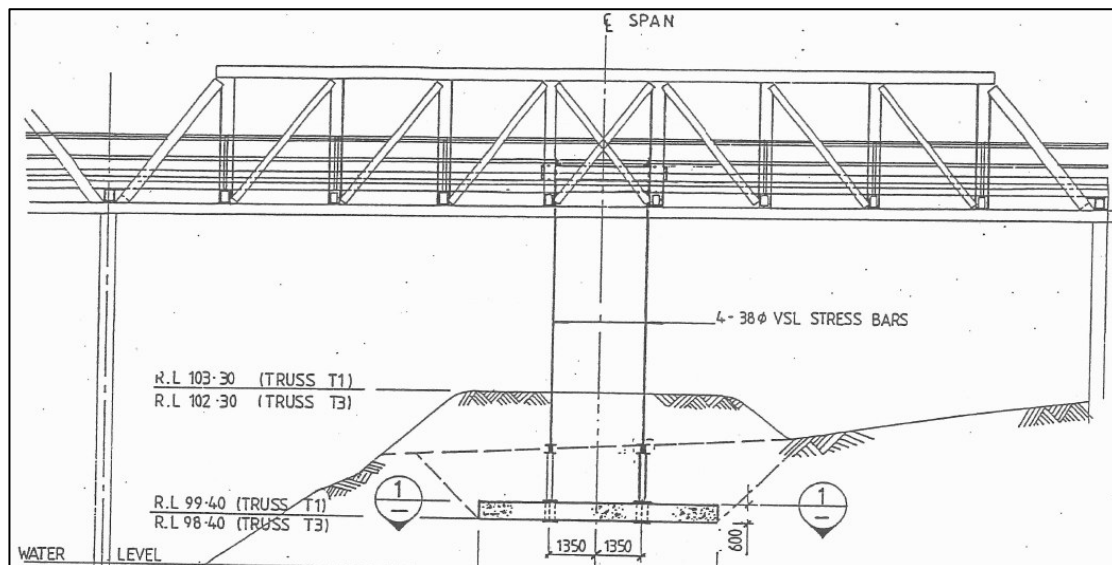
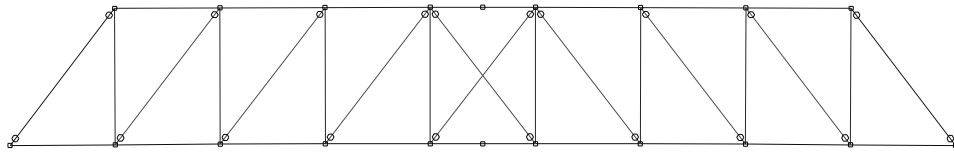


Figure 4.1: Setup for Full Scale Ultimate Load Testing – Euminbah Bridge

- <sup>49</sup> MBK 1994 “Report on Test Loading of Allan Truss Bridges (Euminbah Bridge) and Dare Truss Bridges (Dangar Bridge) in February and June 1993”, RTA File 92M1768



The MBK report does not give details of the forces in the failed members, and so a Microstran model must be prepared to determine the effects of the stated applied loads in the truss. A very simple two dimensional model of a single truss was prepared for this purpose:



The approximate axial forces in the first three diagonals (excluding principals) are as follows:

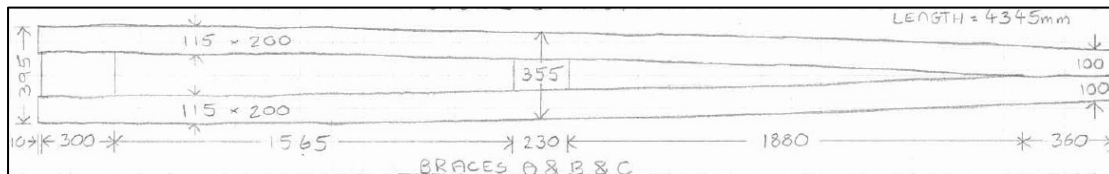
Member	Dead Load	Applied Test Load		Total Member Force	
Brace A	N* = 140 kN	N* <sub>1</sub> = 475	N* <sub>2</sub> = 610	N* <sub>1</sub> = 615	N* <sub>2</sub> = 750
Brace B	N* = 95 kN	N* <sub>1</sub> = 480	N* <sub>2</sub> = 620	N* <sub>1</sub> = 575	N* <sub>2</sub> = 715
Brace C	N* = 50 kN	N* <sub>1</sub> = 465	N* <sub>2</sub> = 600	N* <sub>1</sub> = 515	N* <sub>2</sub> = 650

Therefore, the forces in the member that failed in each truss (Brace B) can now be calculated:

$$N^*_{c1} \text{ First Failure (single flitch)} = 287.5 \text{ kN} \quad (\text{duration: 5 hours})$$

$$M^* \text{ (including 35\% reduction)} = 4.2 \text{ kNm} \quad (\text{duration: 5 hours})$$

And now the capacity of that member (Brace B) can also be calculated:



Bending moments (phi here is excluded as we are seeking to match ultimate failure loads):

$$M = k_1 k_4 k_6 k_9 k_{12} f'_b Z$$

$$= 0.97 \times 55 \times 200 \times 115^2 / 6 = 23.5 \text{ kNm}$$

Material compression failure must be considered (again without phi):

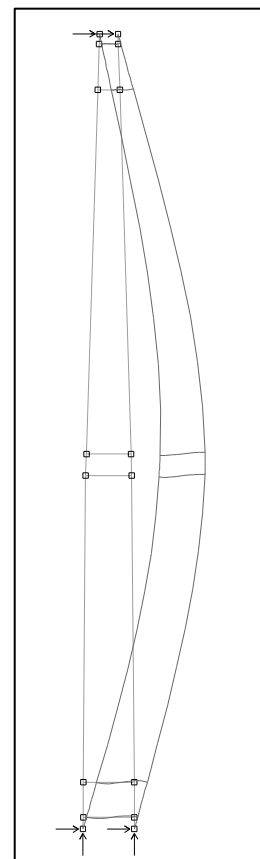
$$N = k_1 k_4 k_6 f'_c A_c$$

$$= 0.97 \times 42 \times 200 \times 115 = 937$$

The MBK report seems to indicate that an average modulus of elasticity of 16,000MPa is reasonable, and so this was used in the Microstran model of the column assembly to find the critical buckling load, which turns out to be 768 kN (equivalent to 384 kN per flitch).

Brace B	
$M^*_y / M =$	$4.2 / 23.5 = 0.18$
$N^*_{c1} / N =$	$287.5 / 384 = 0.75$
$(M^*_y / M) + (N^* / N) =$	$0.18 + 0.75 = 0.93$

We see that the result (0.93) is very close to unity, and because we have included no capacity reduction factors in this assessment, this does seem to indicate that the approach given provides a reasonable prediction of failure load of the member in question. It is important to note here that there were other identical members in the bridge which achieved higher loads without failure (compare member forces in Brace A with Brace B). Due to the variability in timber, there will always be significant differences in capacity, but the approach outlined seems to give a reasonable estimate of the lower bound, and the full scale test reported by MBK seems to confirm this.



Finally, we can look at how the findings and recommendations outlined in this paper compare with the results achieved in the testing of the 1/3 size scale model column assemblies. Two sets of Microstran Models were prepared, each using actual MoE values determined from the tests. The first set is just as described by this paper, the second set of models are more detailed in order to take into account SLT holes and the extra stiffness of the top bolt due to the fact that it was fitted into a steel shoe rather than a timber spacer block. The inclusion of the reduced section at SLT holes only effected results by approximately 2%, but the additional rigidity of the top bolt resulted in a significant (approximately 35%) increase in capacity.

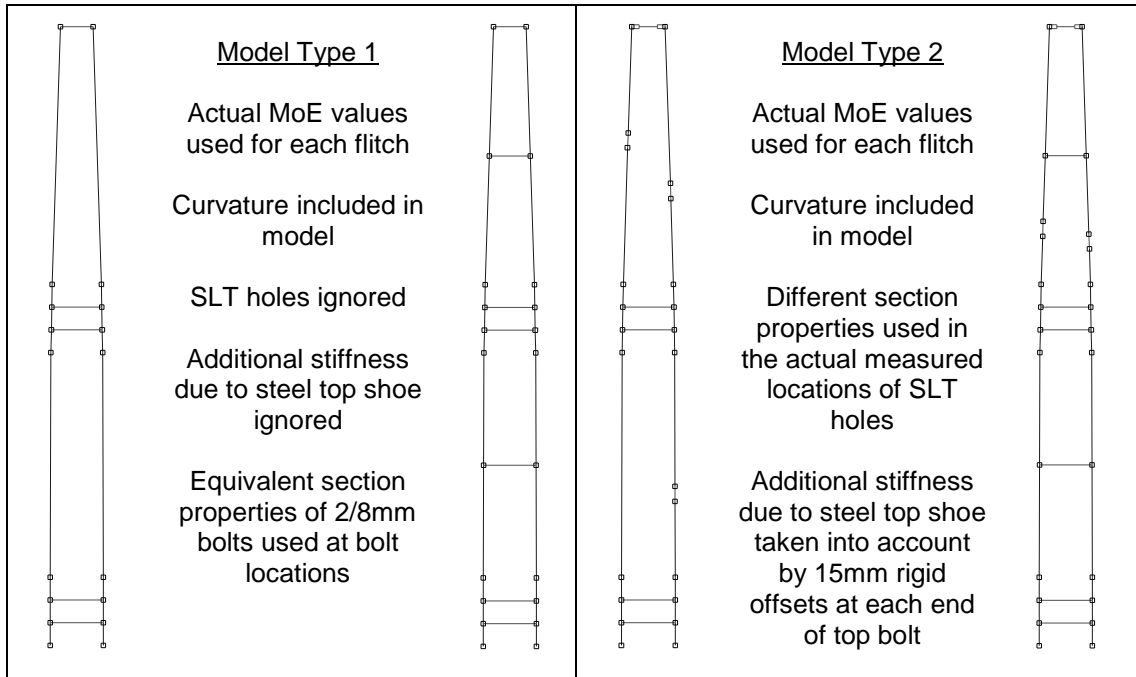


Figure 4.2: Microstran Models used to assess Critical Buckling Load

Assembly	MoE (y)	Microstran		N*1	N*2	N*mat	Actual	Model1 act/cal	Model2 act/cal	material act/cal
		Ncr 1	Ncr 2							
11B 12A	17,619	295.0	402.0	182.4	248.5	411.6	301.0	1.7	1.2	0.7
	17,707									
08A 02A	15,789	271.0	368.0	177.2	240.6	411.6	275.5	1.6	1.1	0.7
	16,228									
11A 10A	16,770	284.0	382.0	180.8	243.1	411.6	331.0	1.8	1.4	0.8
	16,863									
10B 02B	16,336	276.0	374.0	178.6	242.0	411.6	302.5	1.7	1.2	0.7
	16,309									
05A 04A	22,414	355.0	487.0	186.3	255.6	411.6	463.0	2.5	1.8	1.1
	21,543									
07B 07A	25,745	398.0	536.0	182.6	245.9	411.6	457.0	2.5	1.9	1.1
	24,327									
01A 01B	20,034	323.0	435.0	186.0	250.5	411.6	454.5	2.4	1.8	1.1
	19,197									
04B 05B	21,075	341.0	462.0	186.4	252.6	411.6	345.5	1.9	1.4	0.8
	20,857									
06A 12B	17,732	295.0	401.0	182.0	247.4	411.6	364.0	2.0	1.5	0.9
	17,710									
06B 09B	20,366	332.0	453.0	186.6	254.6	411.6	444.5	2.4	1.7	1.1
	20,144									

Figure 4.3: Table comparing Two Microstran Models & Material Strength with Test Results (note that reductions for bending moment are included in the results listed in this table)

We can see here the difficulty in matching a formula to the experimental data due to the fact that there is no clear relationship between the maximum loads obtained and either the modulus of elasticity of the timber or the layout of the assembly (ie. number of spacers). This is most likely due to the fact that premature failure occurred at the SLT bolt hole locations.

Another important factor to note here is that the maximum loads obtained in some cases exceed the code value for the compressive capacity of the timber itself, even excluding phi:

$$N = k_1 k_4 k_6 f'_c A_c = 1.0 \times 1.0 \times 1.0 \times 1.0 \times 1.0 \times 2 \times 42 \times 140 \times 35 = 411.6$$

Four out of ten assemblies tested achieved higher loads than this limiting material strength criterion. Furthermore, if  $\phi = 0.75$  then seven out of the ten assemblies tested achieved higher loads than the code value for the compressive strength of the F22 timber used. From the tests which investigated the actual compressive strength of the timber used in these scale models, we know that the actual ultimate strength of the timber far exceeds the code values.

We can see that when the method recommended in this paper is applied to the scale models tested, the method generally underestimates capacity by 60% to 250%. However, when the more detailed Microstran model was used, the predicted loads were closer to experimental results, underestimating capacity by 10% to 90%. If the simple criterion of material strength is used then calculated capacity ranges from overestimating by 30% to underestimating by 10%.

A very critical thing to note here is that it is impossible to construct a scale model which accurately scales down all the various strengths, sizes and stiffnesses of the different elements that make up a column assembly in an RTA timber truss bridge. Most probably, the reason for the Microstran models underestimating the strength of the scale model assemblies is simply that the relative stiffness of the 8mm bolts compared with the timber spacers would be significantly different to the relative stiffness of 20mm bolts through timber spacers.

The shear capacity experiments on the timber spacers with 20mm bolts showed that the timber spacers contribute almost zero resistance in most cases. This is because the 20mm bolt has a significantly higher stiffness and strength than the timber loaded perpendicular to grain. However, in the scale models, we were using similar timber (F22) loaded in a similar fashion (perpendicular to grain), but we were using 8mm bolts rather than 20 mm bolts. Therefore, it would not be surprising if the timber in the timber spacers contributed more to the shear stiffness in the scale models than they did in the full size shear capacity tests.

Therefore, although the scale model experiment does not particularly verify the model proposed in this paper, it certainly does not disprove it either. One thing that the scale model experiment did confirm was the buckling mode of these assemblies, which is a good outcome.

One final comparison must be made here, which involves revisiting the spaced column provisions in AS1720.1, and here they are applied to the Type A (single spacer) assemblies:

(a)	S	=	$g_{13}L/d = 0.85 \times 1225 / 140 = 7.4375$
	$\rho_c$	=	1.01
	$K_{12}$	=	1
	$N_{(case1)}$	=	$\phi k_1 k_4 k_6 k_{12} f'_c A_c = 0.75 \times 42 \times 9,800 = \mathbf{309 \text{ kN (solid column)}}$
(b)	$S_5$	=	$0.3 g_{13} g_{28} L (A/I)^{1/2} = 0.3 \times 0.85 \times 2.7 \times 1225 (9,800 / 25.5 \times 10^6)^{1/2} = 16.5$
	$\rho_c$	=	1.01
	$K_{12}$	=	$1.5 - 0.05 \rho_c S = 1.5 - 0.05 (1.01 \times 16.5) = 0.665$
	$N_{(case2)}$	=	$\phi k_1 k_4 k_6 k_{12} f'_c A_c = 0.75 \times 0.665 \times 42 \times 9,800 = \mathbf{205 \text{ kN (spaced column)}}$
(c)	S	=	$L/d = 580 / 35 = 16.6$
	$\rho_c$	=	1.01
	$K_{12}$	=	$1.5 - 0.05 \rho_c S = 1.5 - 0.05 (1.01 \times 16.6) = 0.66$
	$N_{(case3)}$	=	$\phi k_1 k_4 k_6 k_{12} f'_c A_c = 2 \times 0.75 \times 0.66 \times 42 \times 4,900 = \mathbf{205 \text{ kN (single flitch)}}$

The thing to note here is that the spaced column provisions conclude that there are two equally possible modes of failure (buckling of assembly as a whole and buckling of a single flitch between spacers). It is highly significant, therefore, that the second mode of failure (buckling of a single flitch between spacers) did not occur in any of the assemblies tested.

**CONCLUSIONS AND RECOMMENDATIONS:**

The recommended guidelines that can be used by bridge design staff to allow reasonable prediction of compression strength of members in RTA timber truss bridges are as follows:

Recommended departures from AS1720.1-2010 are highlighted for clarity.

This simplification of the biaxial bending formula in AS 1720.1 Appendix E shall be used:

$$\left( \frac{M^*_{y}}{M_{d,y}} \right) + \left( \frac{N^*_{c}}{N_{d,cy}} \right) \leq 1.0$$

A bending strength assessment of an individual flitch shall be undertaken as follows:

$$M_d \geq M^* \text{ where } M_d = \phi k_1 k_4 k_6 k_9 k_{12} f'_b Z$$

- $M_d$  = design capacity in bending
- $M^*$  = design action effect in bending
  - for ultimate live loads, secondary moments due to the applied axial forces must be calculated and added to fabrication forces.
  - **Apply a factor of 0.65 to bending moments due to permanent deflections induced at fabrication where fabrication occurs a minimum of 12 months prior to installation into the bridge**
- $\phi$  = capacity factor (0.75 for F22 timber)
- $k_1$  = duration of load factor
  - 0.57 for dead loads
  - 0.80 for serviceability live loads (T44, Load Factor=1, DLA=20%)
  - 0.97 for ultimate live loads (T44, Load Factor=2.0, DLA=20%)
  - **0.65 for bending moments due to permanent deflections**
- $k_4$  = partial seasoning factor (1.0 for RTA truss timbers)
- $k_6$  = modification factor for temperature (1.0 for RTA truss bridges)
- $k_9$  = strength sharing factor (1.0 for RTA truss members)
- $k_{12}$  = stability factor (1.0 for bending about the minor axis)
- $f'_b$  = characteristic value in bending (55MPa for F22)
- $Z$  = section modulus which equals  $db^2/6$  for bending about minor axis

A compressive strength assessment of an individual flitch shall be undertaken as follows:

$$N_{d,c} \geq N^*_c$$

where  $N_{d,c}$  is the lesser of:

$$= \phi k_1 k_4 k_6 f'_c A_c; \text{ or}$$

$$= \phi k_4 k_6 N_{cr}$$

- $N_{d,c}$  = design capacity in compression
- $N^*_c$  = design action effect in compression
- $\phi$  = capacity factor (0.75 for F22 timber)
- $k_1$  = duration of load factor
  - 0.57 for dead loads
  - 0.80 for serviceability live loads (T44, Load Factor=1, DLA=20%)
  - 0.97 for ultimate live loads (T44, Load Factor=2.0, DLA=20%)
- $k_4$  = partial seasoning factor (1.0 for RTA truss timbers)
- $k_6$  = modification factor for temperature (1.0 for RTA truss bridges)
- $f'_c$  = characteristic value in compression parallel to grain (42MPa for F22)
- $A_c$  = cross-sectional area of column
- $N_{cr}$  = **0.5 x critical elastic axial buckling load of the column assembly**

The critical elastic axial buckling load of the column assembly shall be determined as follows:

A model shall be prepared in Microstran, with careful attention being paid to ensuring correct dimensions are used, including the actual length of the timber (not including any steel shoes) and the actual shape of the timber (including the curvature shown on the drawings whereby each flitch is generally offset from straight at the central spacer by approximately 25mm).

Section properties of the timber flitches shall match the dimensions shown on the drawings. However, timber spacers shall not be included in the model. Instead, any bolts that are included through the timber spacers shall be included in the model. Therefore, if 20mm bolts are specified, then the section and material properties of a 20mm steel bolt shall be used.

In the case where there are two bolts side by side, an equivalent section property can be calculated by doubling the second moment of area (I) for one bolt.

$$I = \frac{\pi d^4}{64} = \frac{\pi 220^4}{64} = 7854 \text{ mm}^4$$

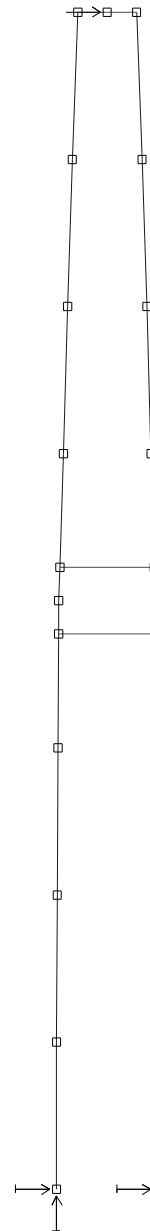
$$2I = 2 \times 7854 = 15708$$

Care shall be taken in determining appropriate supports. Generally in timber truss bridges, pinned supports would be most appropriate. Only in the case of bridges with steel bottom chords and steel cross girders with significant connection rigidity should fixed connections be used at the base.

The top of the column assembly shall be restrained from horizontal movement both laterally and longitudinally, but free to move vertically so that compressive loads can be applied. Design forces obtained from the global truss model shall be applied to the top of the flitches (50% of load to each flitch). An Elastic Critical Load (ECL) Analysis shall then be performed in Microstran. This is a rational buckling analysis to computer the elastic critical load for the assembly and the associated buckling mode shapes.

$N_{cr}$  for a single flitch shall be half of the critical load of the column assembly.

When checking for combined bending and compression, the same modulus of elasticity shall be used when calculating the design bending moments as when calculating the critical elastic axial buckling load. Checks shall be carried out for three cases (E=8,000MPa; E=16,000MPa; E=24,000MPa).



**FURTHER RESEARCH NEEDS:**

Significant benefit could be gained by further research in the following specific areas:

- **Interaction equation for bending moment and axial force:** An investigation is required using actual bridge timbers, and full size sections as used in RTA bridges to determine the real behaviour in combined compression and bending.
- **Stress relaxation in timber subject to constant deflection:** Long term (minimum 24 months) timber stress relaxation tests are required using actual bridge timbers and full section sizes, but at a variety of stress levels and environmental conditions.
- **Relaxation rupture in timber with constant deflection:** This can be done in conjunction with the previous test, but looking specifically at failure due to time effects of timber subject to constant deflection. This may result in new  $k_1$  factors for bending.
- **Optimisation of bolt sizes in timber spacer connections:** A study needs to be done into the effect of increasing shear stiffness by increasing bolt diameters without excessively decreasing the compressive strength of the timber, which is also critical.
- **Influence of direction of grain of timber spacers:** Some trusses have spacers where direction of grain is different, and effects of this requires further investigation.

# APPENDIX A

## SPACED COLUMN TEST RESULTS

### DIMENSIONS OF TIMBERS FOR SPACED COLUMNS:

In order to be able to properly assess the behaviour of the spaced columns, accurate dimensions were taken prior to the first four point bending tests for modulus of elasticity.

	<b>width left</b>	<b>width centre</b>	<b>width right</b>	<b>thickness left</b>		<b>thickness centre</b>		<b>thickness right</b>	
1	139.82	139.45	138.75	35.65	35.25	35.45	35.55	35.52	35.39
2	139.00	139.38	139.42	34.20	34.10	34.40	34.00	34.30	34.50
3	138.84	139.17	138.10	34.32	34.46	34.25	34.65	34.50	34.40
4	139.59	139.70	139.24	35.40	35.30	35.41	35.37	35.00	35.16
5	139.65	139.46	139.24	35.37	35.37	35.53	35.23	35.25	34.98
6	139.97	140.00	140.40	35.48	35.24	35.56	35.33	35.54	35.57
7	139.37	138.84	138.97	35.68	35.05	34.98	35.37	35.76	34.96
8	138.57	138.47	138.59	34.61	34.86	34.18	34.68	34.15	34.13
9	139.97	139.85	141.20	35.04	35.48	35.20	35.63	35.88	35.54
10	139.06	139.44	138.46	33.91	34.27	34.51	34.73	34.04	34.27
11	141.10	141.40	140.75	35.47	35.76	35.78	35.60	35.71	35.19
12	139.34	139.56	139.50	34.21	34.11	34.26	34.36	34.41	34.40
<b>av</b>	<b>139.52</b>	<b>139.56</b>	<b>139.39</b>	<b>34.95</b>	<b>34.94</b>	<b>34.96</b>	<b>35.04</b>	<b>35.01</b>	<b>34.87</b>

*Figure A.1: measured dimensions for 2.8m lengths of F22 timber*

Because the 140x35mm lengths of F22 timber had previously been used to make a Stress Laminated Timber (SLT) deck, they had a number of holes in them. The holes were measured, and were all 35mm in diameter. The locations of the holes were then recorded:

Specimen 1: 1000; 2200; 2600 mm from left end of timber to centre of hole

Specimen 2: 100; 700; 1300; 1900; 2500 mm from left end of timber to centre of hole

Specimen 3: 300; 900; 1500; 2100; 2700 mm from left end of timber to centre of hole

Specimen 4: 200; 1400; 2600 mm from left end of timber to centre of hole

Specimen 5: 1000; 2200; 2600 mm from left end of timber to centre of hole

Specimen 6: 200; 1400; 2600 mm from left end of timber to centre of hole

Specimen 7: 600; 1800 mm from left end of timber to centre of hole

Specimen 8: 300; 900; 1500; 2100; 2700 mm from left end of timber to centre of hole

Specimen 9: 200; 1400; 2600 mm from left end of timber to centre of hole

Specimen 10: 300; 900; 1500; 2100; 2700 mm from left end of timber to centre of hole

Specimen 11: 200; 600; 1800 mm from left end of timber to centre of hole

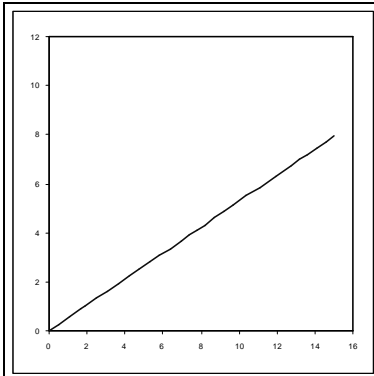
Specimen 12: 300; 900; 1500; 2100; 2700 mm from left end of timber to centre of hole

### MODULUS OF ELASTICITY ABOUT X AND Y AXES:

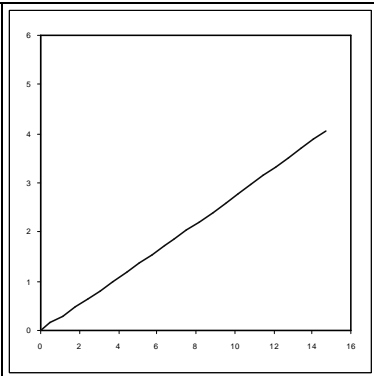
After dimensions were measured, four point bending tests were conducted to determine the modulus of elasticity about both the x-axis and the y-axis for each piece of timber. Twelve lengths of timber each 2.8m long labelled 1 to 12 were first tested about the x-axis.

The 12 pieces were then cut in half, labelled 1A to 12B and tested about their y-axis.

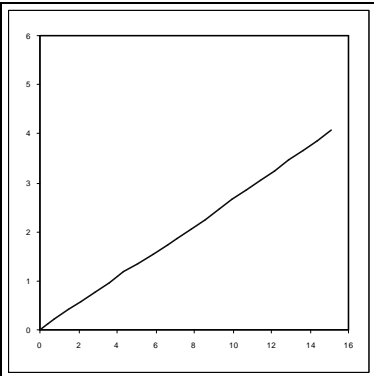
The load was increased at a constant rate until the central deflection reached 15mm for all tests (both about the x-axis and about the y-axis). Plots of load vs deflection for each test are shown on the following pages. Load (max 12kN for x-axis; max 6kN for y-axis) is plotted on the vertical axis, and deflection (max 16mm for all graphs) is plotted on the horizontal axis.



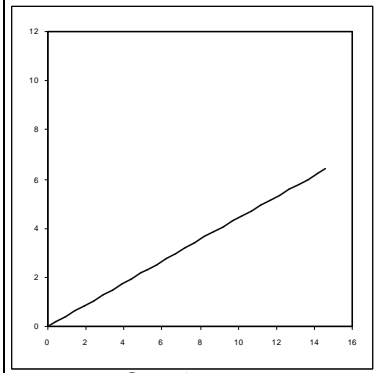
Specimen 1  
Modulus of Elasticity (x-axis)  
= 18,674



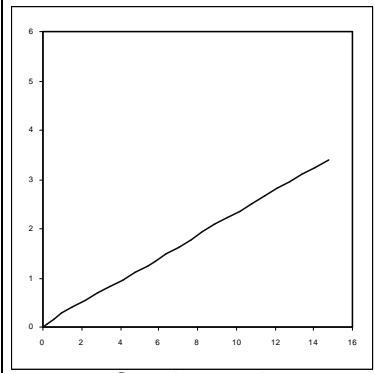
Specimen 1A  
Modulus of Elasticity (y-axis)  
= 20,034



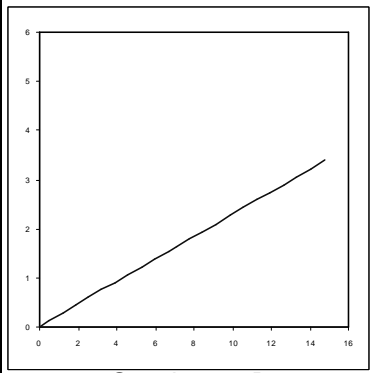
Specimen 1B  
Modulus of Elasticity (y-axis)  
= 19,197



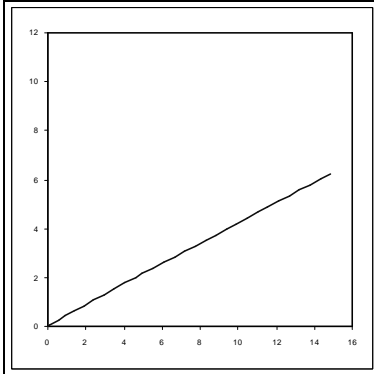
Specimen 2  
Modulus of Elasticity (x-axis)  
= 15,539



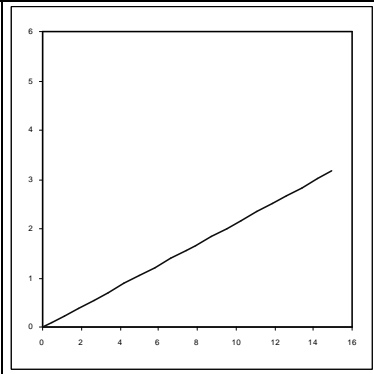
Specimen 2A  
Modulus of Elasticity (y-axis)  
= 16,228



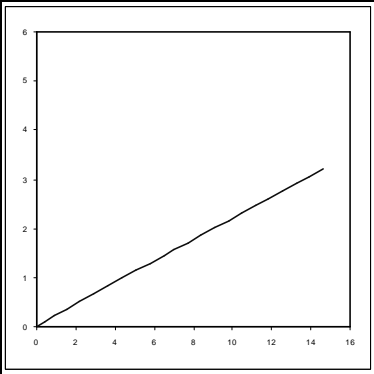
Specimen 2B  
Modulus of Elasticity (y-axis)  
= 16,309



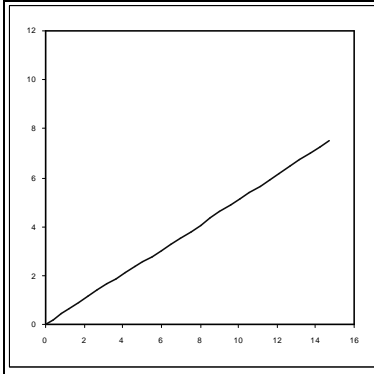
Specimen 3  
Modulus of Elasticity (x-axis)  
= 14,735



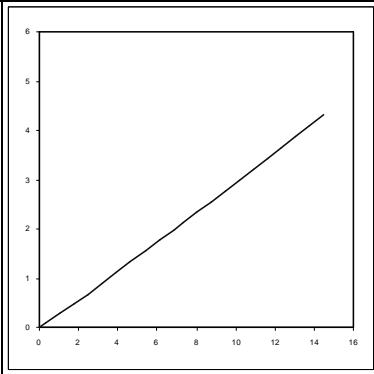
Specimen 3A  
Modulus of Elasticity (y-axis)  
= 15,137



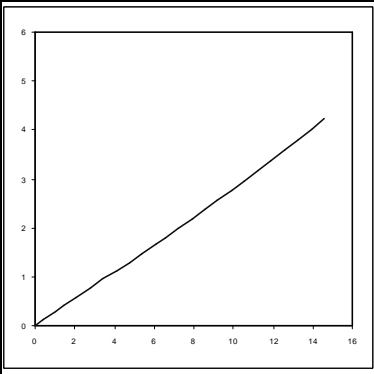
Specimen 3B  
Modulus of Elasticity (y-axis)  
= 15,421



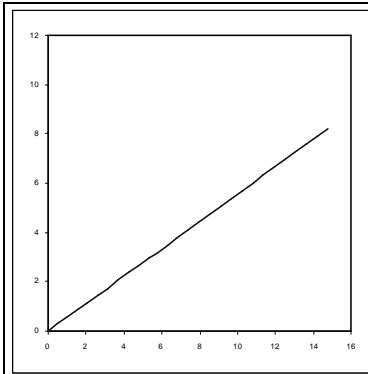
Specimen 4  
Modulus of Elasticity (x-axis)  
= 18,064



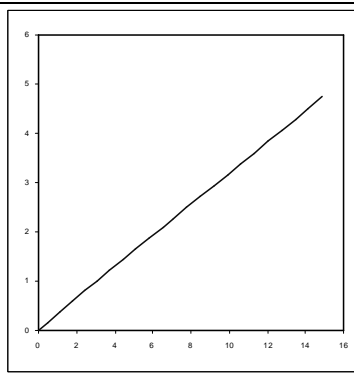
Specimen 4A  
Modulus of Elasticity (y-axis)  
= 21,543



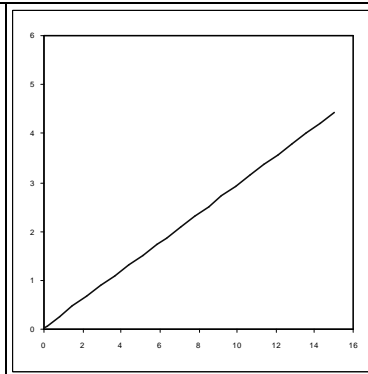
Specimen 4B  
Modulus of Elasticity (y-axis)  
= 21,075



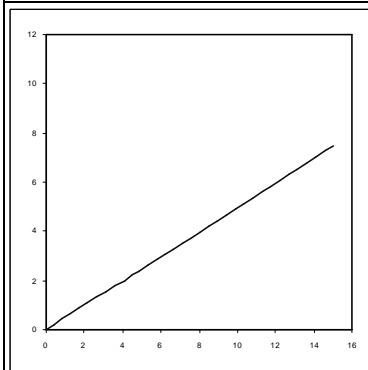
Specimen 5  
Modulus of Elasticity (x-axis)  
= 19,824



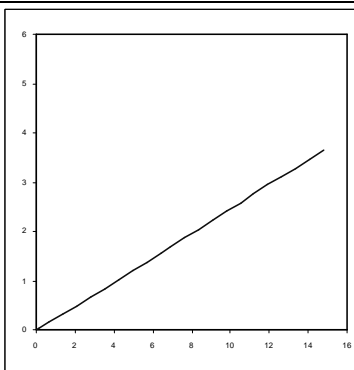
Specimen 5A  
Modulus of Elasticity (y-axis)  
= 22,414



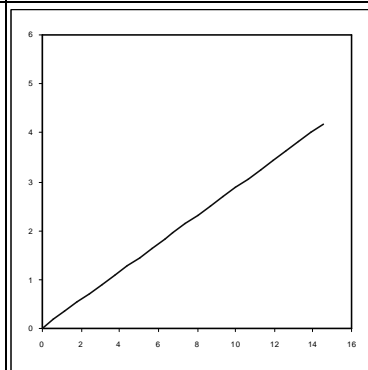
Specimen 5B  
Modulus of Elasticity (y-axis)  
= 20,857



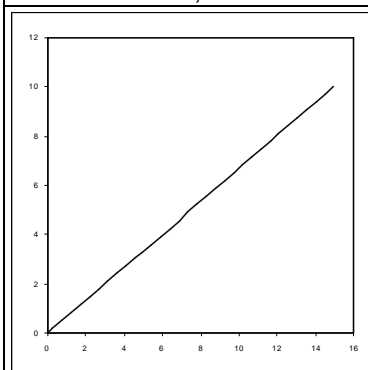
Specimen 6  
Modulus of Elasticity (x-axis)  
= 17,868



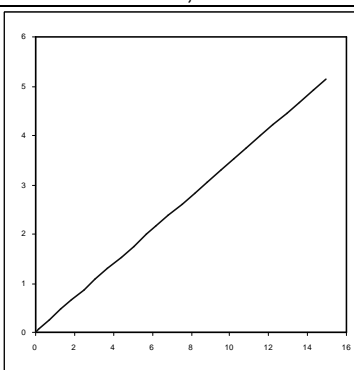
Specimen 6A  
Modulus of Elasticity (y-axis)  
= 17,732



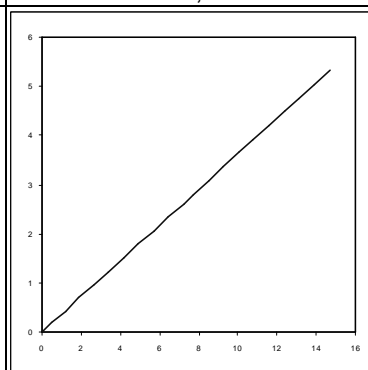
Specimen 6B  
Modulus of Elasticity (y-axis)  
= 20,366



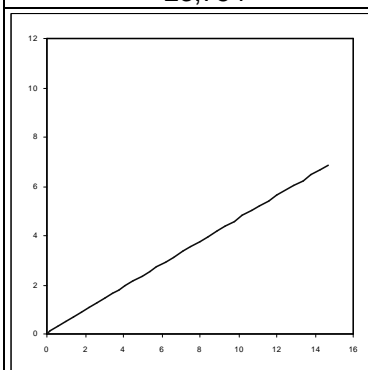
Specimen 7  
Modulus of Elasticity (x-axis)  
= 23,754



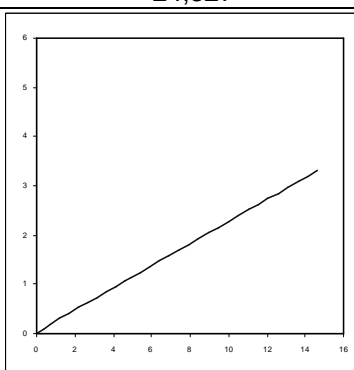
Specimen 7A  
Modulus of Elasticity (y-axis)  
= 24,327



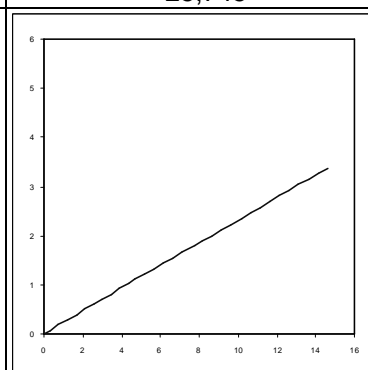
Specimen 7B  
Modulus of Elasticity (y-axis)  
= 25,745



Specimen 8  
Modulus of Elasticity (x-axis)  
= 16,456

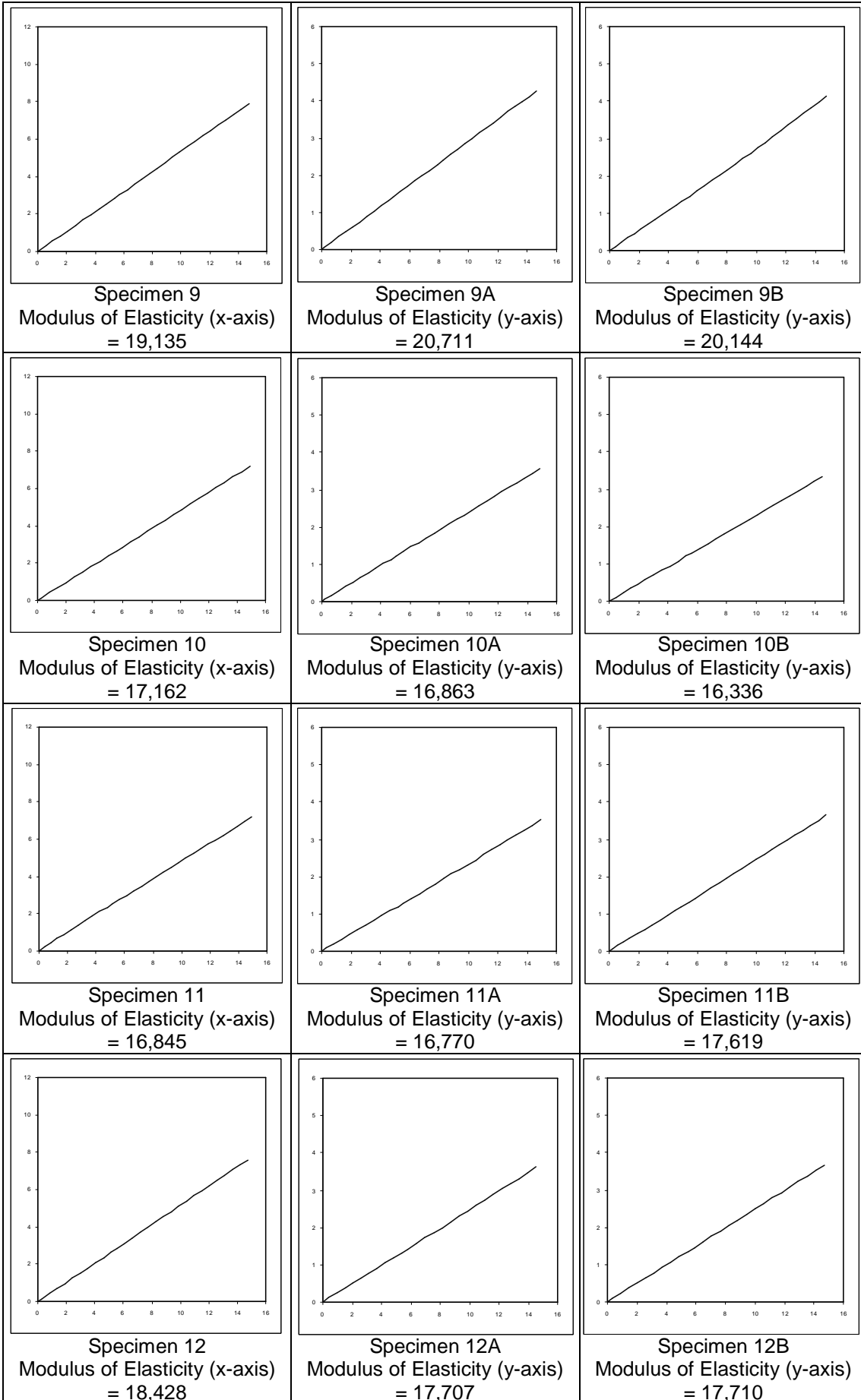


Specimen 8A  
Modulus of Elasticity (y-axis)  
= 15,789



Specimen 8B  
Modulus of Elasticity (y-axis)  
= 16,284





**COMPRESSIVE STRENGTH OF TIMBERS FOR SPACED COLUMNS:**

In order to be able to compare the experimental results with the code provisions, and also to determine the effects of the 35mm SLT holes, the compressive strength of the timber was tested. The 24 pieces of timber were sorted in order of their modulus of elasticity, and matched into pairs. The timbers were then cut to size (1225mm), and the ends of most of the timbers were tested for compressive strength (some were not due to irregular lengths).

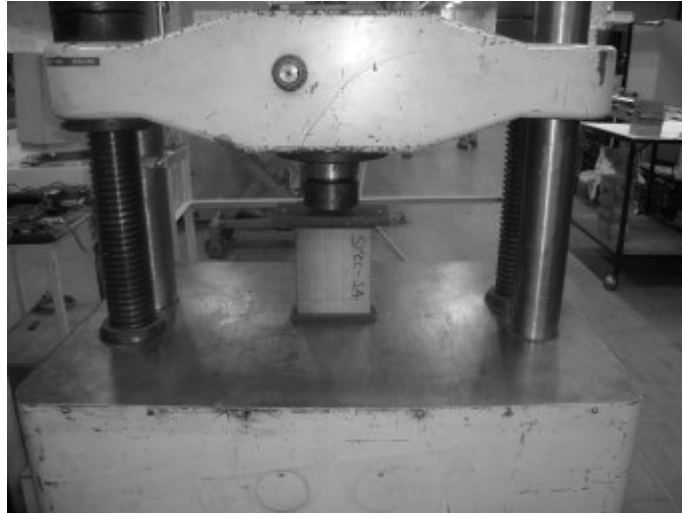
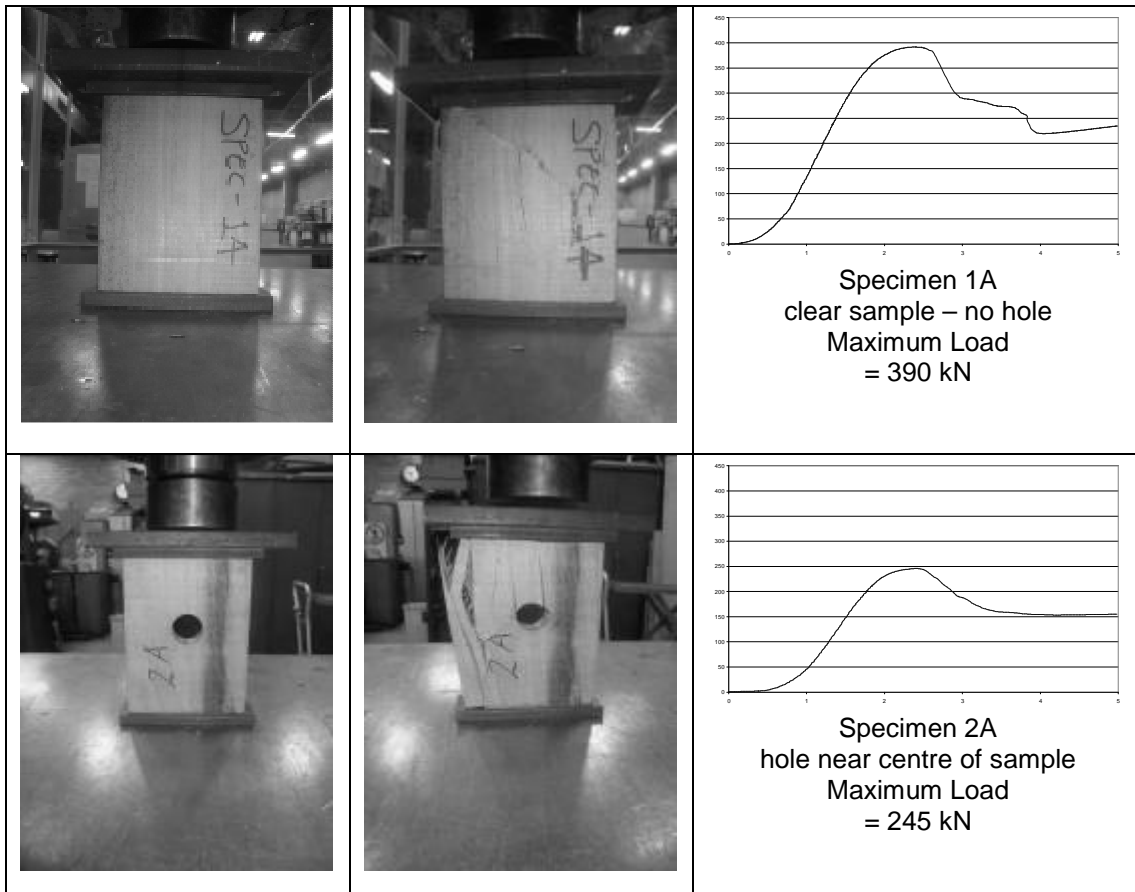
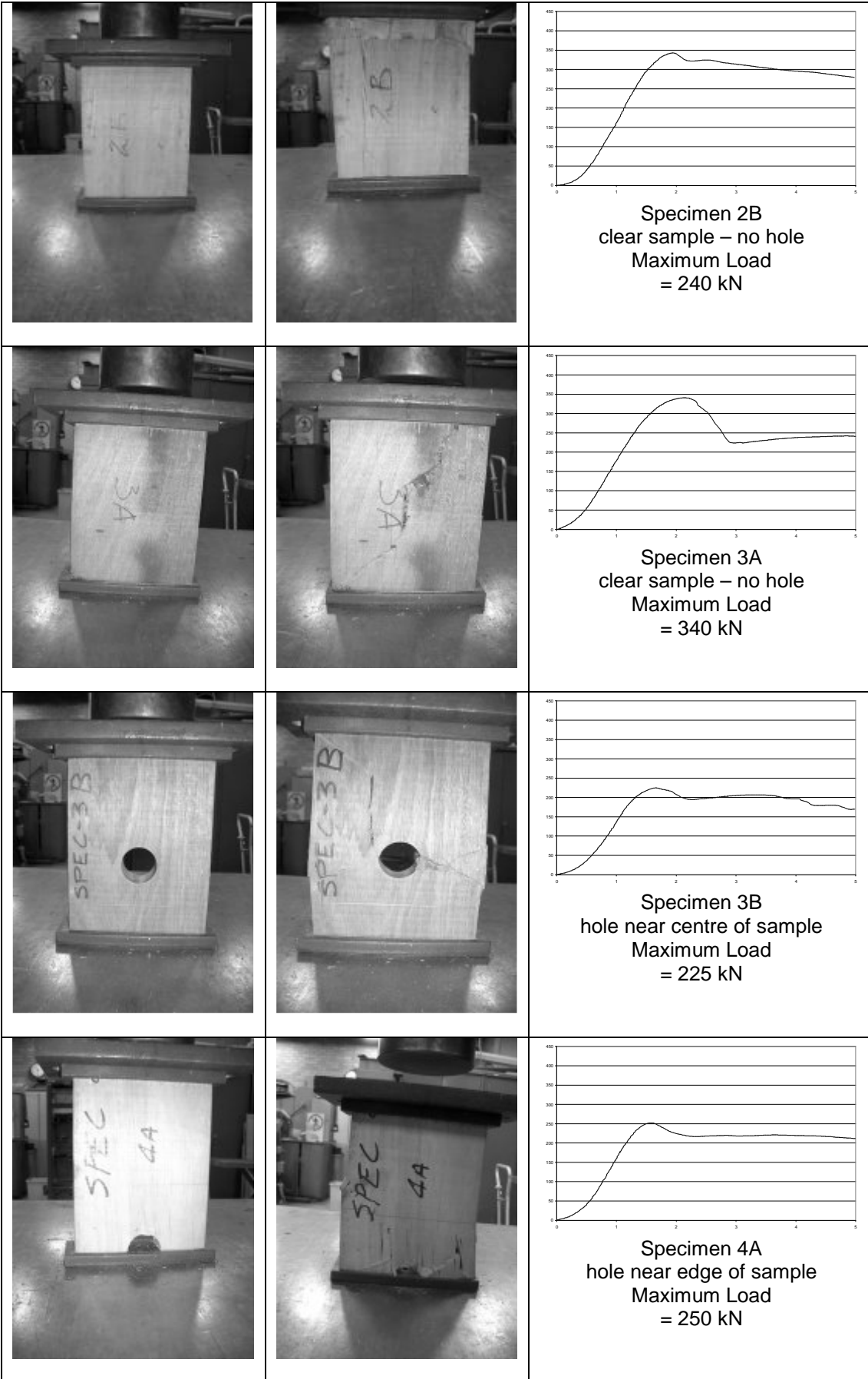
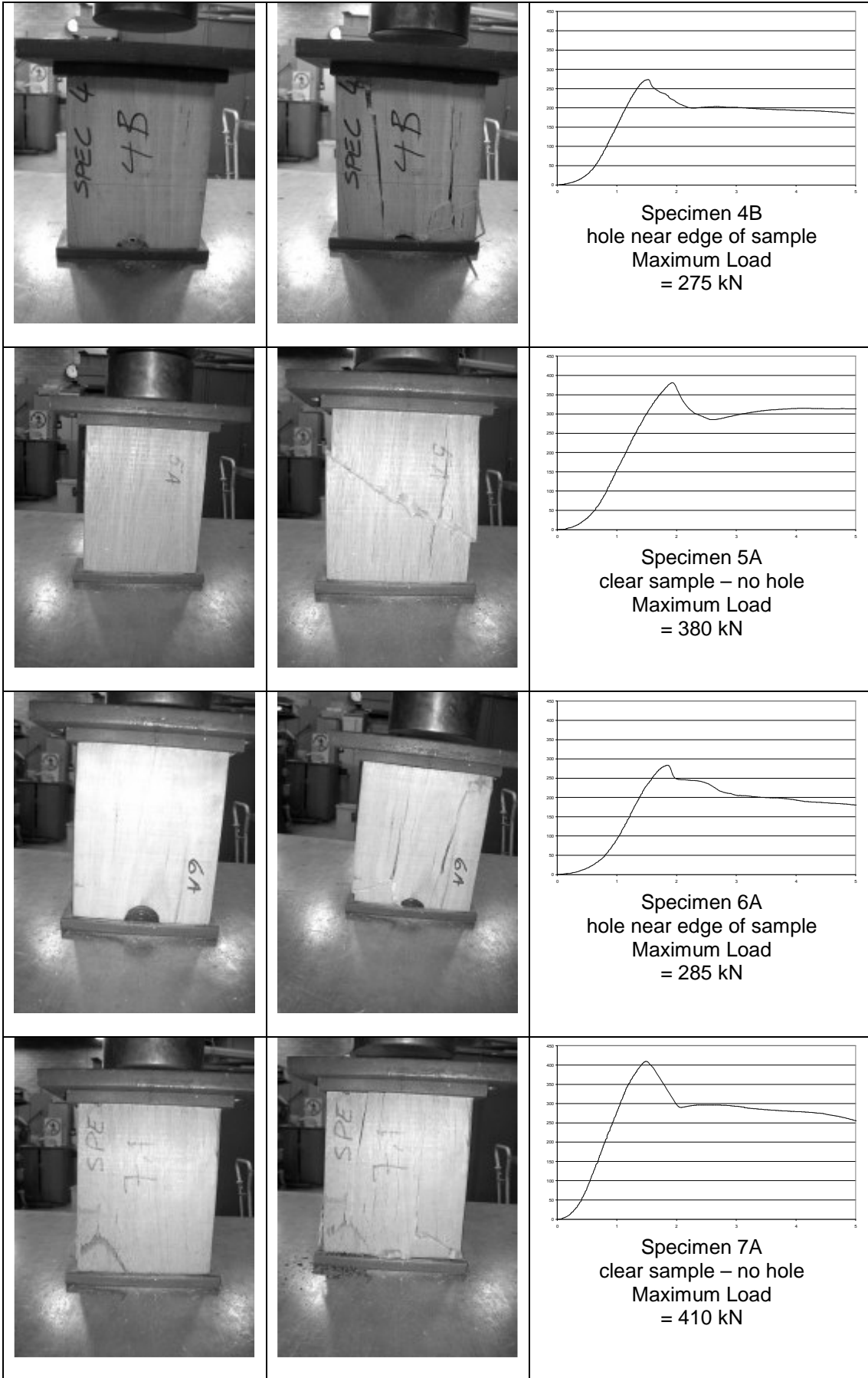


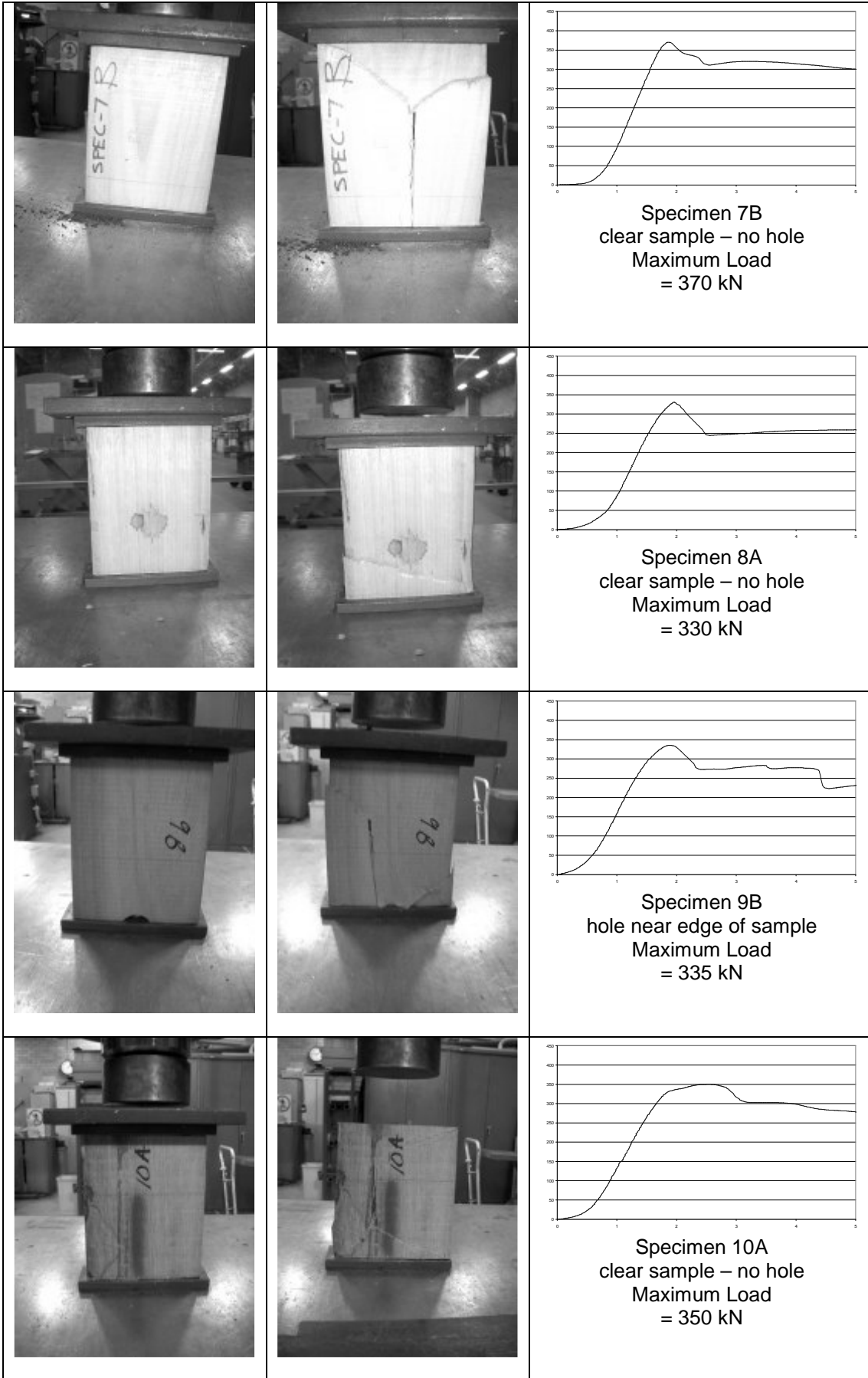
Figure A.2: Shimadzu Universal Testing Machine (500kN capacity)

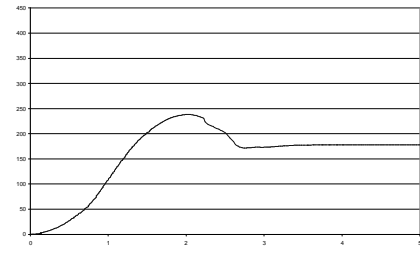
Results below show photographs of each sample before and after testing to show the modes of failure. A plot is also included of load vs cross head travel for each compression test. Load is on the vertical axis to a maximum of 450kN. Cross Head Travel (ie. vertical movement of the testing machine) is plotted on the horizontal axis to a maximum of 5mm.



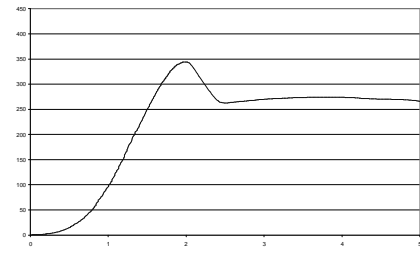




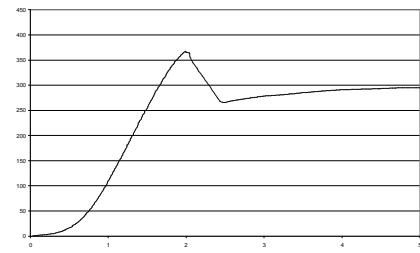




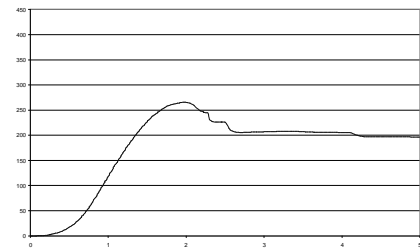
Specimen 10B  
hole near centre of sample  
Maximum Load  
= 240 kN



Specimen 11B  
clear sample – no hole  
Maximum Load  
= 345 kN



Specimen 12A  
clear sample – no hole  
Maximum Load  
= 365 kN



Specimen 12B  
hole near centre of sample  
Maximum Load  
= 265 kN

**EXPERIMENTAL RESULTS FOR SPACED COLUMN ASSEMBLY 11B12A:**

	11B	12A
Modulus of Elasticity (x axis)	16,845	18,428
Modulus of Elasticity (y axis)	17,619	17,707
Compressive Strength	345 (no hole)	365 (no hole)
Assembly Buckling Load	301.0 kN	

Figure A.3: Summary of Results for Assembly 11B12A

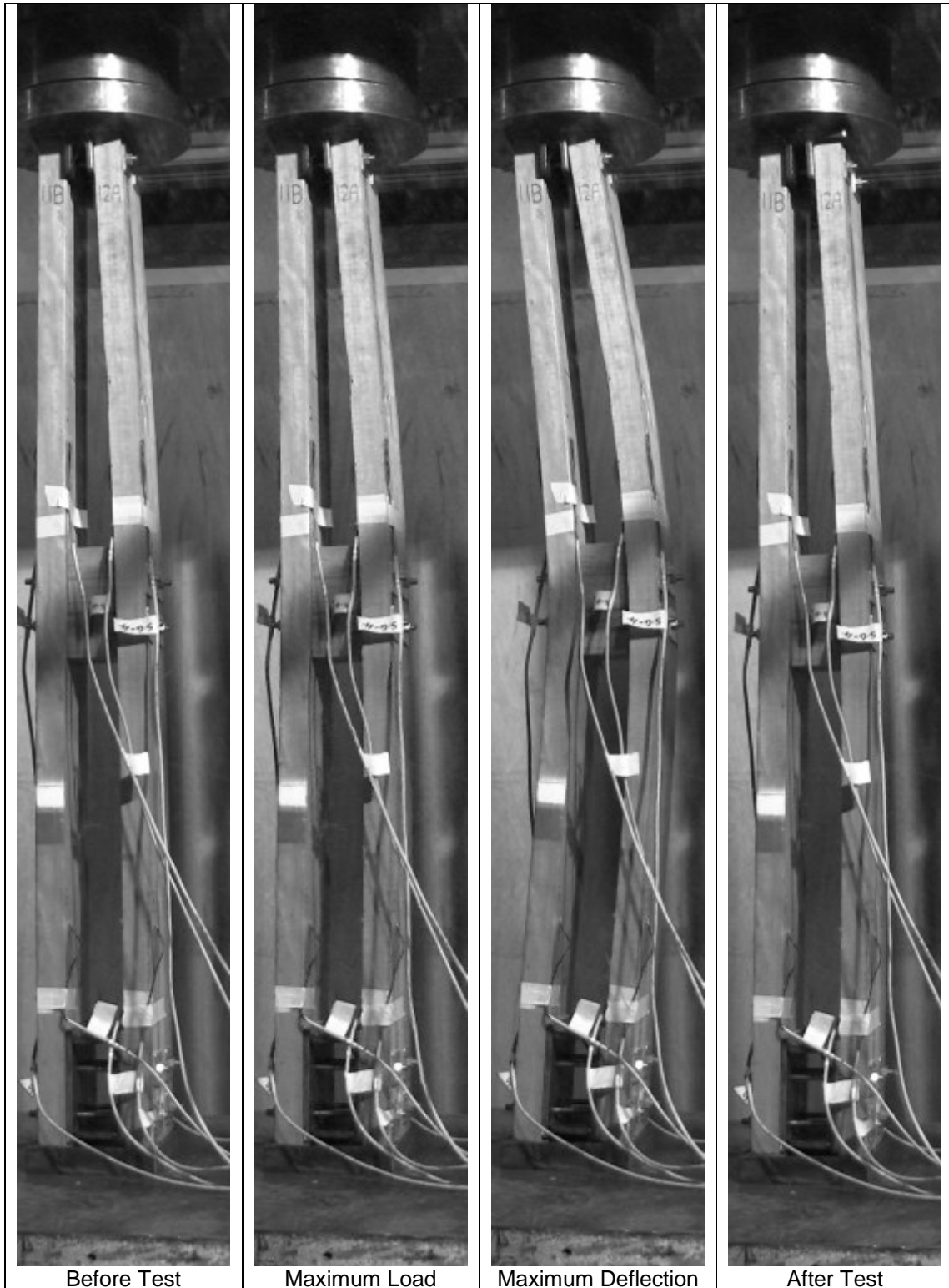
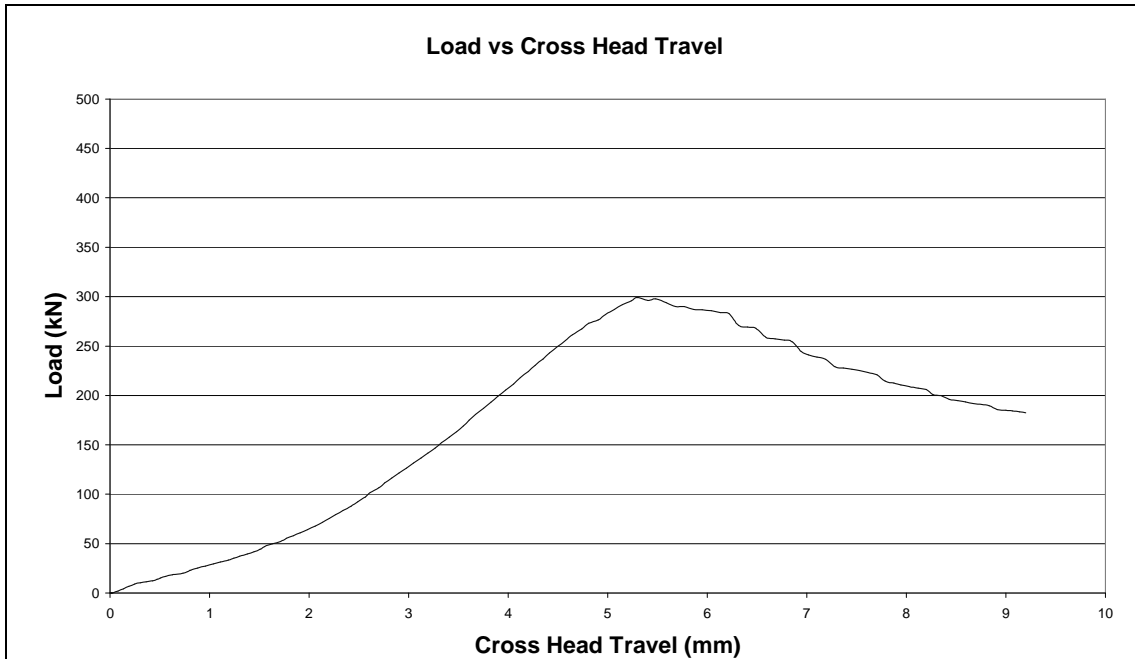


Figure A.4: Photographs of test for Assembly 11B12A



Figure A.5: Photographs of failure locations for Assembly 11B12A





The graph below shows the strains recorded at each of the strain gauges during the test.

Gauges 1 to 4 were located 135mm above the top line of bolts for the central timber spacer:

- Strain Gauge 1 is on the left hand outer face.
- Strain Gauge 2 is on the left hand inner face.
- Strain Gauge 3 is on the right hand inner face.
- Strain Gauge 4 is on the right hand outer face.

Gauges 5 to 8 were located 135mm above the top line of the bolts for the bottom steel box:

- Strain Gauge 5 is on the left hand outer face.
- Strain Gauge 6 is on the left hand inner face.
- Strain Gauge 7 is on the right hand inner face.
- Strain Gauge 8 is on the right hand outer face.

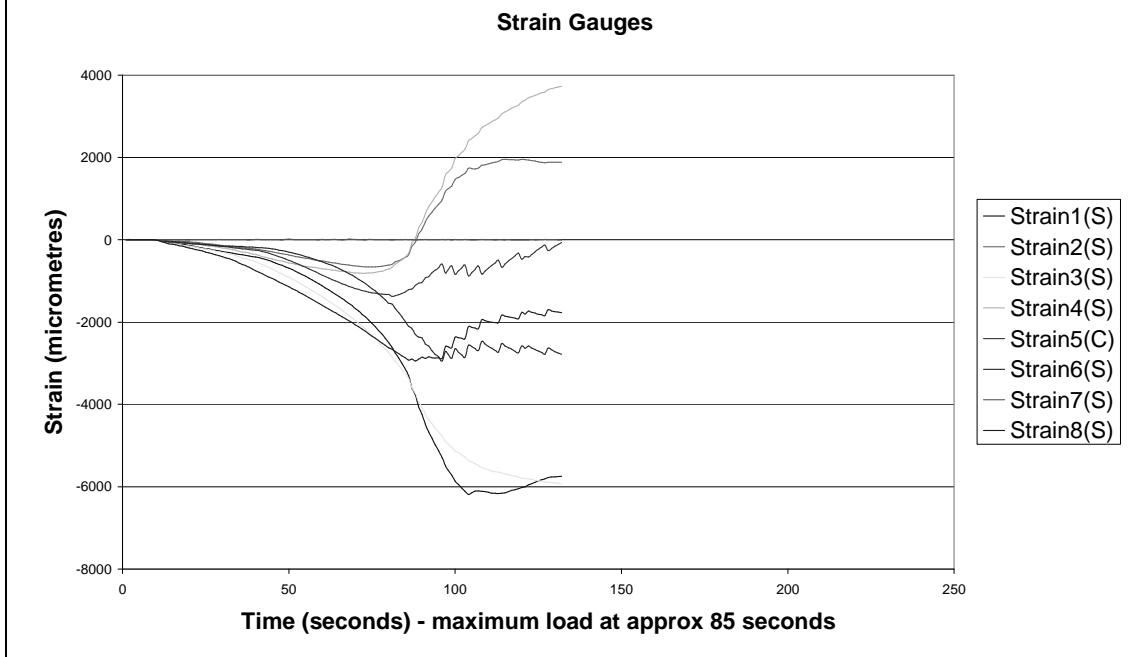


Figure A.6: Graphs for Assembly 11B12A

**EXPERIMENTAL RESULTS FOR SPACED COLUMN ASSEMBLY 08A02A:**

	08A	02A
Modulus of Elasticity (x axis)	16,456	15,539
Modulus of Elasticity (y axis)	15,789	16,228
Compressive Strength	330 (no hole)	245 (at hole)
Assembly Buckling Load	275.5 kN	

Figure A.7: Summary of Results for Assembly 08A02A

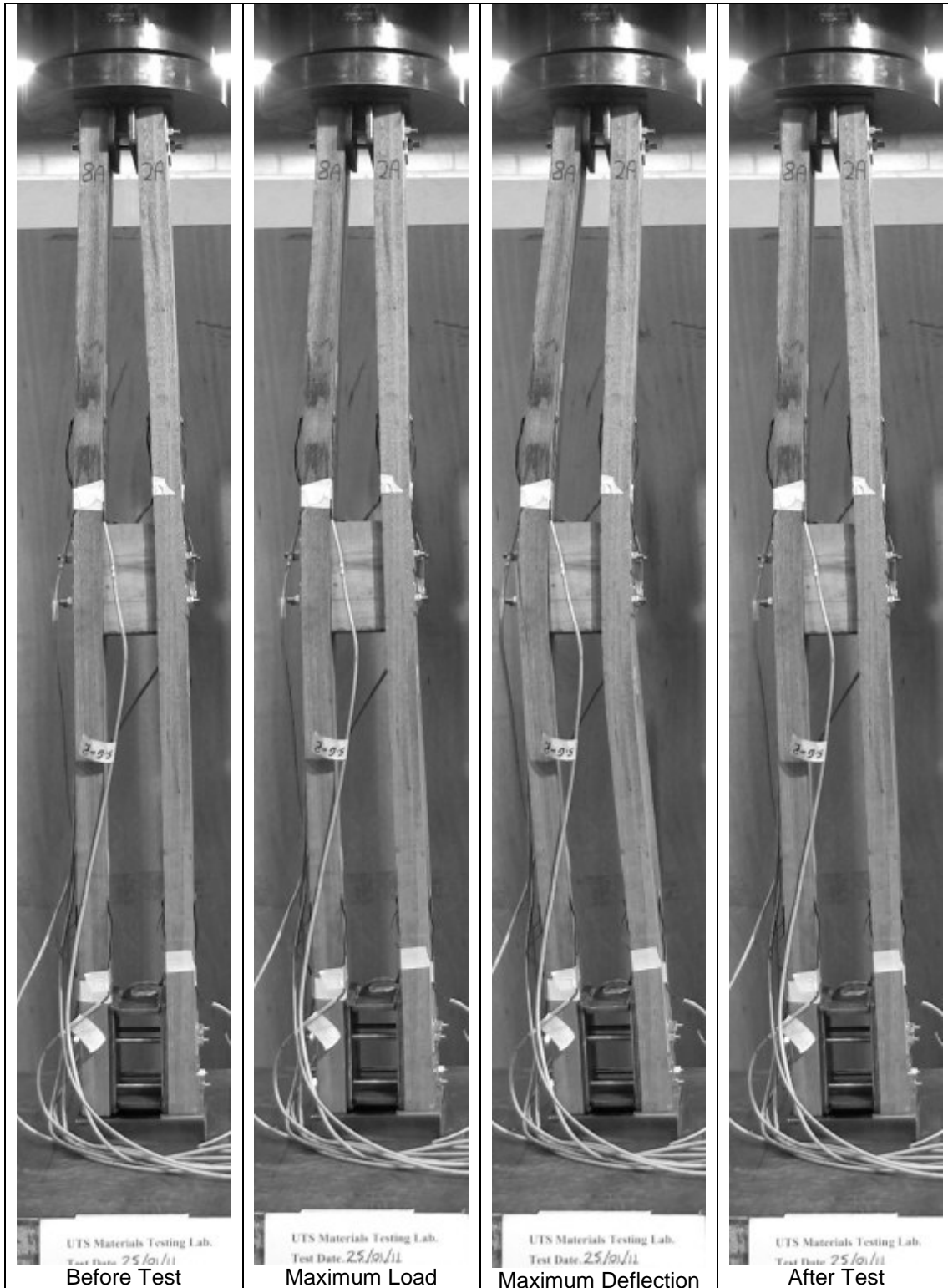
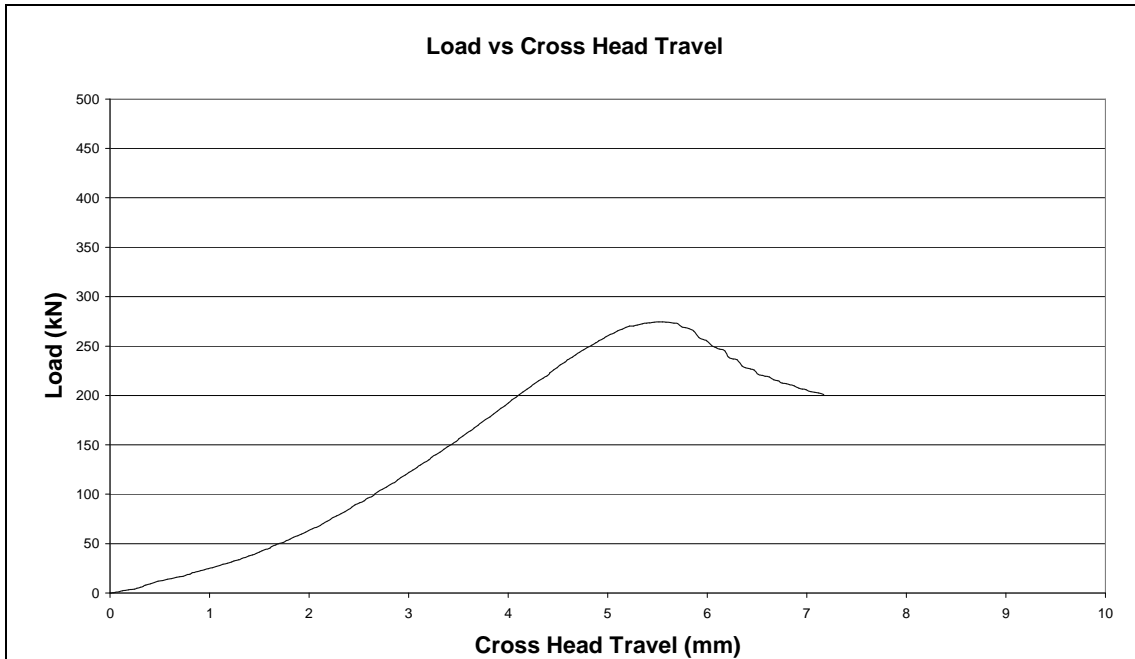


Figure A.8: Photographs of test for Assembly 08A02A



*Figure A.9: Photographs of failure locations for Assembly 08A02A*



The graph below shows the strains recorded at each of the strain gauges during the test.

Gauges 1 to 4 were located 135mm above the top line of bolts for the central timber spacer:

- Strain Gauge 1 is on the left hand outer face.
- Strain Gauge 2 is on the left hand inner face.
- Strain Gauge 3 is on the right hand inner face.
- Strain Gauge 4 is on the right hand outer face.

Gauges 5 to 8 were located 135mm above the top line of the bolts for the bottom steel box:

- Strain Gauge 5 is on the left hand outer face.
- Strain Gauge 6 is on the left hand inner face.
- Strain Gauge 7 is on the right hand inner face.
- Strain Gauge 8 is on the right hand outer face.

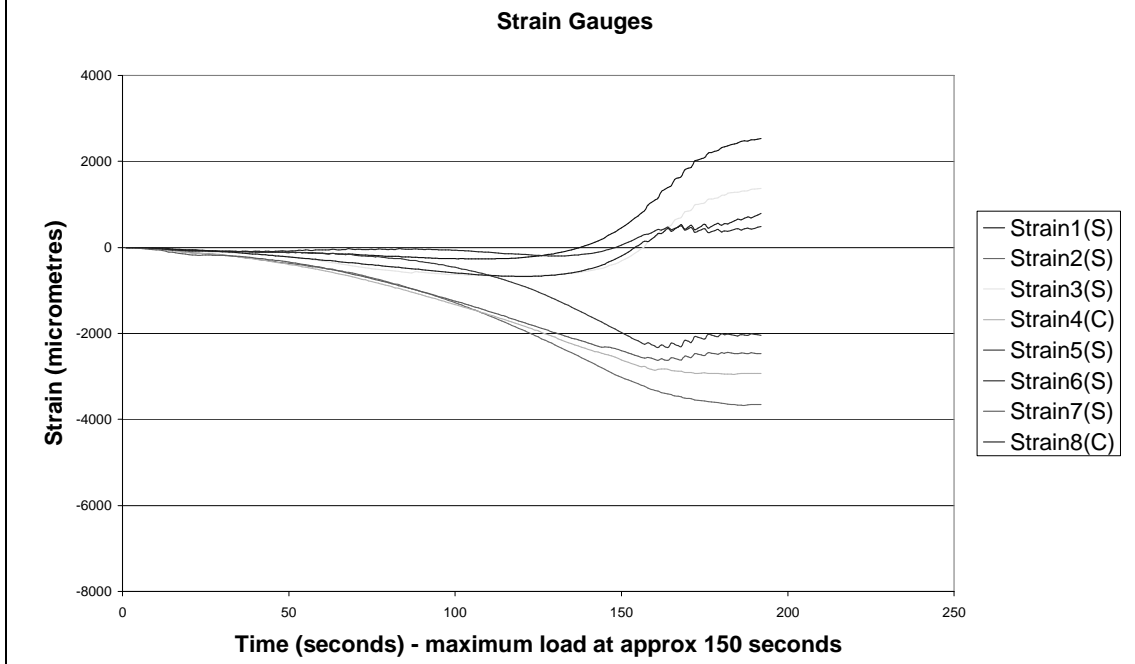


Figure A.10: Graphs for Assembly 08A02A

**EXPERIMENTAL RESULTS FOR SPACED COLUMN ASSEMBLY 11A10A:**

	11A	10A
Modulus of Elasticity (x axis)	16,845	17,162
Modulus of Elasticity (y axis)	16,770	16,863
Compressive Strength	no result	350 (no hole)
Assembly Buckling Load	331.0 kN	

Figure A.11: Summary of Results for Assembly 11A10A

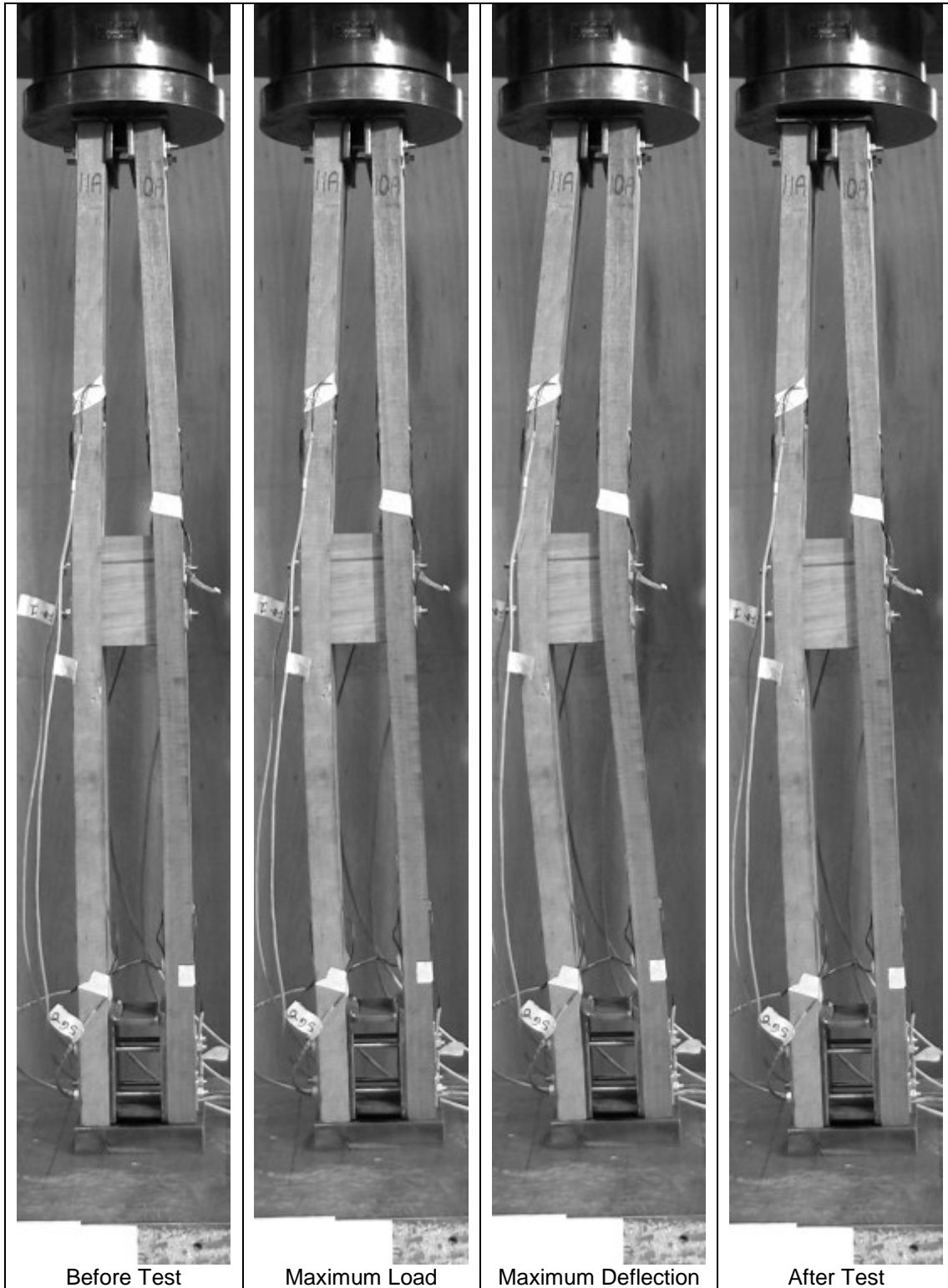
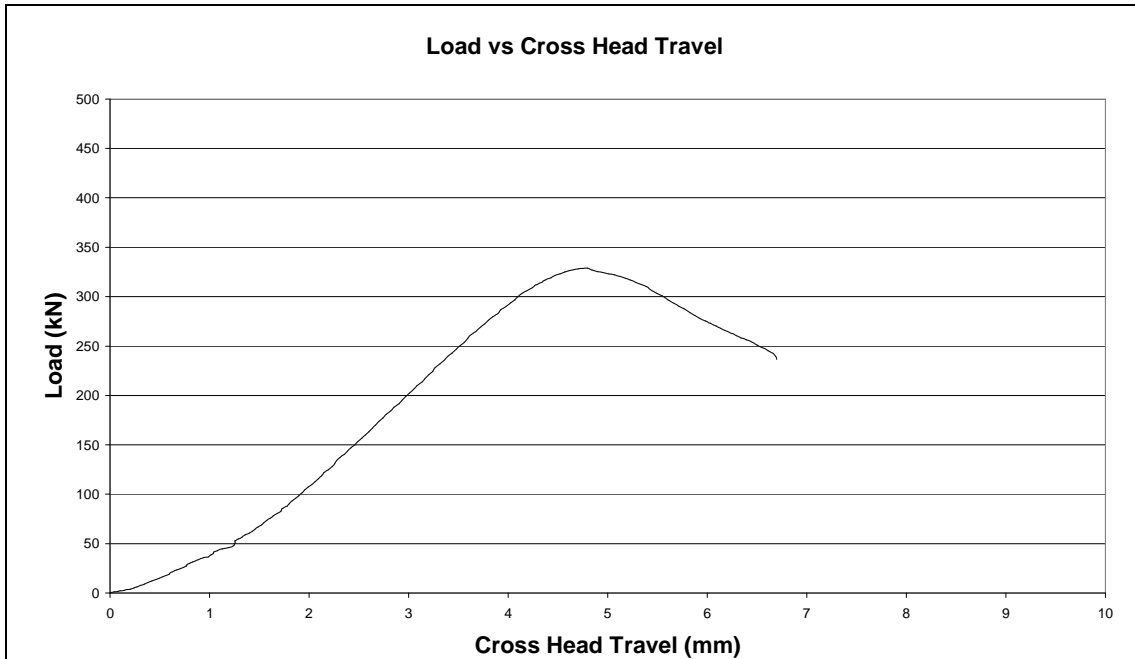


Figure A.12: Photographs of test for Assembly 11A10A



Figure A.13: Photographs of failure locations for Assembly 11A10A



The graph below shows the strains recorded at each of the strain gauges during the test.

Gauges 1 to 4 were located 135mm above the top line of bolts for the central timber spacer:

- Strain Gauge 1 is on the left hand outer face.
- Strain Gauge 2 is on the left hand inner face.
- Strain Gauge 3 is on the right hand inner face.
- Strain Gauge 4 is on the right hand outer face.

Gauges 5 to 8 were located 135mm above the top line of the bolts for the bottom steel box:

- Strain Gauge 5 is on the left hand outer face.
- Strain Gauge 6 is on the left hand inner face.
- Strain Gauge 7 is on the right hand inner face.
- Strain Gauge 8 is on the right hand outer face.

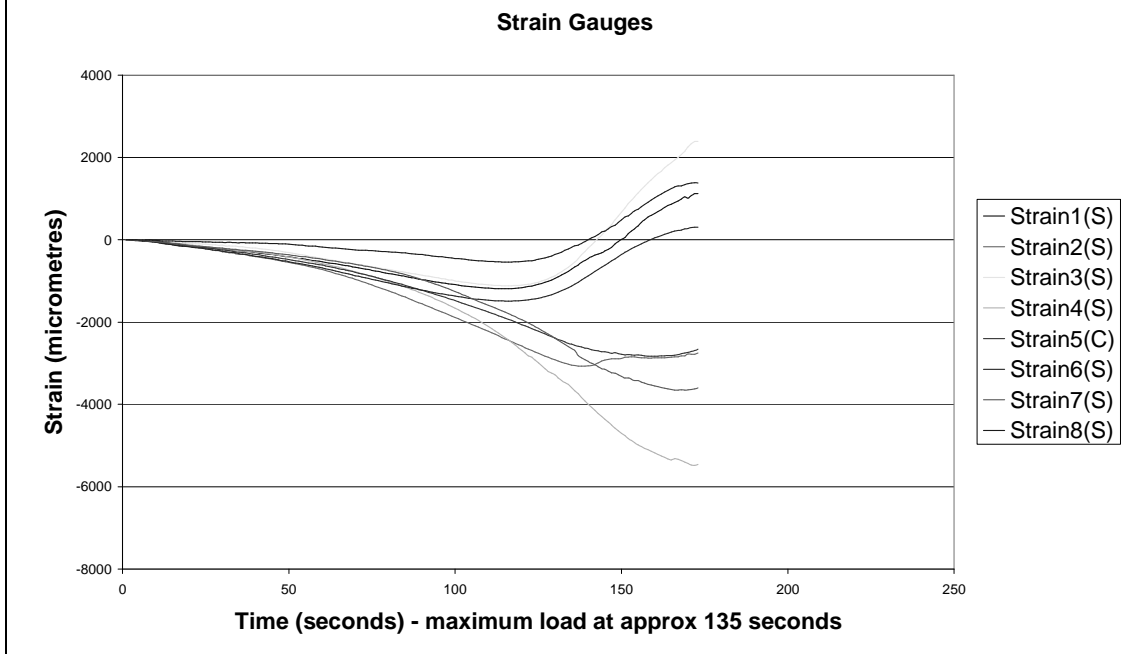


Figure A.14: Graphs for Assembly 11A10A

**EXPERIMENTAL RESULTS FOR SPACED COLUMN ASSEMBLY 10B02B:**

	10B	02B
Modulus of Elasticity (x axis)	17,162	15,539
Modulus of Elasticity (y axis)	16,336	16,309
Compressive Strength	240 (at hole)	340 (no hole)
Assembly Buckling Load	302.5 kN	

Figure A.15: Summary of Results for Assembly 10B02B

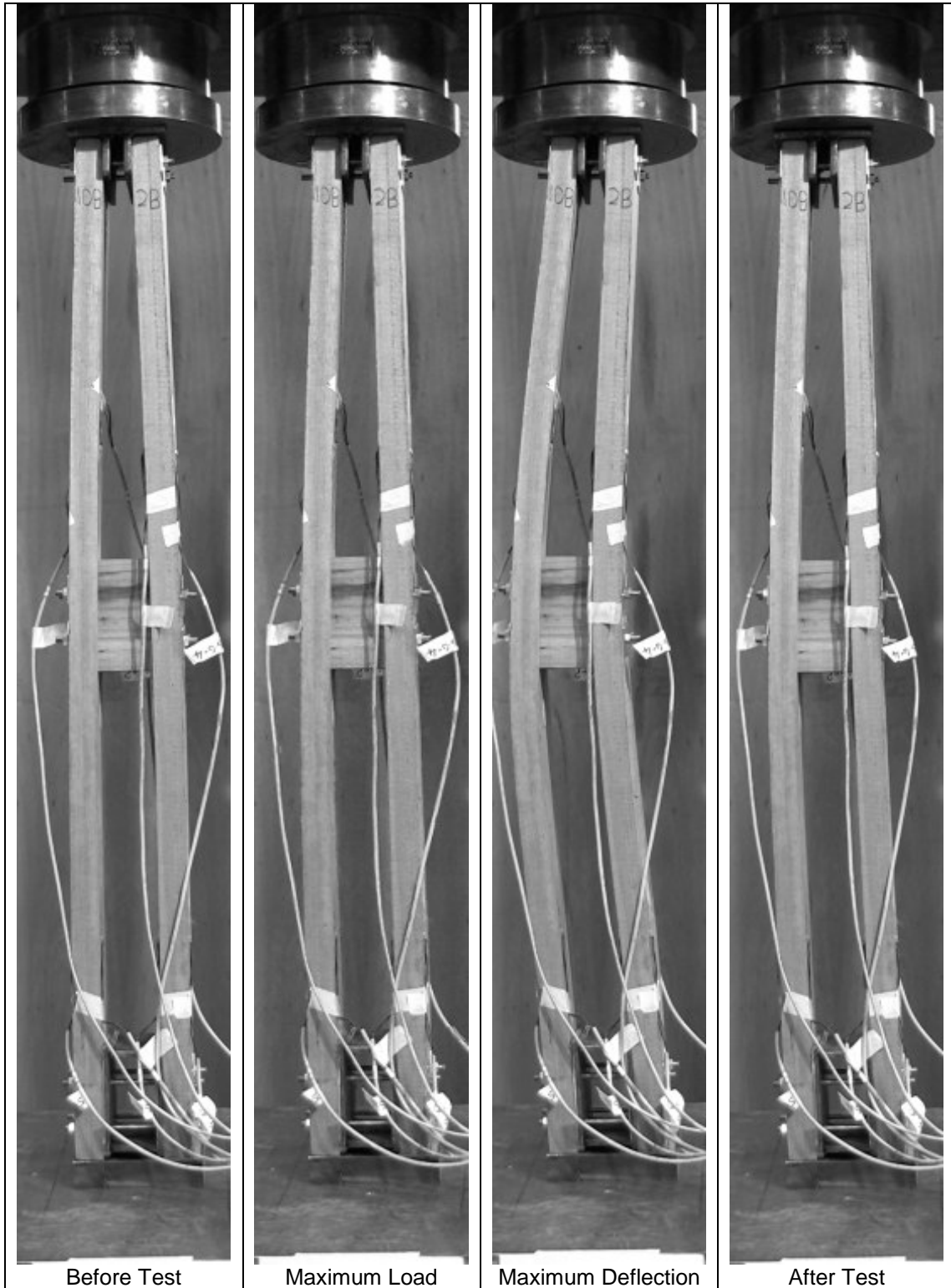


Figure A.16: Photographs of test for Assembly 10B02B



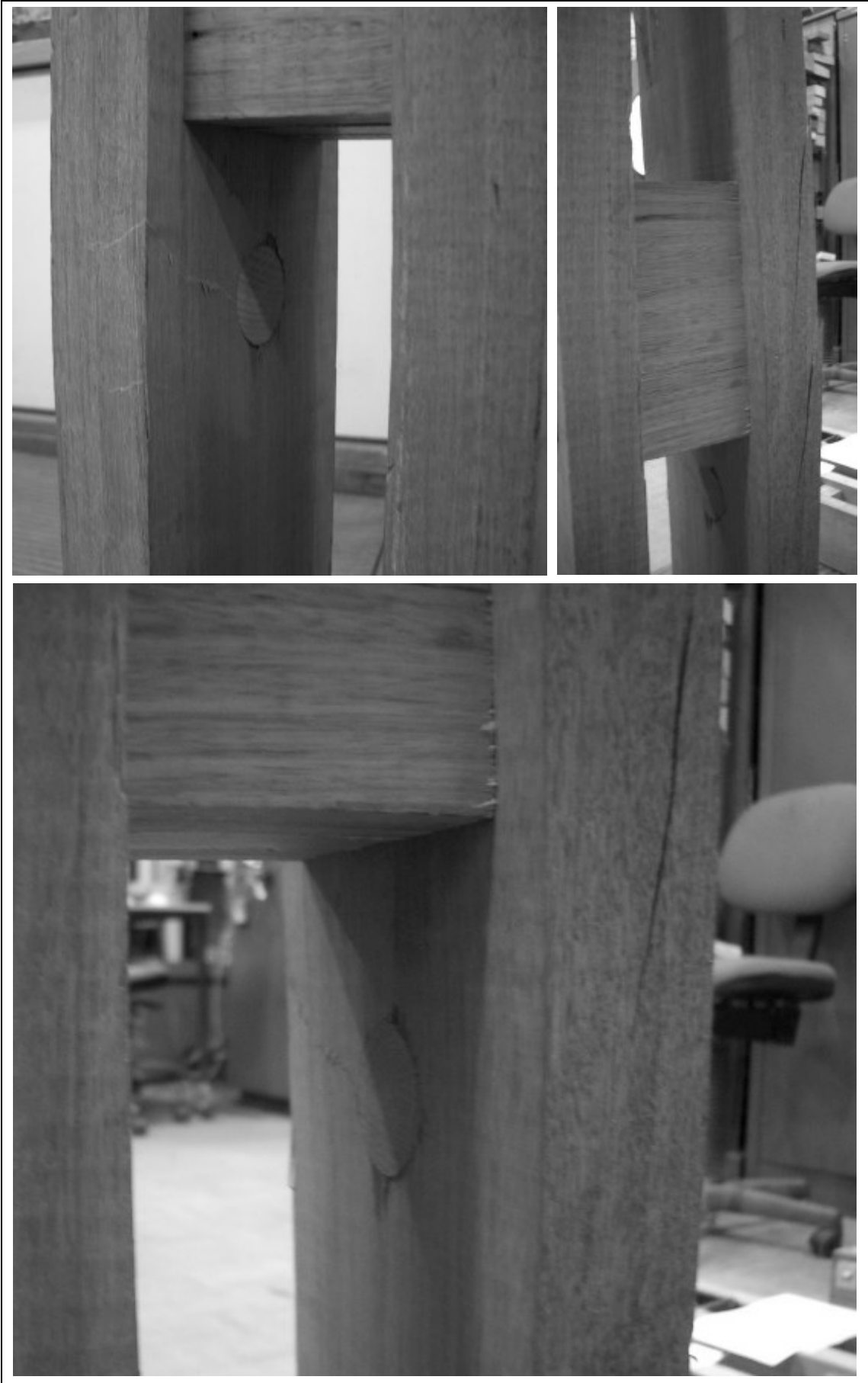
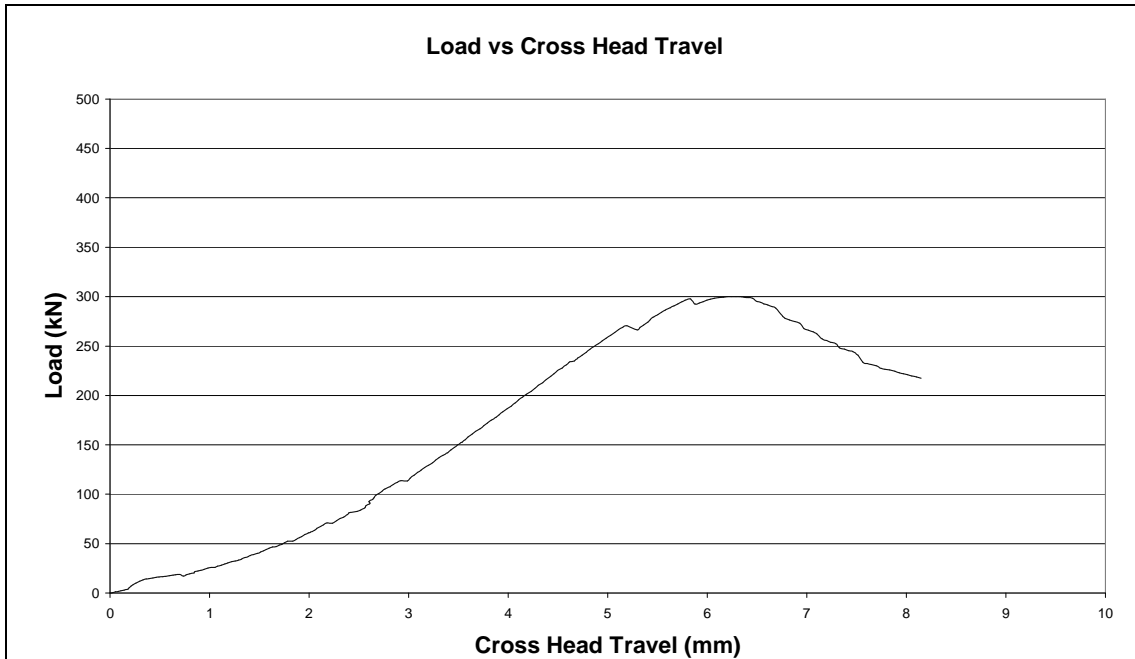


Figure A.17: Photographs of failure locations for Assembly 10B02B



The graph below shows the strains recorded at each of the strain gauges during the test.

Gauges 1 to 4 were located 135mm above the top line of bolts for the central timber spacer:

- Strain Gauge 1 is on the left hand outer face.
- Strain Gauge 2 is on the left hand inner face.
- Strain Gauge 3 is on the right hand inner face.
- Strain Gauge 4 is on the right hand outer face.

Gauges 5 to 8 were located 135mm above the top line of the bolts for the bottom steel box:

- Strain Gauge 5 is on the left hand outer face.
- Strain Gauge 6 is on the left hand inner face.
- Strain Gauge 7 is on the right hand inner face.
- Strain Gauge 8 is on the right hand outer face.

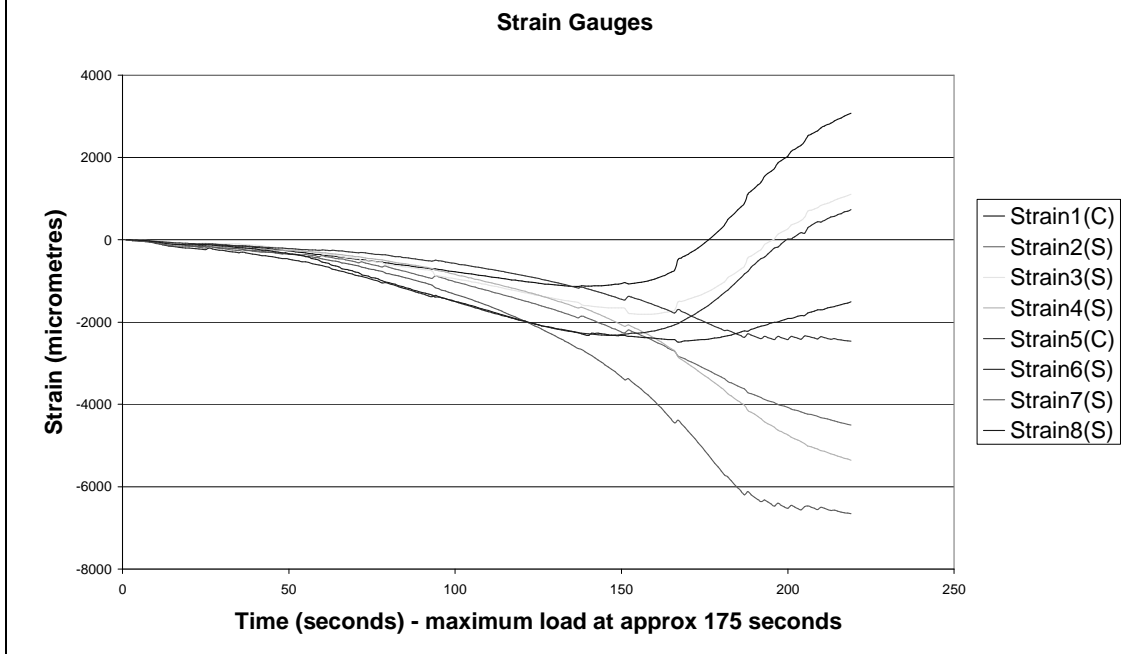


Figure A.18: Graphs for Assembly 10B02B

**EXPERIMENTAL RESULTS FOR SPACED COLUMN ASSEMBLY 05A04A:**

	05A	04A
Modulus of Elasticity (x axis)	19,824	18,064
Modulus of Elasticity (y axis)	22,414	21,543
Compressive Strength	380 (no hole)	250 (at hole)
Assembly Buckling Load	463.0 kN	

Figure A.19: Summary of Results for Assembly 05A04A

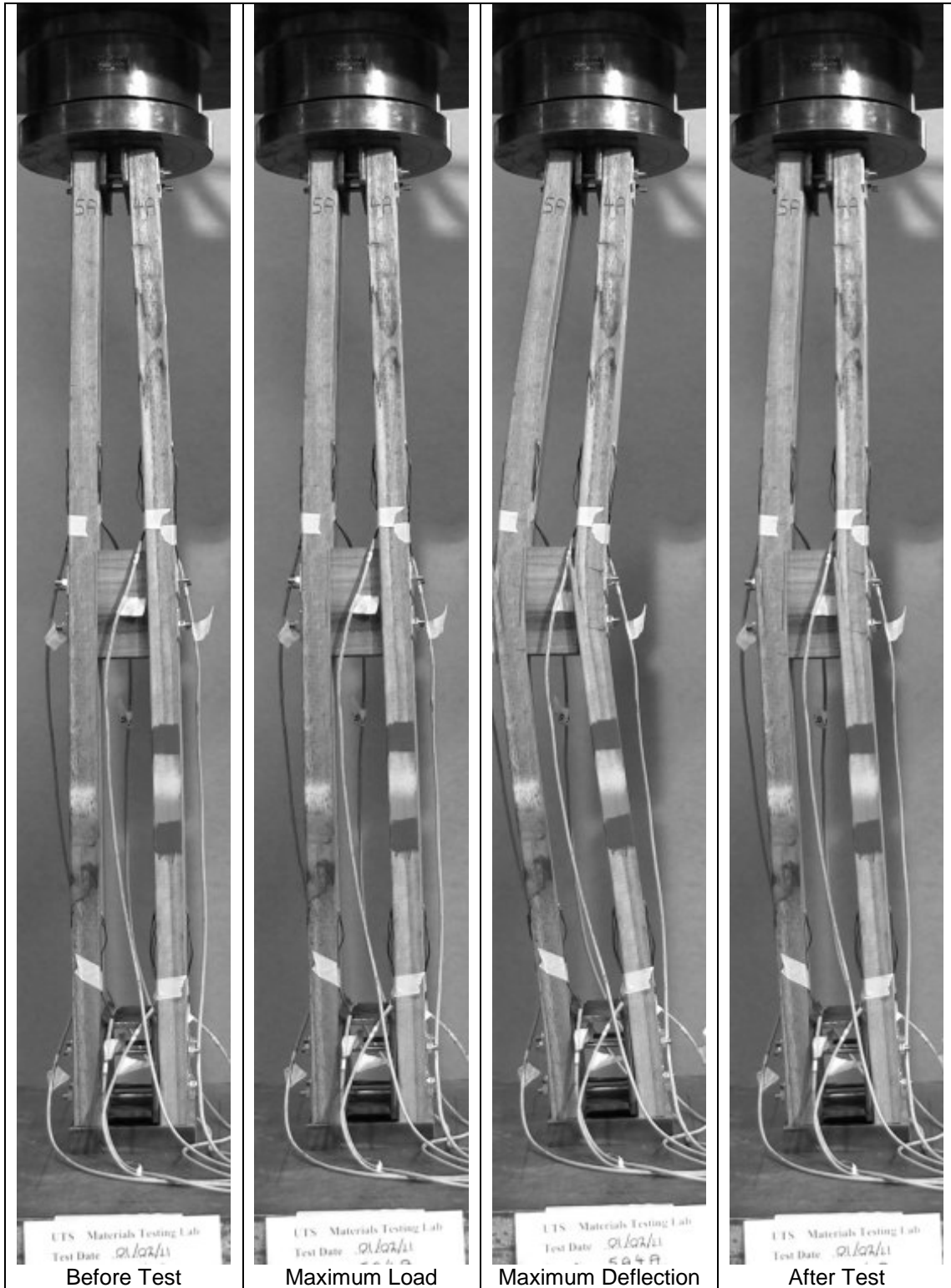


Figure A.20: Photographs of test for Assembly 05A04A

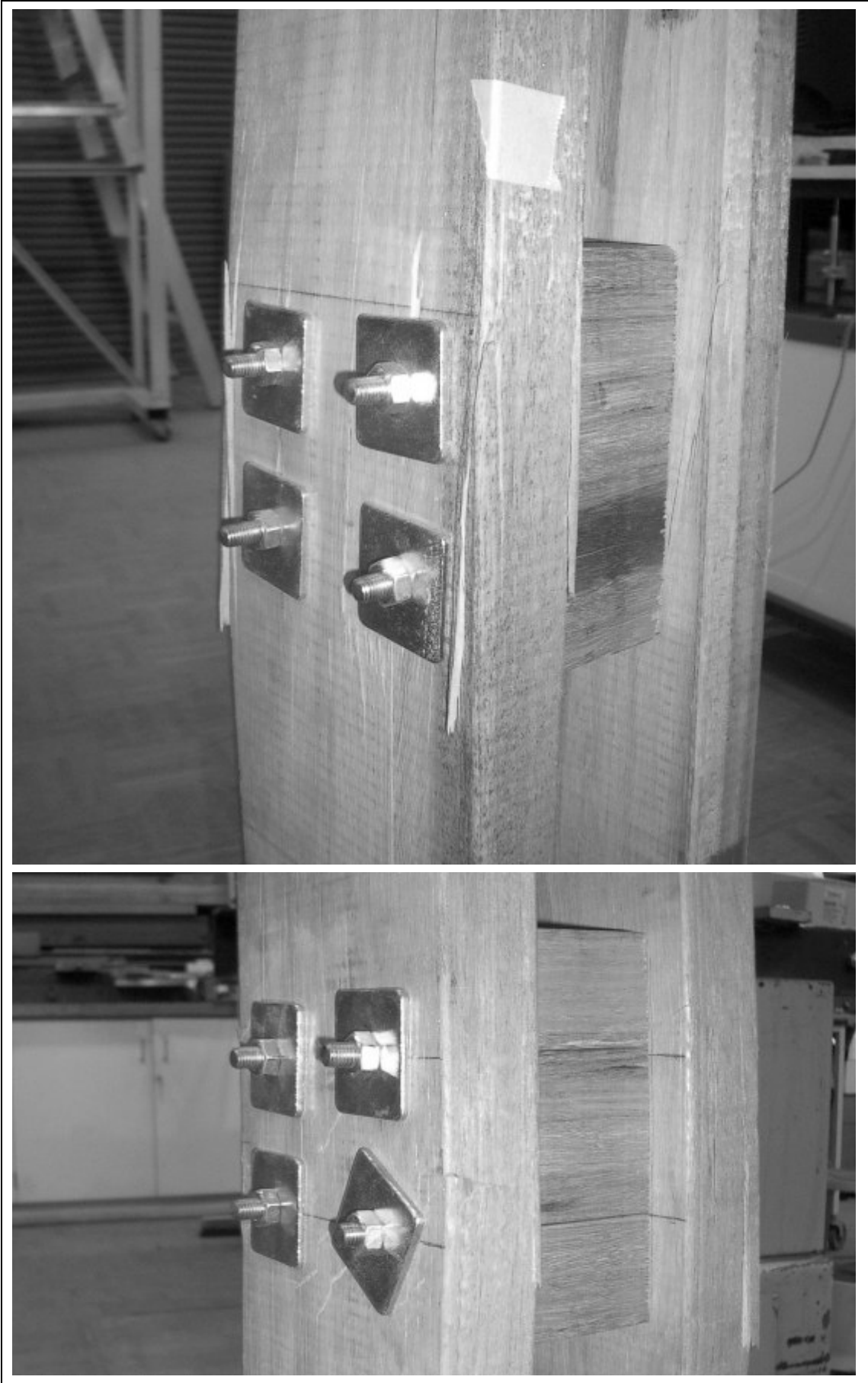
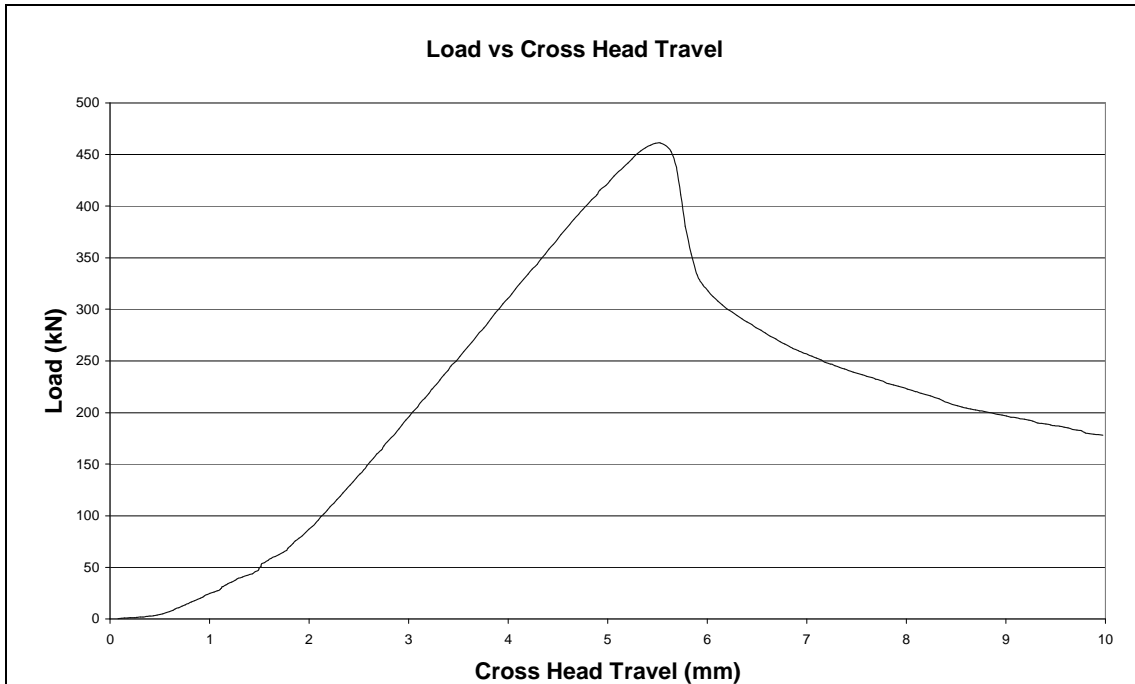


Figure A.21: Photographs of failure locations for Assembly 05A04A



The graph below shows the strains recorded at each of the strain gauges during the test.

Gauges 1 to 4 were located 135mm above the top line of bolts for the central timber spacer:

- Strain Gauge 1 is on the left hand outer face.
- Strain Gauge 2 is on the left hand inner face.
- Strain Gauge 3 is on the right hand inner face.
- Strain Gauge 4 is on the right hand outer face.

Gauges 5 to 8 were located 135mm above the top line of the bolts for the bottom steel box:

- Strain Gauge 5 is on the left hand outer face.
- Strain Gauge 6 is on the left hand inner face.
- Strain Gauge 7 is on the right hand inner face.
- Strain Gauge 8 is on the right hand outer face.

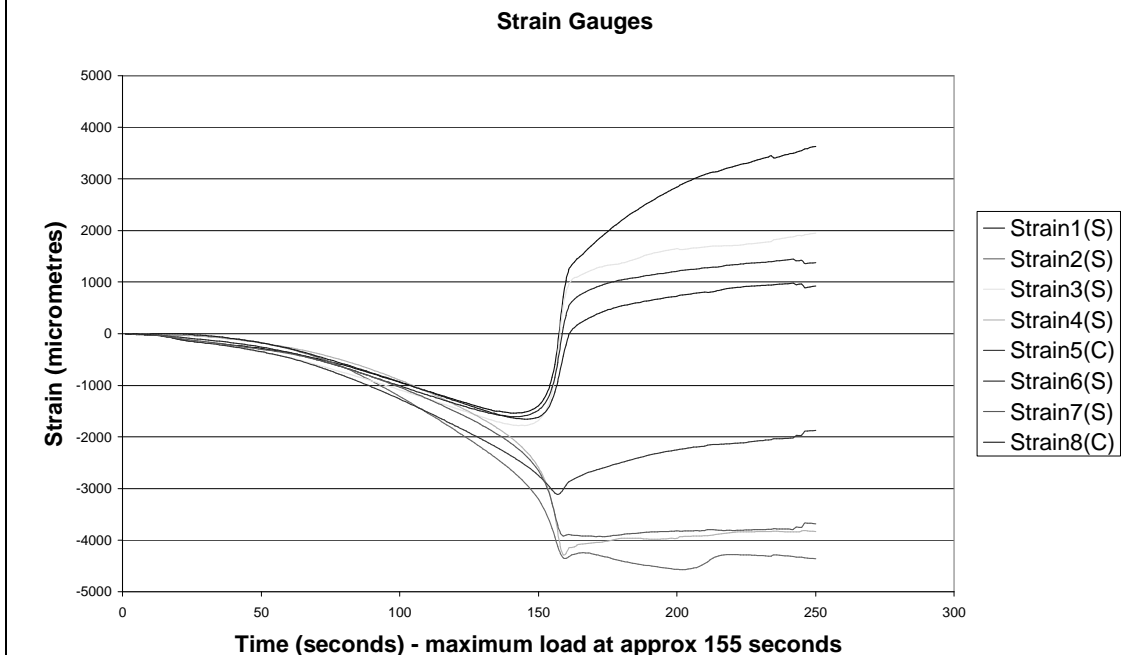


Figure A.22: Graphs for Assembly 05A04A

**EXPERIMENTAL RESULTS FOR SPACED COLUMN ASSEMBLY 07B07A:**

	07B	07A
Modulus of Elasticity (x axis)	23,754	23,754
Modulus of Elasticity (y axis)	25,745	24,327
Compressive Strength	370 (no hole)	410 (no hole)
Assembly Buckling Load	457.0 kN	

Figure A.23: Summary of Results for Assembly 07B07A

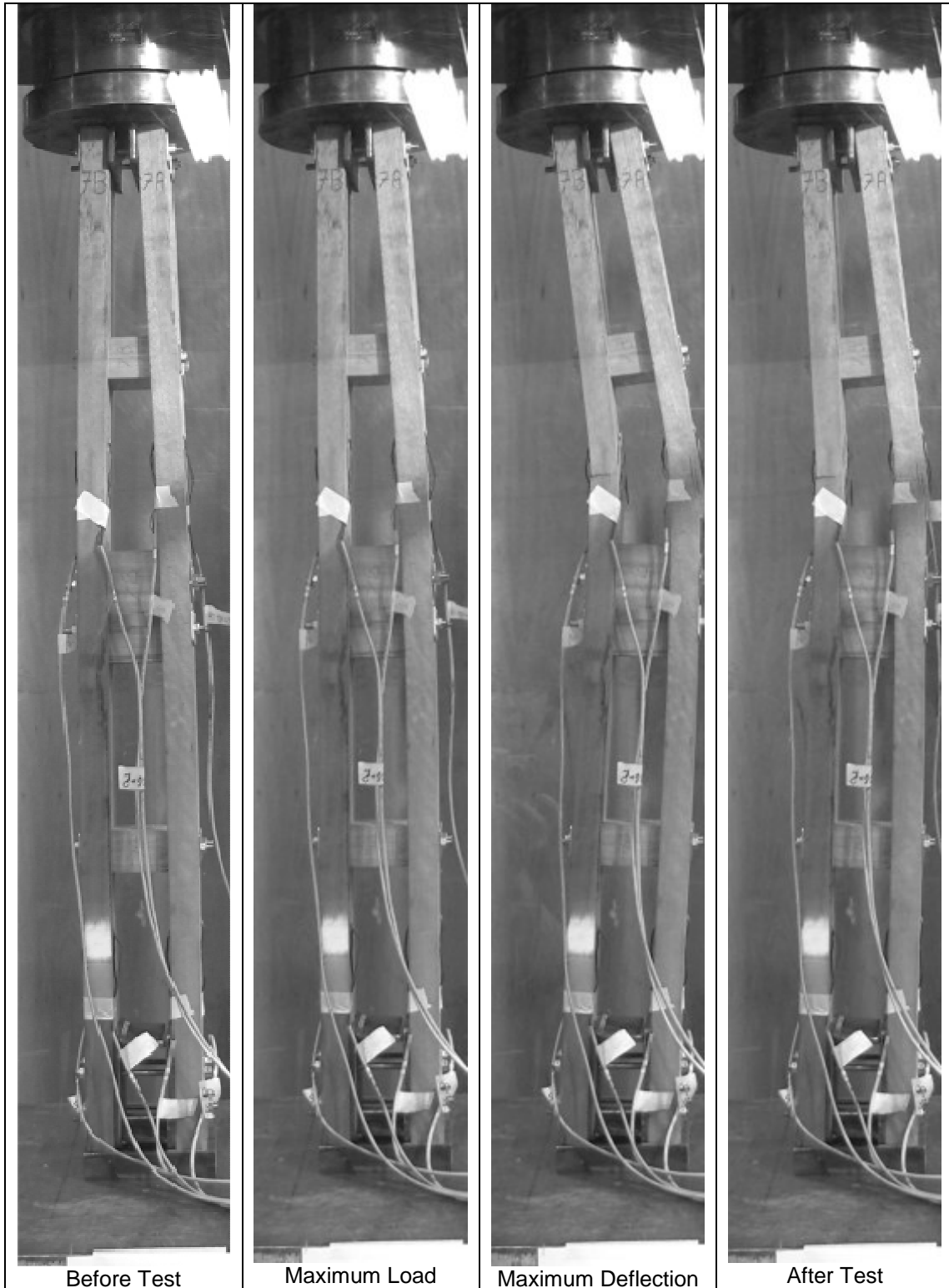


Figure A.24: Photographs of test for Assembly 07B07A

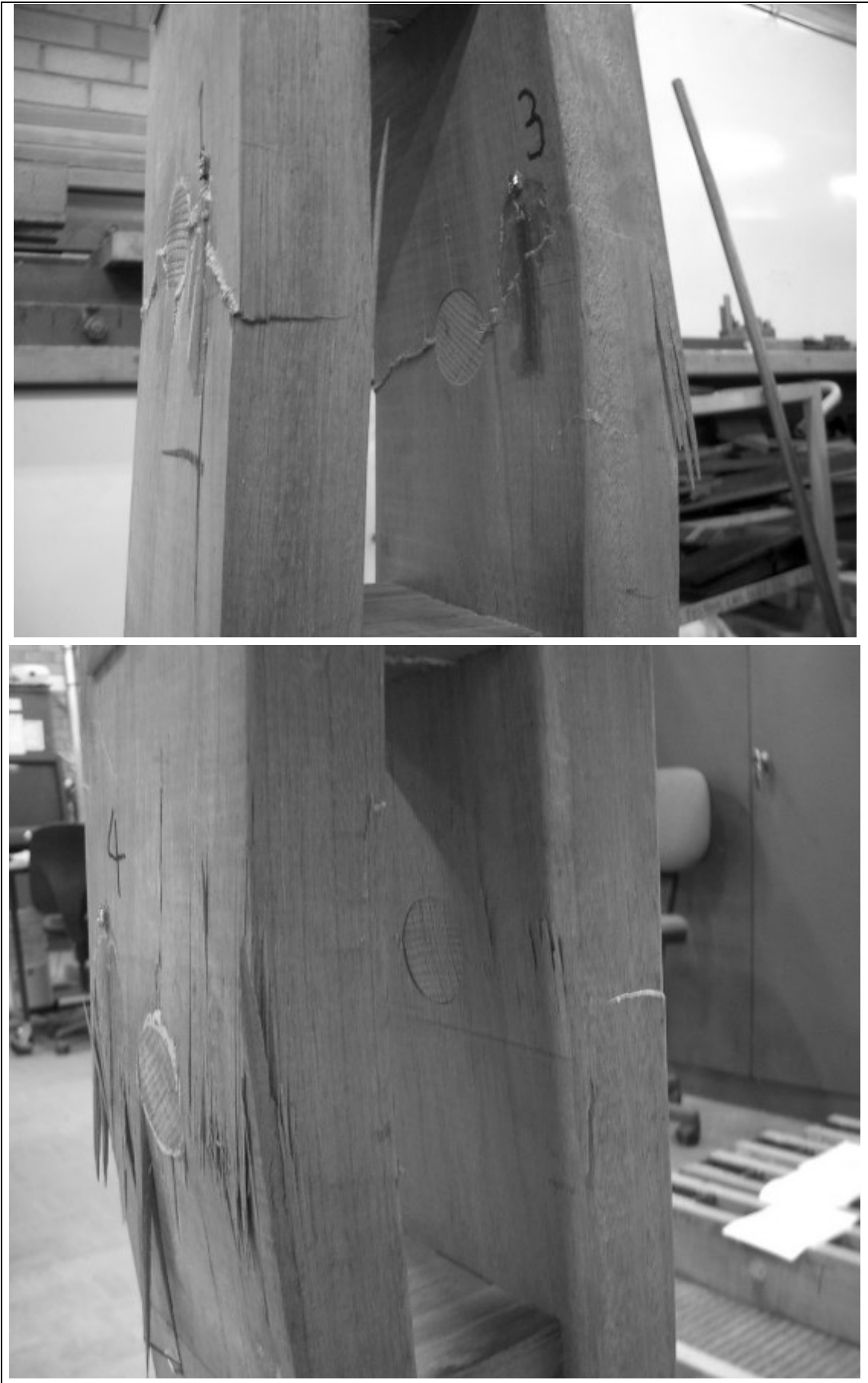
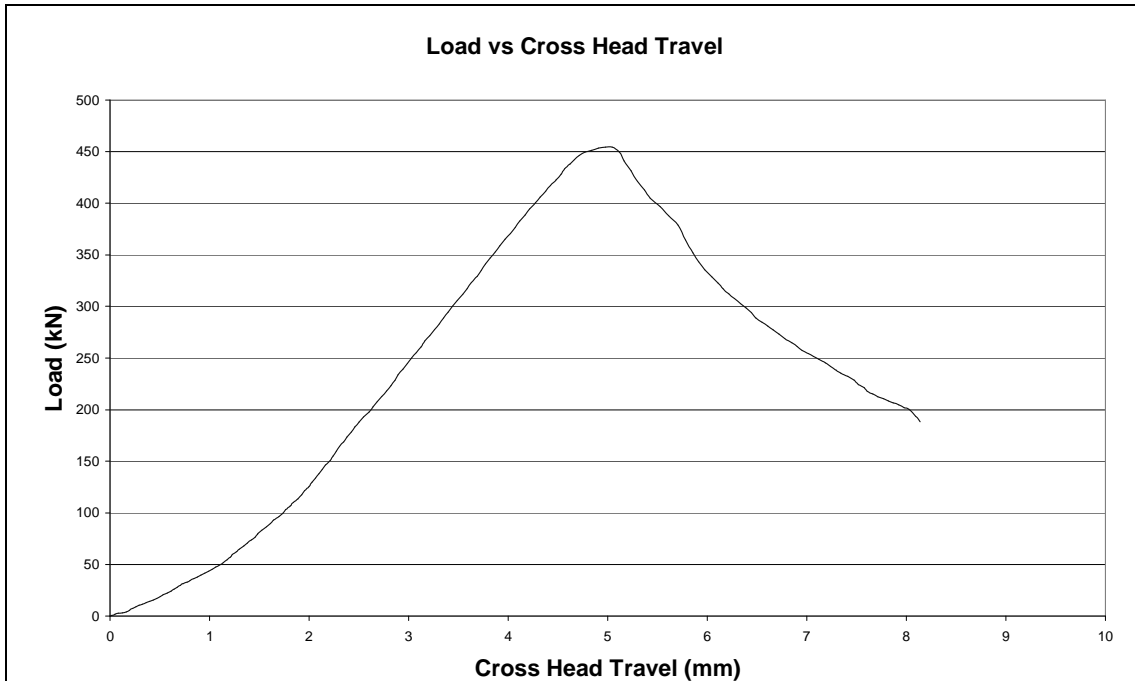


Figure A.25: Photographs of failure locations for Assembly 07B07A



The graph below shows the strains recorded at each of the strain gauges during the test.

Gauges 1 to 4 were located 135mm above the top line of bolts for the central timber spacer:

- Strain Gauge 1 is on the left hand outer face.
- Strain Gauge 2 is on the left hand inner face.
- Strain Gauge 3 is on the right hand inner face.
- Strain Gauge 4 is on the right hand outer face.

Gauges 5 to 8 were located 135mm above the top line of the bolts for the bottom steel box:

- Strain Gauge 5 is on the left hand outer face.
- Strain Gauge 6 is on the left hand inner face.
- Strain Gauge 7 is on the right hand inner face.
- Strain Gauge 8 is on the right hand outer face.

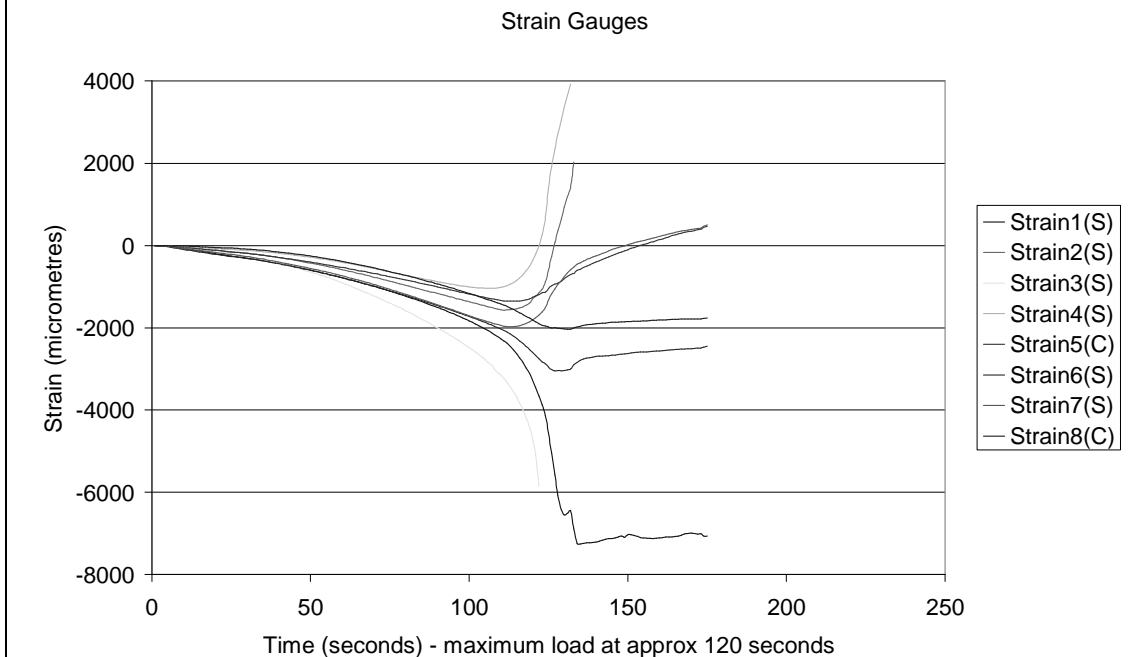


Figure A.26: Graphs for Assembly 07B07A



**EXPERIMENTAL RESULTS FOR SPACED COLUMN ASSEMBLY 01A01B:**

	01A	01B
Modulus of Elasticity (x axis)	18,674	18,674
Modulus of Elasticity (y axis)	20,034	19,197
Compressive Strength	390 (no hole)	no result
Assembly Buckling Load	454.5 kN	

Figure A.27: Summary of Results for Assembly 01A01B

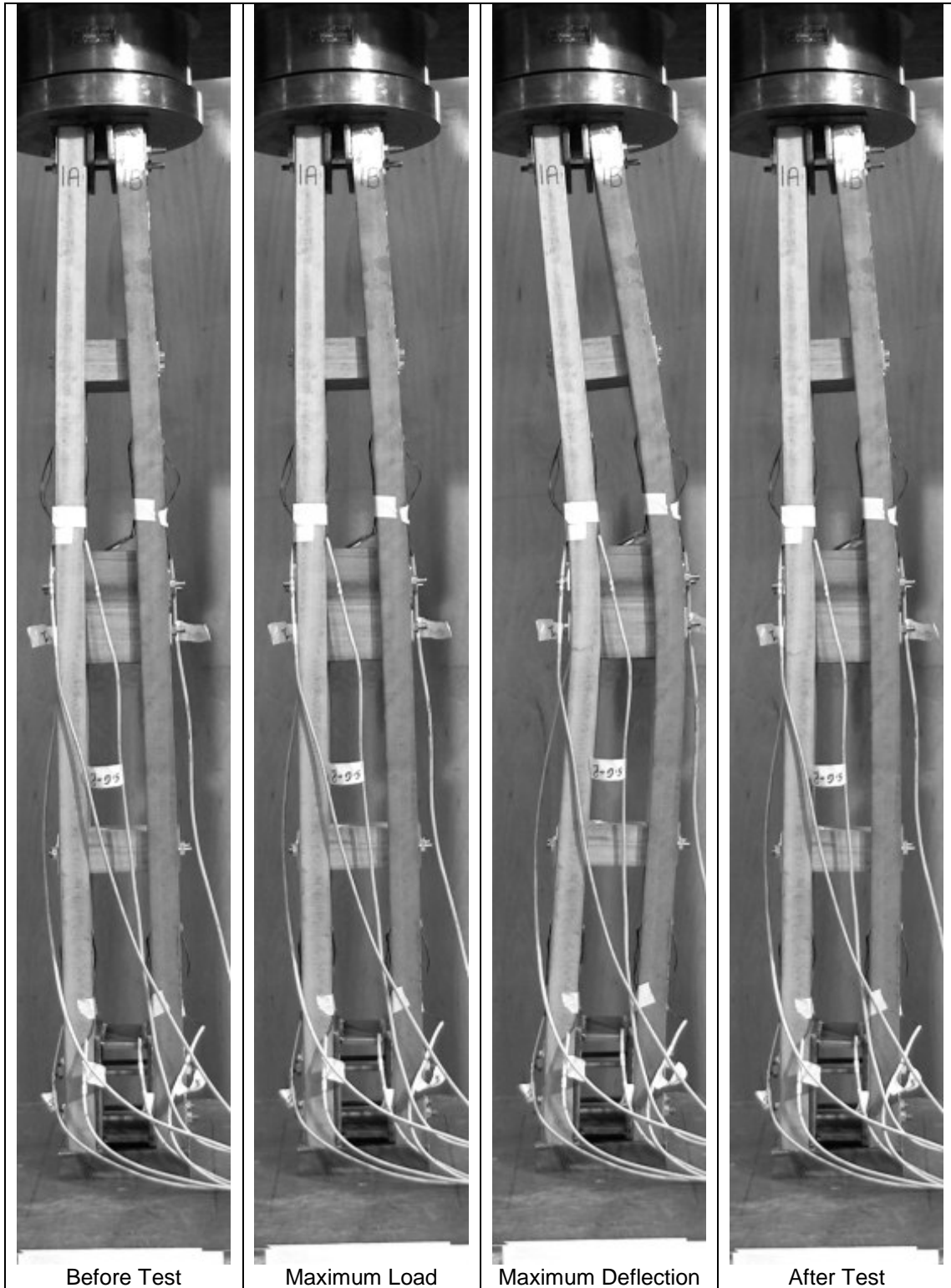


Figure A.28: Photographs of test for Assembly 01A01B

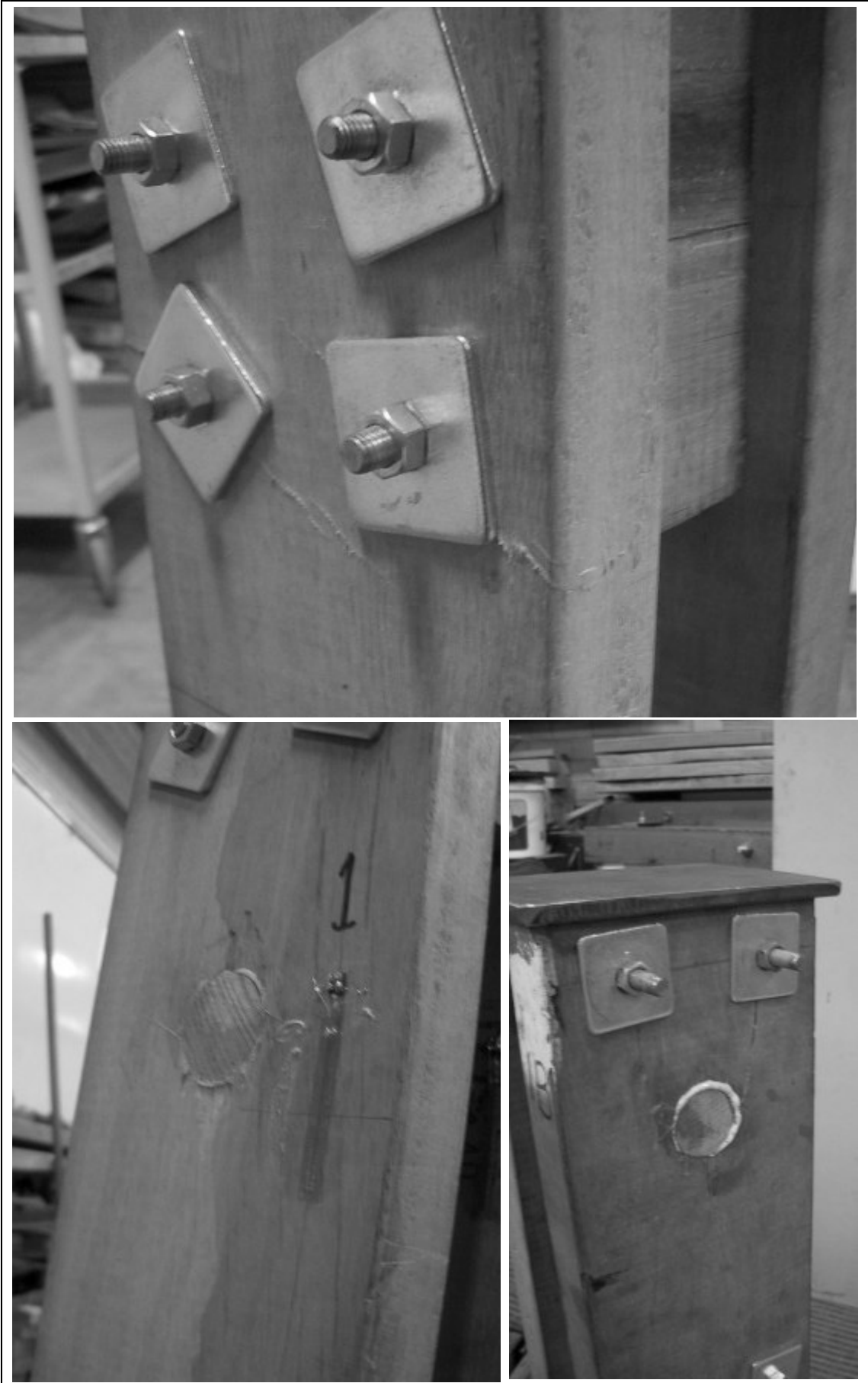
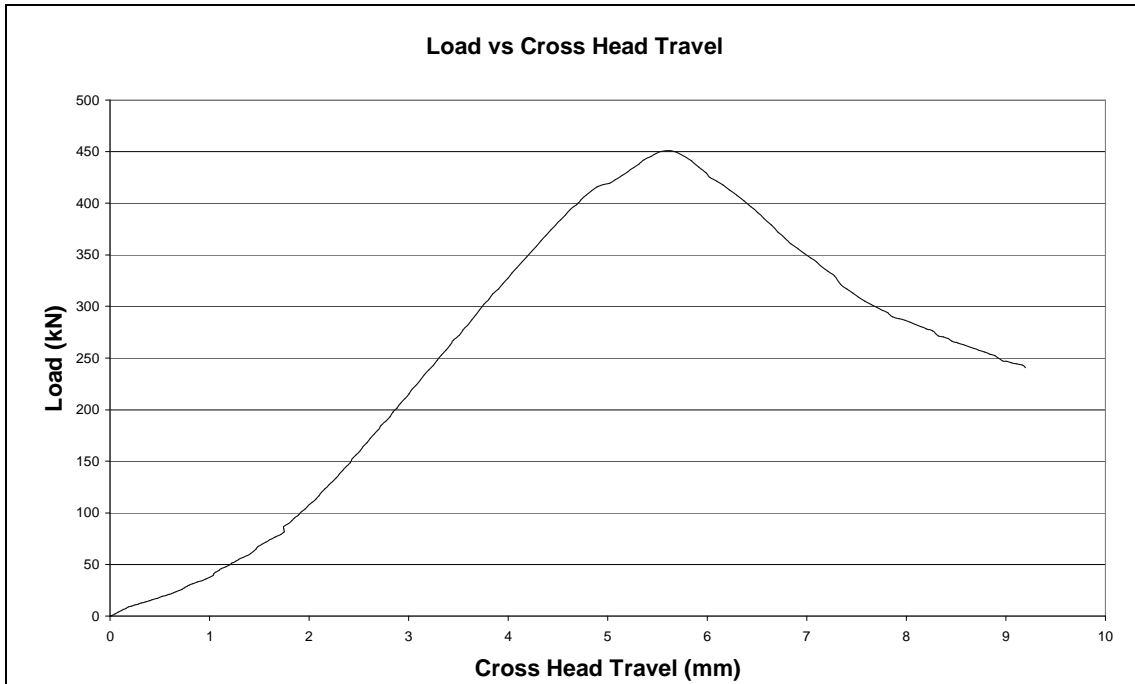


Figure A.29: Photographs of failure locations for Assembly 01A01B



The graph below shows the strains recorded at each of the strain gauges during the test.

Gauges 1 to 4 were located 135mm above the top line of bolts for the central timber spacer:

- Strain Gauge 1 is on the left hand outer face.
- Strain Gauge 2 is on the left hand inner face.
- Strain Gauge 3 is on the right hand inner face.
- Strain Gauge 4 is on the right hand outer face.

Gauges 5 to 8 were located 135mm above the top line of the bolts for the bottom steel box:

- Strain Gauge 5 is on the left hand outer face.
- Strain Gauge 6 is on the left hand inner face.
- Strain Gauge 7 is on the right hand inner face.
- Strain Gauge 8 is on the right hand outer face.

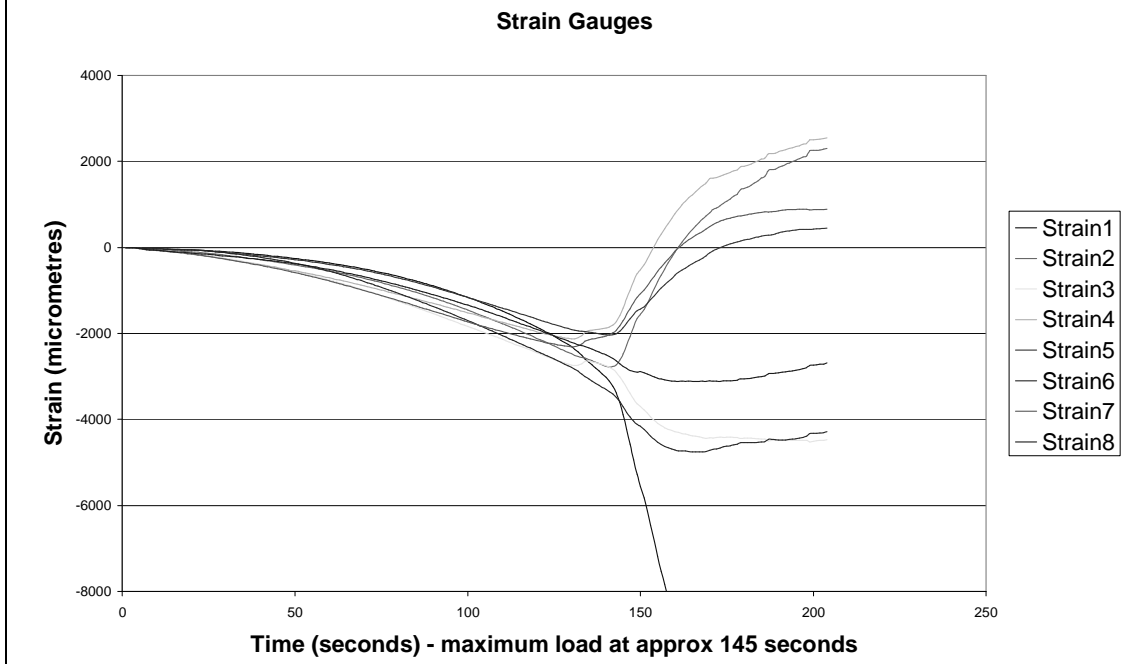


Figure A.30: Graphs for Assembly 01A01B

**EXPERIMENTAL RESULTS FOR SPACED COLUMN ASSEMBLY 04B05B:**

	04B	05B
Modulus of Elasticity (x axis)	18,064	19,824
Modulus of Elasticity (y axis)	21,075	20,857
Compressive Strength	275 (edge hole)	no result
Assembly Buckling Load	345.5 kN	

Figure A.31: Summary of Results for Assembly 04B05B

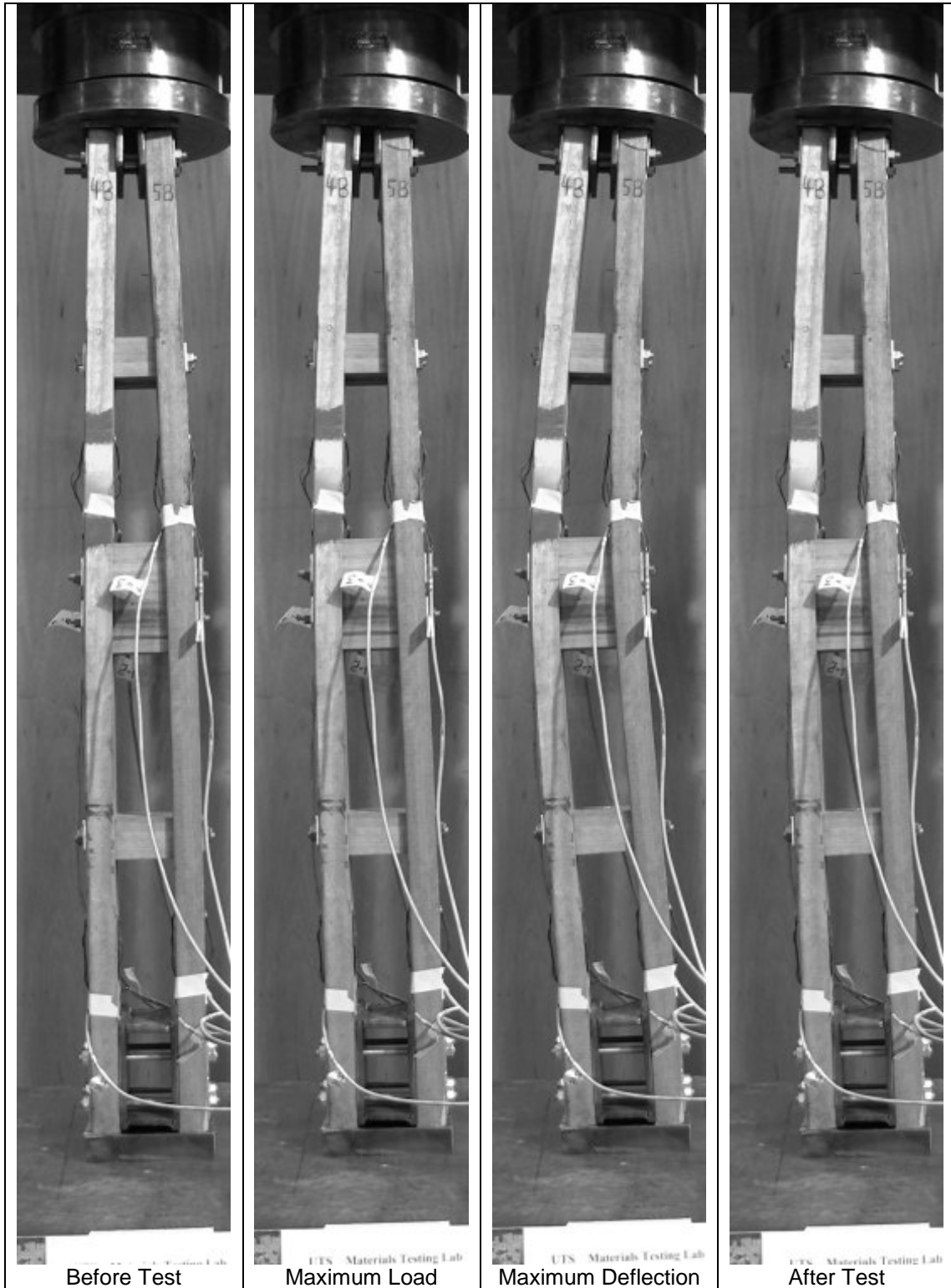


Figure A.32: Photographs of test for Assembly 04B05B

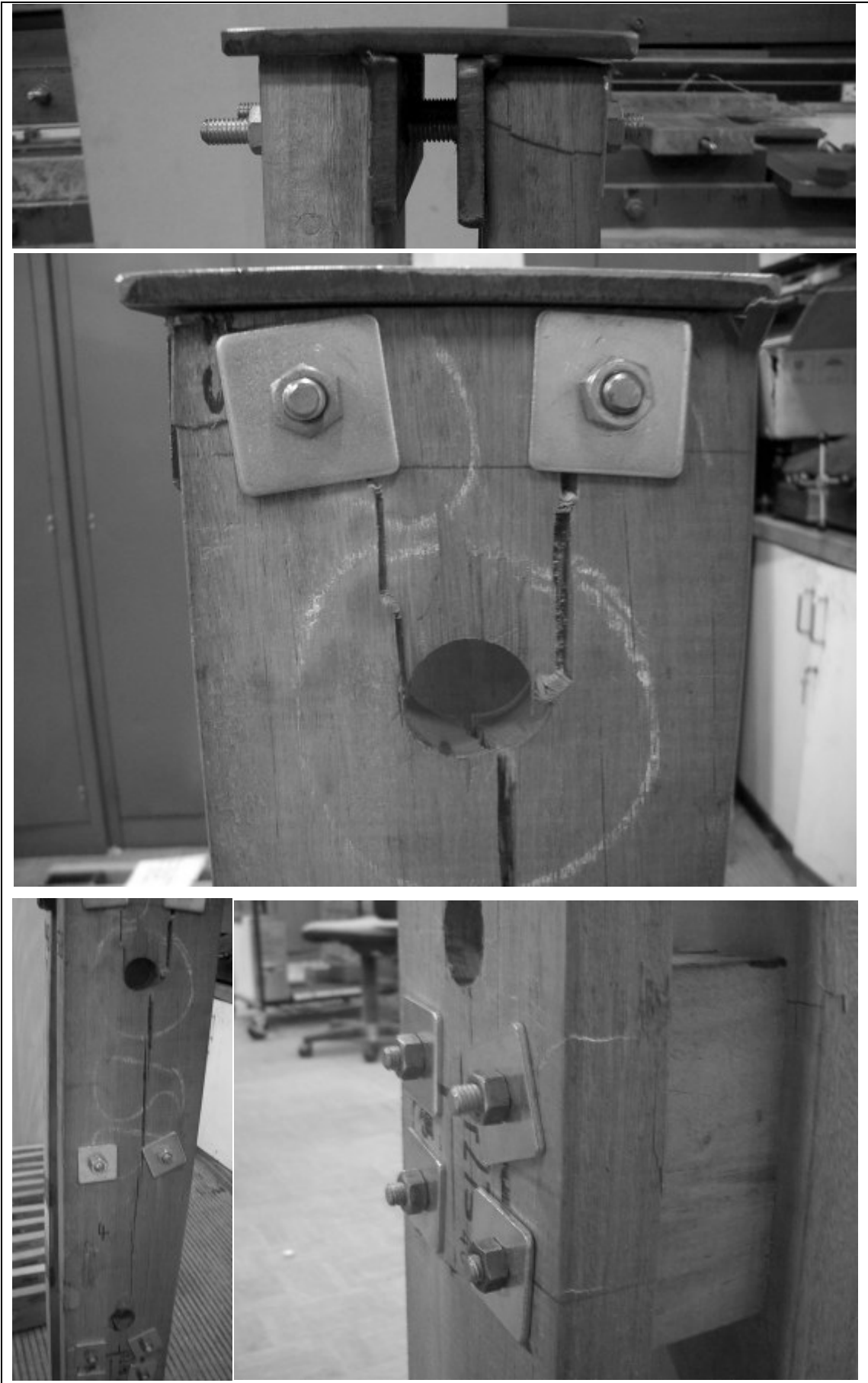
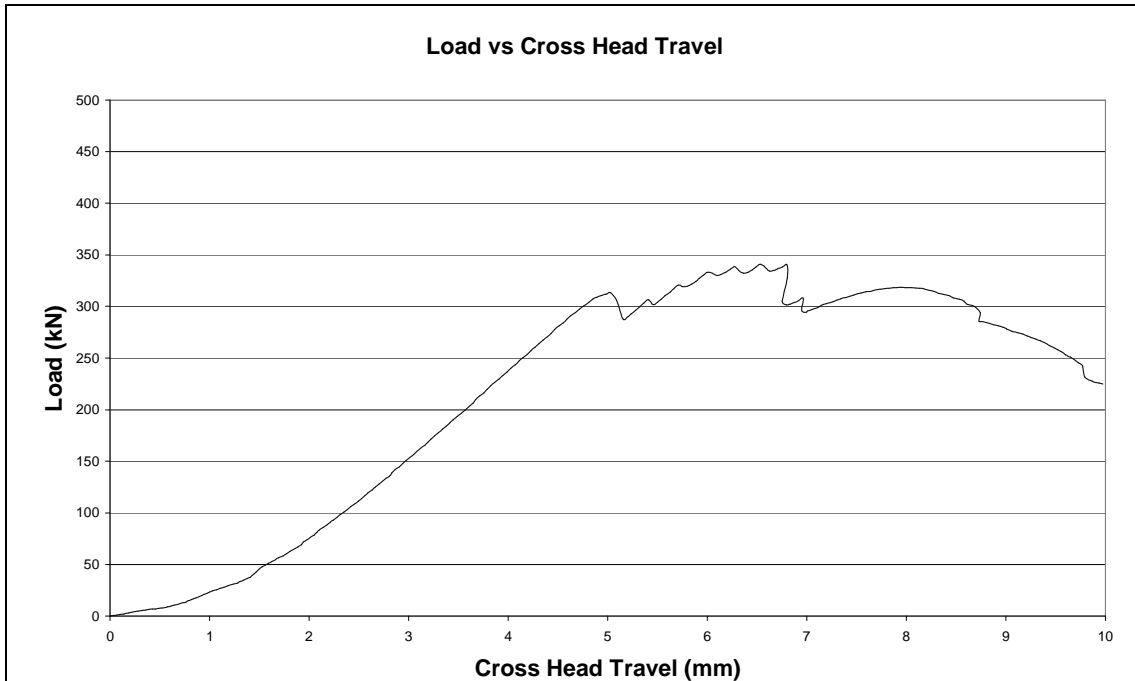


Figure A.33: Photographs of failure locations for Assembly 04B05B



The graph below shows the strains recorded at each of the strain gauges during the test.

Gauges 1 to 4 were located 135mm above the top line of bolts for the central timber spacer:

- Strain Gauge 1 is on the left hand outer face.
- Strain Gauge 2 is on the left hand inner face.
- Strain Gauge 3 is on the right hand inner face.
- Strain Gauge 4 is on the right hand outer face.

Gauges 5 to 8 were located 135mm above the top line of the bolts for the bottom steel box:

- Strain Gauge 5 is on the left hand outer face.
- Strain Gauge 6 is on the left hand inner face.
- Strain Gauge 7 is on the right hand inner face.
- Strain Gauge 8 is on the right hand outer face.

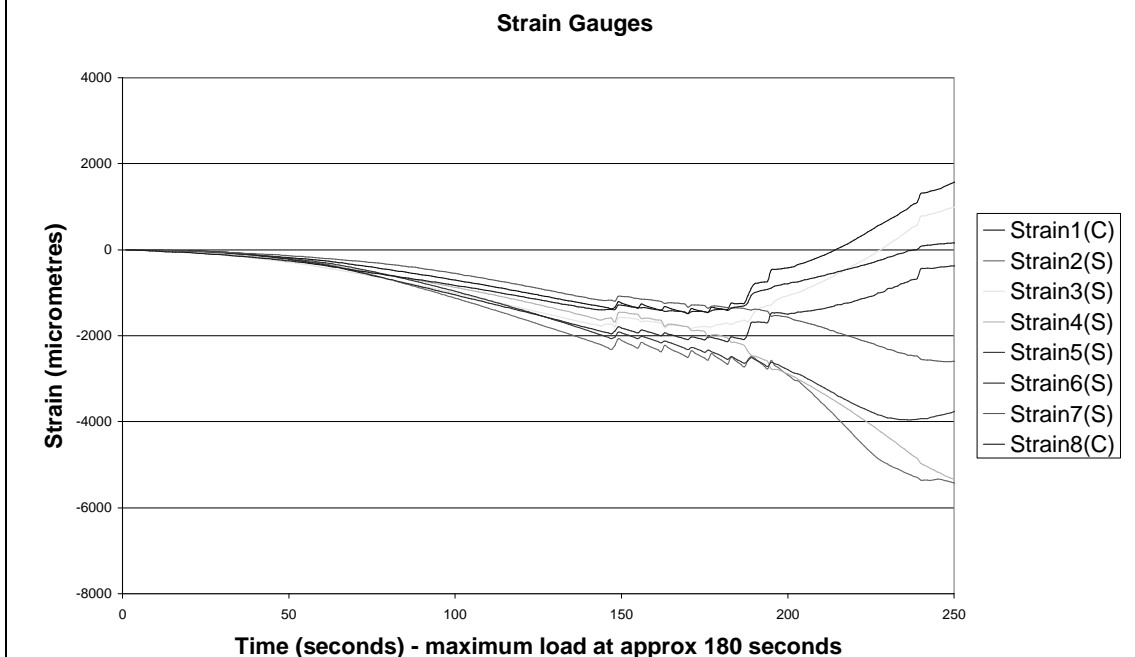


Figure A.34: Graphs for Assembly 04B05B

**EXPERIMENTAL RESULTS FOR SPACED COLUMN ASSEMBLY 06A12B:**

	06A	12B
Modulus of Elasticity (x axis)	17,868	18,428
Modulus of Elasticity (y axis)	17,732	17,710
Compressive Strength	285 (edge hole)	265 (at hole)
Assembly Buckling Load	364.0 kN	

Figure A.35: Summary of Results for Assembly 06A12B

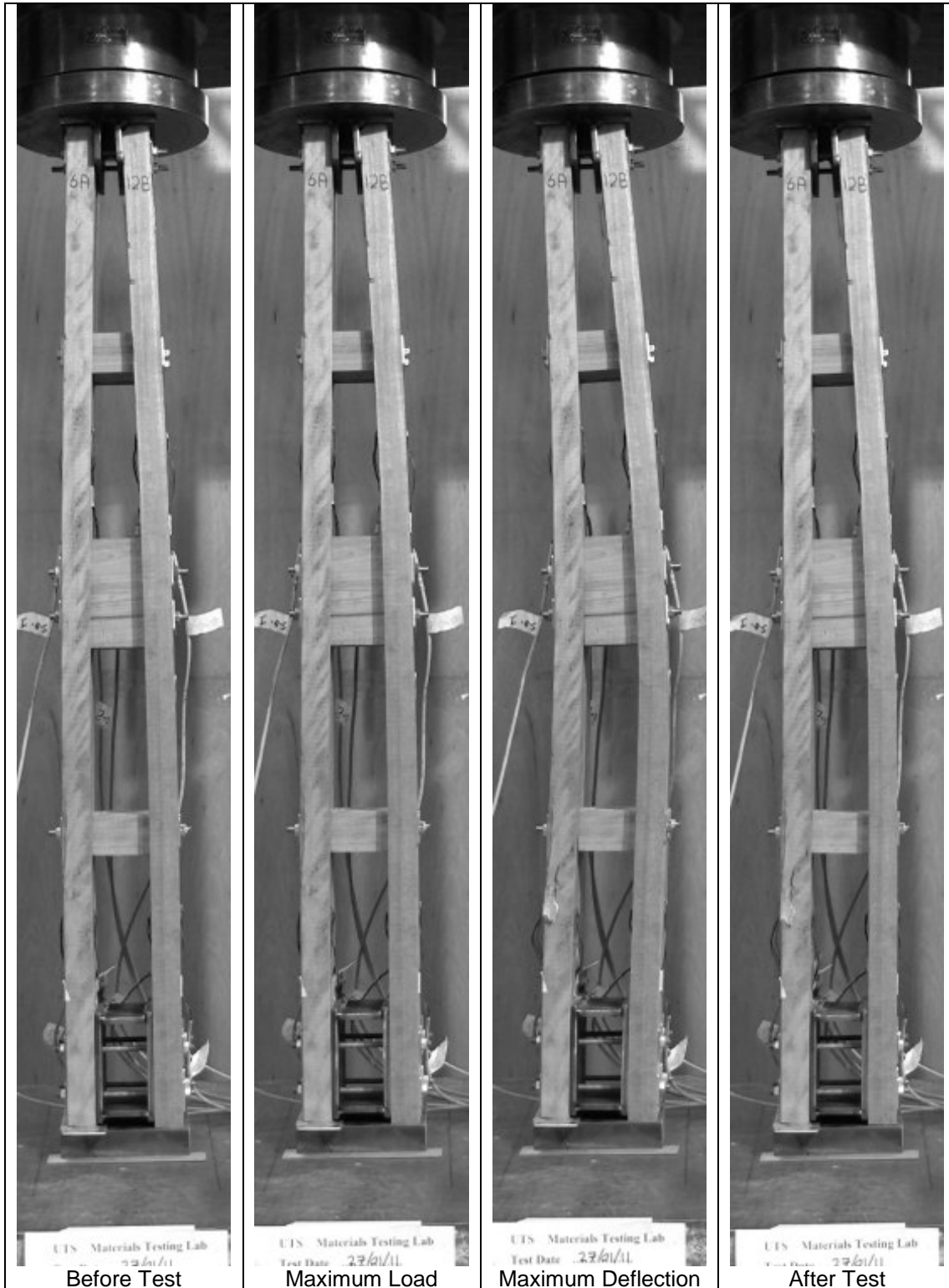


Figure A.36: Photographs of test for Assembly 06A12B

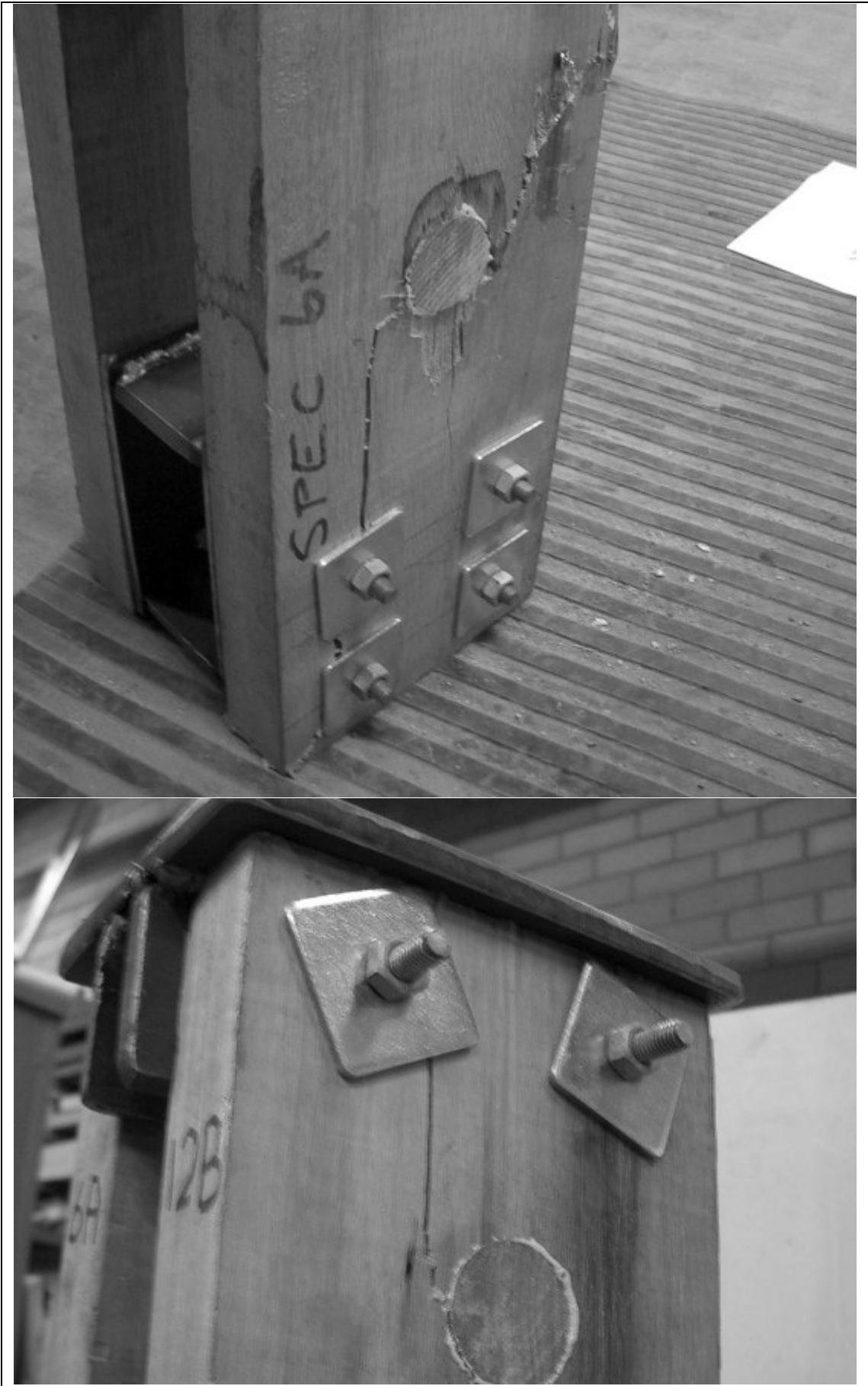
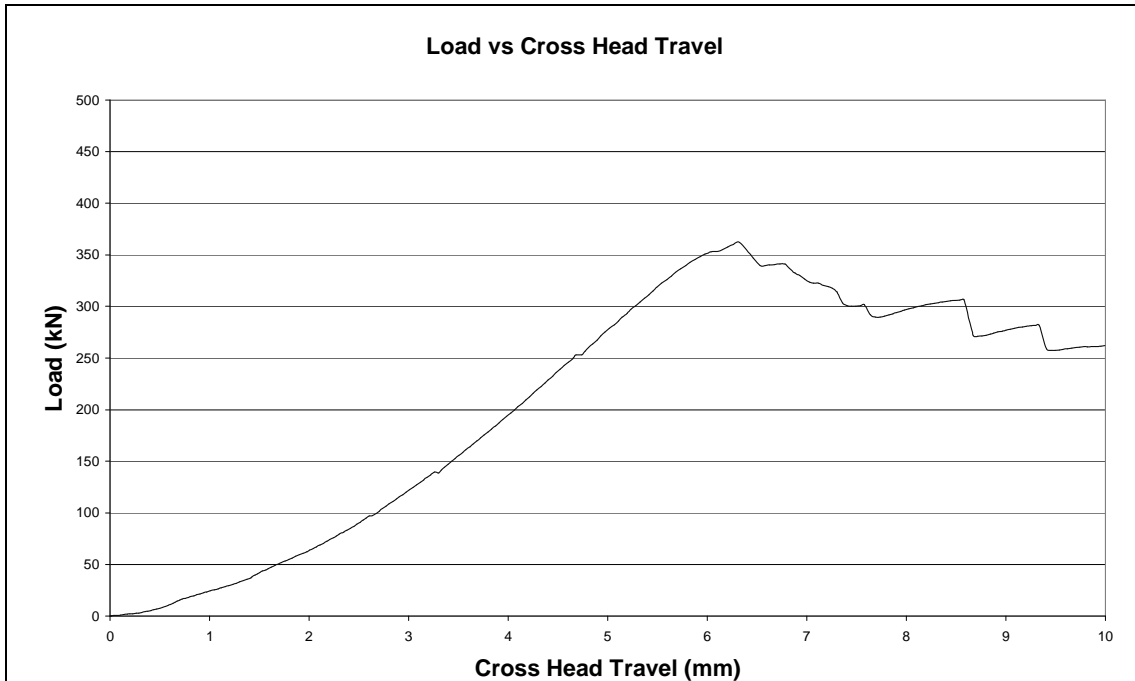


Figure A.37: Photographs of failure locations for Assembly 06A12B





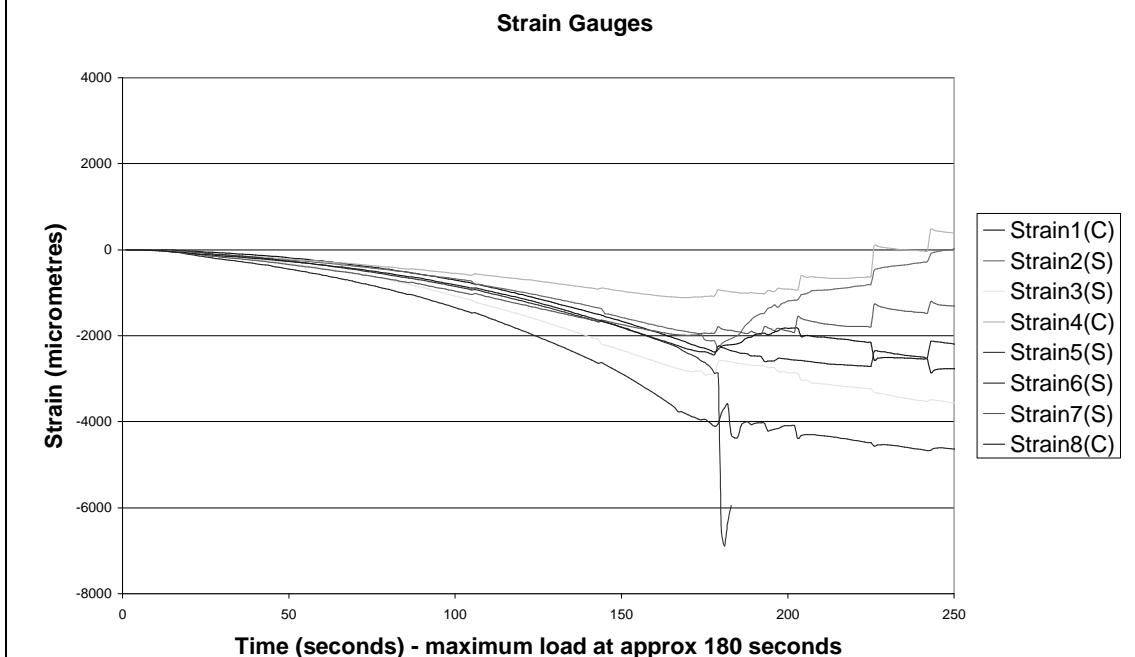
The graph below shows the strains recorded at each of the strain gauges during the test.

Gauges 1 to 4 were located 135mm above the top line of bolts for the central timber spacer:

- Strain Gauge 1 is on the left hand outer face.
- Strain Gauge 2 is on the left hand inner face.
- Strain Gauge 3 is on the right hand inner face.
- Strain Gauge 4 is on the right hand outer face.

Gauges 5 to 8 were located 135mm above the top line of the bolts for the bottom steel box:

- Strain Gauge 5 is on the left hand outer face.
- Strain Gauge 6 is on the left hand inner face.
- Strain Gauge 7 is on the right hand inner face.
- Strain Gauge 8 is on the right hand outer face.



Time (seconds) - maximum load at approx 180 seconds  
 Figure A.38: Graphs for Assembly 06A12B

**EXPERIMENTAL RESULTS FOR SPACED COLUMN ASSEMBLY 06B09B:**

	06B	09B
Modulus of Elasticity (x axis)	17,868	19,135
Modulus of Elasticity (y axis)	20,366	20,144
Compressive Strength	305 (edge hole)	335 (edge hole)
Assembly Buckling Load	444.5 kN	

Figure A.39: Summary of Results for Assembly 06B09B

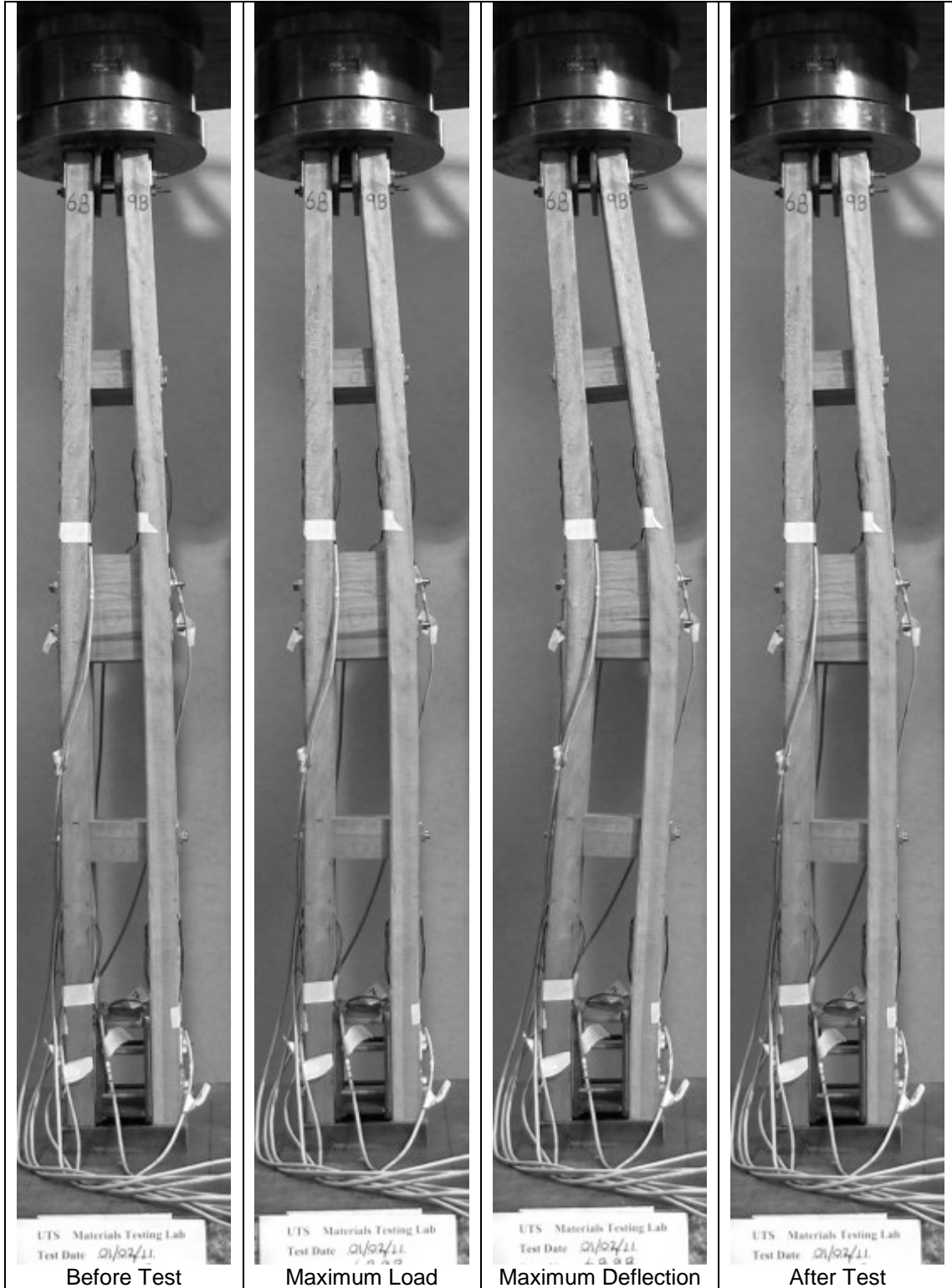


Figure A.40: Photographs of test for Assembly 06B09B

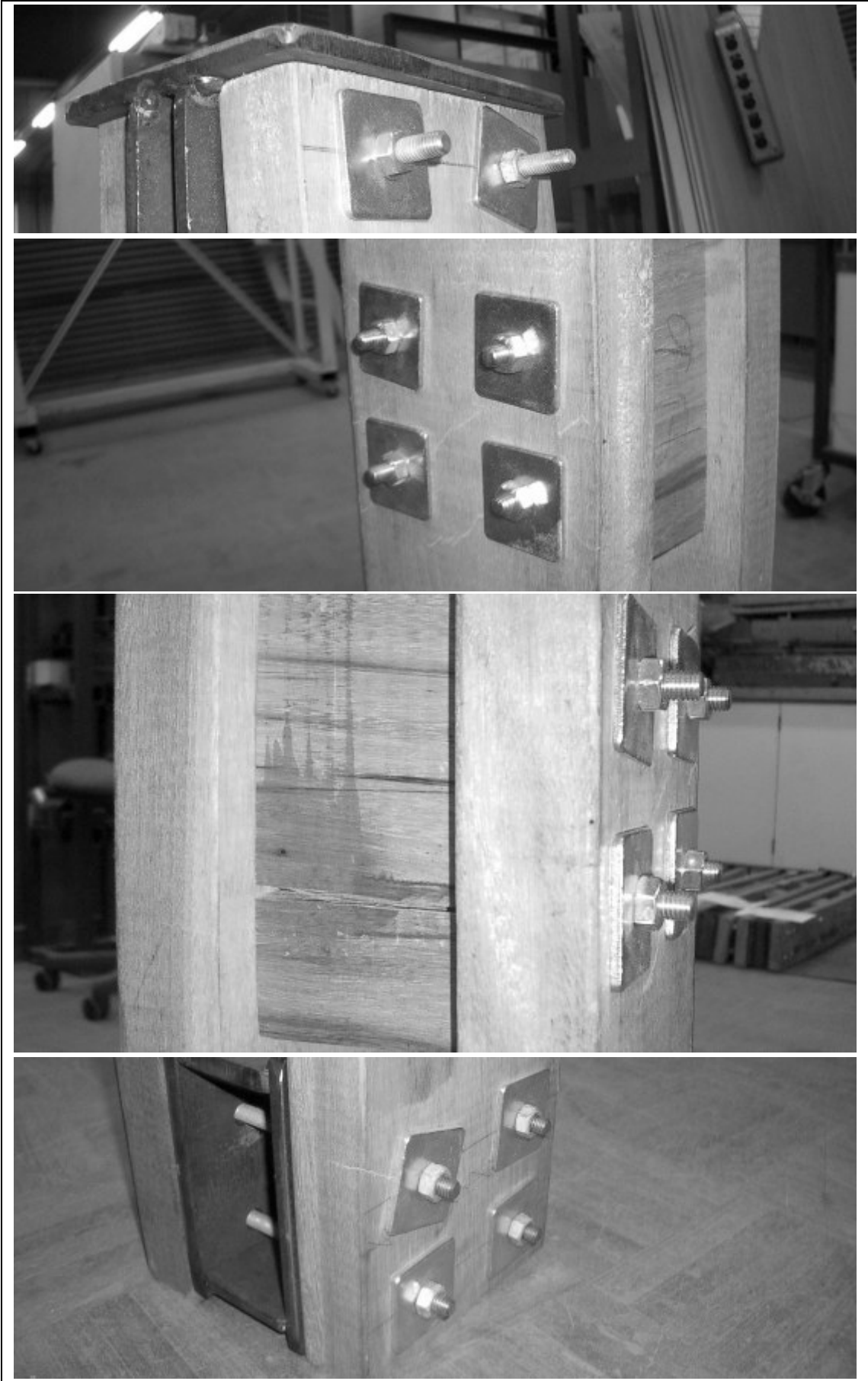
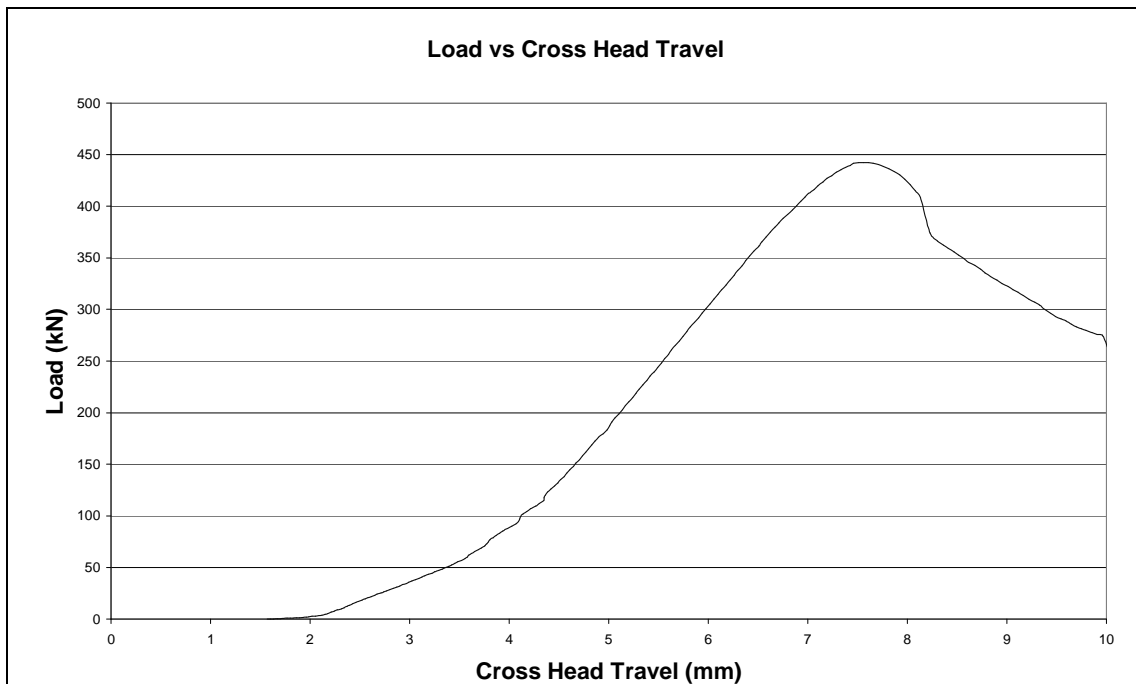


Figure A.41: Photographs of failure locations for Assembly 06B09B



The graph below shows the strains recorded at each of the strain gauges during the test.

Gauges 1 to 4 were located 135mm above the top line of bolts for the central timber spacer:

- Strain Gauge 1 is on the left hand outer face.
- Strain Gauge 2 is on the left hand inner face.
- Strain Gauge 3 is on the right hand inner face.
- Strain Gauge 4 is on the right hand outer face.

Gauges 5 to 8 were located 135mm above the top line of the bolts for the bottom steel box:

- Strain Gauge 5 is on the left hand outer face.
- Strain Gauge 6 is on the left hand inner face.
- Strain Gauge 7 is on the right hand inner face.
- Strain Gauge 8 is on the right hand outer face.

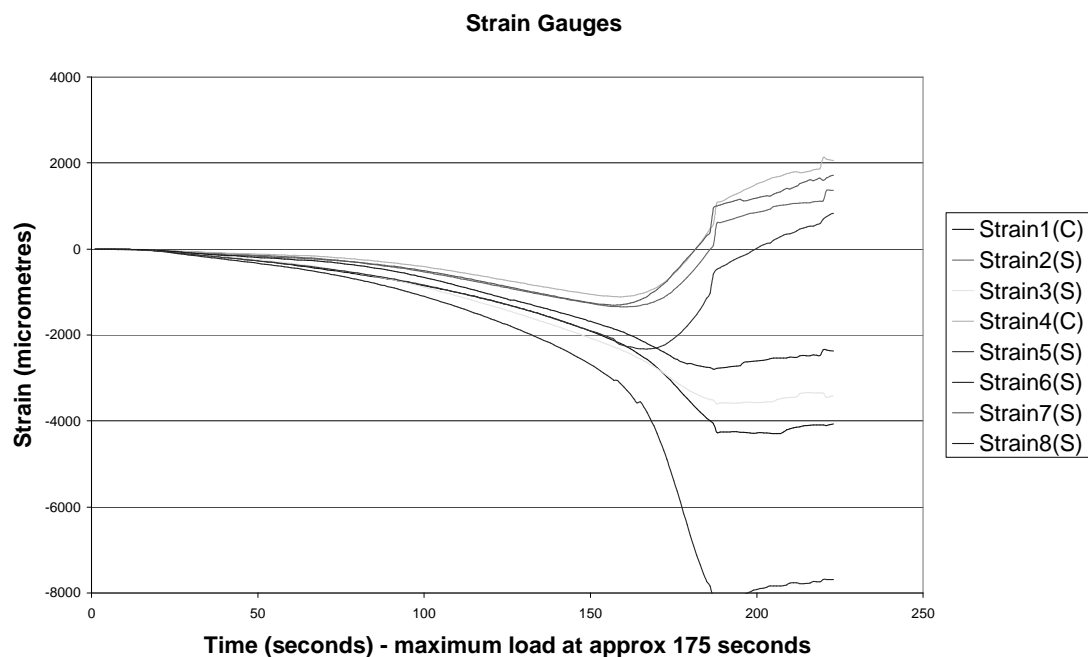


Figure A.42: Graphs for Assembly 06B09B